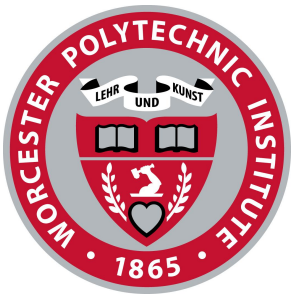

A Design and Analysis of Solid Oxide Electrolysis Cells

A Major Qualifying Project submitted to the Faculty of
WORCESTER POLYTECHNIC INSTITUTE
in partial fulfillment of the requirements for the degree of
Bachelor of Science

by:
Stephen Davis
Alexander Kochling
Samuel Krimmel

Date:
August 19th 2022

Report Submitted to:

Professor Yu Zhong
Worcester Polytechnic Institute

Abstract

Fuel cell systems are a crucial technology in the future energy market. With the renewable energy sector growing, there is a significant need for reversible energy storage and alternative sources of continuous power. Reversible Solid Oxide Cells (R-SOCs) are of particular interest due to their ability to electrochemically convert chemical energy to electrical energy and vice versa with no carbon or other particulate emissions. Solid Oxide Fuel Cell (SOFC) and Solid Oxide Electrolysis Cell (SOEC) mathematical models are developed and analyzed in this study. Additionally, SOFCs and SOECs are modeled using the process simulation software packages Aspen Plus and IDAES, so the processes can be combined to analyze an R-SOC cycle. The mathematical models found that SOEC performance improves with increasing temperature by lowering the voltage and slightly increasing the voltage efficiency. The Aspen Plus simulation determined a similar relationship between voltage and temperature. Therefore, an operating temperature of around 1173K is suggested for SOECs with the current setting. During operation, lower current densities, activation energies, and cell resistance is suggested. For SOFC mode, increasing partial pressure of H_2O relative to H_2 and decreasing partial pressure of O_2 will improve performance. For SOEC mode, increasing the partial pressure of H_2 relative to H_2O and increasing the partial pressure of O_2 will improve performance.

Acknowledgements

Our team would like to acknowledge and thank the individuals and organizations who have supported this research with their guidance and contributions. We thank Dr. Yu Zhong for supporting and advising us throughout the duration of this project and his willingness to help us solve any problems that arose. We would also like to thank Saint-Gobain Research North America for their support, as well as Dr. John Pietras from the SGRNA Process Technology Group for taking the time to go over our research and provide valuable feedback. Without their support, this project would not be possible.

Executive Summary

Today's energy market is highly dependent on unsustainable energy sources, which boosts outdated energy methods such as fossil fuel mining, oil fracking, etc. (Union of Concerned Scientists, 2008). These natural resources produce destructive greenhouse gasses into the environment and come only in a limited supply. Therefore, alternative options such as fuel cell systems are a key component of today's energy market. With the renewable energy sector growing, there is a significant need for energy storage and alternative sources of continuous power. Reversible Solid Oxide Cells (R-SOCs) are of particular interest due to their ability to utilize electrochemistry to convert chemical energy to electrical energy and vice versa with no carbon or particulate emissions. This study developed a Solid Oxide Electrolysis Cell (SOEC) mathematical model. Additionally, a SOEC is modeled using the process simulation software packages Aspen Plus and IDAES. It can be combined with a Solid Oxide Fuel Cell (SOFC) model to analyze an R-SOC. The simulations determine the operating efficiency of the SOEC, and recommendations for improved SOFC design were made using this data.

Methodology

R-SOCs are capable of SOFC and SOEC operational modes, serving as electrical power and fuel generation, respectively. Other research groups have previously modeled R-SOCs and their modes for thermodynamic analysis, typically using chemical simulation software. This study will use mathematical models combined with software to model a SOFC and a SOEC. The software that our group will use to replicate and build on the previous iteration of this project will be IDAES and Aspen Plus. It is important to note that both programs are relatively new,

with IDAES being released just six years ago in 2016 and Aspen Plus being released in 1982. Examples of past R-SOC research utilizing IDAES are comparatively scarce.

Key Findings

Results for the SOFC and SOEC simulations from both software programs produced polarization curves that depicted a voltage variation with temperature. For the SOFC models, it was found that a higher operating temperature led to higher voltages. For the SOEC models, there was a more limited relationship with temperature, but higher temperature required lower voltage. When evaluating voltage efficiency, our models suggest that both cell types benefit from higher temperatures. Additionally, a relationship with current density shows that approaching the limiting current density of the cell negatively impacts the performance, decreasing voltage in SOFC mode and increasing voltage in SOEC mode.

For the mathematical models, the multiple forms of electrochemical loss were isolated and analyzed to assess the effectiveness of our loss models. The electrochemical losses were calculated using the same methods for both the SOFC and SOEC. These losses can be isolated graphically at set temperatures to depict the different behavior of each modeling equation with a variation in current density. The results show that ohmic and activation losses are linearly approximated within this range, increasing with current density. Activation loss is displayed on a log scale for current density. The mathematical models were used to manually generate a set of polarization curves for three different temperatures, 1073 K, 1173 K, and 1273 K. These results rely strictly on the equations covered in Section 3.3 and proved to be simple and software-free way to simulate the SOFC and SOEC.

Broader Impacts

Engineering Ethics

Engineers are tasked with following the principles described in the ASME (American Society of Mechanical Engineers) Code of Ethics. This needs to be done in order to maintain and guide engineers' ethics and morals to make sure that the profession is used for the benefit of society. These principles state the following:

1. [Engineers uphold and advance the integrity, honor and dignity of the engineering profession by] using their knowledge and skill for the enhancement of human welfare (ASME, 2012).
2. [...] being honest and impartial, and serving with fidelity their clients (including their employers) and the public (ASME, 2012).
3. [...] striving to increase the competence and prestige of the engineering profession (ASME, 2012).

We can see through these principles that our team has satisfied each of them. The main objective of our project has been to improve the reversible solid oxide cell efficiency so that they may be used as environmentally friendly low-cost energy sources domestically and globally. Additionally, our research, models, simulations, and paper content were all conducted and created using accurate information from reliable sources (Note: Some sources vary on the type of equations used in SOFC/SOEC models. However, we used the equations that fit our models appropriately and accurately with the input parameters. Future groups may want to change said equations based on their needs for parameters or the needs of their sponsor). Finally, all the findings of our projects are delivered in such a way that we have strived to educate engineers and increase the positive reliability of the engineering profession.

Societal Impact

R-SOCs create large amounts of energy relative to their assembly, operation, and maintenance costs. Because of this, they possess the potential to provide entire populated areas with electricity, not just single-family homes. Additionally, concerning the ongoing climate crisis, the fact that R-SOCs are entirely environmentally friendly is a big plus for implementing them in cities and suburban neighborhoods. This research focuses primarily on modeling and analyzing R-SOC systems. Any effort to implement energy storage systems coupled with renewable energy production should pay attention to environmental justice issues. R-SOC technology should be utilized to aid communities in the transition away from harmful and polluting sources of power.

Environmental & Sustainability Impact

Fossil fuels are currently the standard when it comes to energy production, both domestically and abroad. Fuel cells are beginning to show themselves as a more environmentally friendly alternative to these fossil fuels. Furthermore, solid oxide cells are proving to additionally be one of the most sustainable types of these fuel cells. This is due to the fact that the only byproduct of the whole R-SOC process is water and heat, leading to lower pollutant outputs and less greenhouse gasses in the atmosphere. Additionally, they don't require power lines, so they can be easily accessible to remote communities without centralizing an energy system. This would reduce the environmental impact of said transmission lines. These factors strengthen our belief in the importance of our research, as well as the hope that further development of R-SOCs will create a positive impact on both the environment and our society (Stambouli & Traversa, 2002).

Table of Contents

1.0 Introduction

A fuel cell is any device that uses a chemical reaction to generate electricity. The first fuel cell was utilized to conduct electrolysis of water in 1839 by Sir William Grove. Despite the successful output of its intended products from the reaction, it did not produce enough electricity to be considered useful. Since then, fuel cell development led by companies such as Siemens Westinghouse Power Corporation and Sulzer has improved their overall efficiency, gradually evolving the technology to a point where it now stands on the precipice of being able to operate effectively alongside other modern means of electric power generation.

A Solid Oxide Fuel Cell (SOFC) is a specific type of fuel cell where the majority of its components are constructed of ceramic (as opposed to metal) that are operated at high temperatures, performing reverse electrolysis to generate electricity. It was first discovered in 1937 by Walter Nernst, with the use of ZrO_2 as an ion conductor for oxygen (Steinberger-Wilckens, 2016). In 1963, the US Electrical Power Corporation of North America created the first Reversible Solid Oxide Cell (R-SOC), combining a SOFC and a Solid Oxide Electrolyzer Cell (SOEC), the latter of which consumes electricity to perform electrolysis of water, separating hydrogen and water (Service, 2020). R-SOCs have the potential to play a major role in the transition of modern societies to renewable energy, as in addition to generating electricity, they can also perform electrolysis to consume electricity and store the energy chemically as hydrogen gas. The R-SOC can store electricity chemically in times of excess production, and release the stored energy at times of high demand (Gómez & Hotza, 2016). The current design of these cells can theoretically be improved upon even further by lowering the cost of materials and manufacturing, and devising ways to increase their overall efficiency and operational lifetimes.

The previous iteration of this project focused primarily on creating a simplified simulation of a SOFC in chemical process simulation softwares Aspen Plus and IDAES. These models were compared to existing literature and experimental observations for validation. It was found through the previous iteration of this research that greater efficiency for SOFCs could be obtained by increasing the operational temperature, fuel utilization, and inlet fuel pressure of the cells.

The transition to renewable energies requires the use of energy storage to manage grid demand and supply. R-SOCs have significant potential to fulfill this need, but require additional research to increase efficiency and operational lifetime. Therefore, the goal of this work is to not only verify the results found in the previous iteration of this research, but incorporate a SOEC module into the simulations. In doing this, we hope to gain additional understanding of these systems, and provide recommendations on how to solve the current design flaws and increase R-SOC efficiency.

2.0 Literature Review

In this section, we will review the basic concepts important to understand for this study, covering the thermodynamic and chemical behavior of reversible solid oxide cells. This will lead to the methods for modeling reversible solid oxide cells (R-SOCs) and a review of existing literature on the topic. Assessing current progress in software modeling of reversible solid oxide cells will aid us in determining how to appropriately construct our models. Additionally, we will cover the challenges we expect to encounter in our attempts to model these systems.

2.1 Thermodynamic Properties

There are a few fundamental thermodynamic properties that we need to have a thorough understanding of before we can begin to understand the behavior of reversible solid oxide cells: energy, work, heat, entropy, Gibbs free energy. By reviewing these concepts and their relations to each other we can better understand the efficiency evaluations of reversible cells, as well as their inner workings and how to properly model them. The properties are covered in the sections below.

2.1.1 Energy

Energy as a concept is the capacity to do work, and it can come in various forms; mechanical, chemical, electrical, or thermal primarily. In thermodynamics, energy is transferred by either heat or work. This brings us to the first law of thermodynamics, which states that the energy in a system must be conserved. A system can be thought of as having boundaries, and the internal energy change must account for the heat or work transferred across the system boundaries (Denker, 2014).

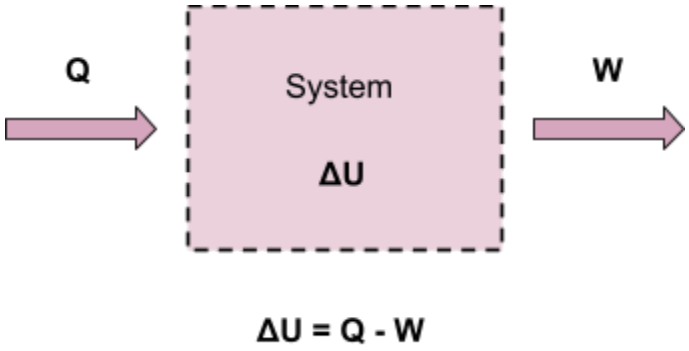

Figure 1: Representation of a system's internal energy change, ΔU (heat transferred in (in, positive), work done by the system on surroundings (out, negative))

2.1.2 Work and Heat

As mentioned above, energy is the capacity to do work. Therefore, when work is performed by a system, it is the transfer of energy from within the system to its surroundings. A simple example could be applying heat to gas in a chamber with a piston. The gas will then do mechanical work by increasing in pressure and applying a force on the piston to move it. In the diagram above, Q can be interpreted as the heat applied to the chamber, and the work is shown as W. In thermodynamics, to transfer energy in the form of heat, there needs to be a temperature difference. Referencing the first law of thermodynamics for the system in Figure 1, the energy is conserved as the internal energy change is equal to the heat applied minus the work done.

2.1.3 Entropy

Entropy can most easily be understood as the disorder that a system is under. As a system becomes more disordered, the number of possible states increases, and so does the entropy. The second law of thermodynamics states that entropy never decreases in a closed system, explaining

why an object at lower temperature can never spontaneously transfer heat to an object of higher temperature. To mathematically define change in entropy, according to the Second Law of Thermodynamics, we simply divide the heat transferred between the system and the surroundings by temperature (Hall, 2021):

Equation 1: $S = \frac{Q}{T}$

2.1.4 Gibbs Free Energy and Exergy

The change in Gibbs free energy is defined as the amount of energy that can be extracted from a chemical reaction. To find Gibbs free energy before and after a reaction, a similar equation to exergy is used:

Equation 2: $B = H - T * S$

where H is the enthalpy of the components, S is the entropy, and T is the temperature. Exergy is defined as the amount of work a system can perform when it is brought into thermodynamic equilibrium with its environment (Jørgensen & Fath, 2008). In simpler terms, this is the amount of work that may be "reversible" within a system. In this case, reversible is referring to work that can be used to return the system to its initial starting state.

2.2 R-SOCs

This section will outline the specifics in the operation and analysis of R-SOCs, including the necessary characteristics to implement in our software model. It is important to first understand the basics of reversible solid oxide cell operation. First, we will cover the chemical reaction that occurs in R-SOCs, and this will lead us to the necessary physical characteristics of

the cells, including materials used in production. Next we will cover the thermodynamics of cell operation, software modeling of R-SOCs, and present roadblocks to development of R-SOCs.

2.2.1 Chemical Reactions of SOFCs

In order for an SOFC to produce an electrical current, a chemical reaction must occur between hydrogen and oxygen gasses to form water vapor. The reactants in this equation are diatomic hydrogen and oxygen gas, and the product is water:

Equation 3: $2H_2\,(g) + O_2\,(g) \rightarrow 2H_2O\,(g)$

The above reaction can be decomposed into two electrochemical half-reactions which more accurately describe the behavior of an SOFC. By separating the above reaction spatially in the fuel cell with an electrically insulating material, it allows for the extraction of current from the process. The electrodes in an SOFC are often referred to as the anode and the cathode, but in this paper we will refer to the fuel side (hydrogen side) and the air side (oxygen side) to avoid confusion when discussing SOEC components. The reaction at the fuel electrode involves hydrogen being oxidized. In this process the hydrogen releases electrons:

Equation 4: $2H_2\,(g) + 2O^{2-} \rightarrow 2H_2O\,(g) + 4e^-$

At the air electrode, the diatomic oxygen atoms undergo a reduction process where they gain four electrons released by the hydrogen atoms at the anode, forming two peroxide anions. These anions flow through the ionic conductor, also known as the electrolyte, where they meet the oxidized hydrogen and combine to form water (Maric & Mirshekari, 2020):

Equation 5: $O_2\,(g) + 4e^- \rightarrow 2O^{2-}$

2.2.2 Chemical Reactions of SOECs

In SOEC mode, the R-SOC consumes electricity to convert water vapor into hydrogen and oxygen gas. This reaction can be used to convert electrical energy to chemical energy, stored as hydrogen which can later be used in the R-SOC in SOFC mode to generate power. The overall reaction can be summarized by the chemical equation below:

Equation 6: $2H_2O\ (g) \rightarrow 2H_2\ (g) + O_2\ (g)$

Just like when operating in SOFC mode, the above reaction can be decomposed into two electrochemical half reactions. At the fuel side, water vapor enters the cell and is reduced, gaining electrons. The hydrogen gas separated in this process flows out of the cell, and the other product, an oxygen anion, is carried through the electrolyte. The reaction can be characterized by the equation below:

Equation 7: $2H_2O\ (g) + 4e^- \rightarrow 2H_2\ (g) + 2O^{2-}$

The second electrochemical half reaction describes the chemical process at the air electrode. Here, the oxygen anions that traveled through the electrolyte are oxidized, releasing their electrons and becoming diatomic oxygen gas (Gómez & Hotza, 2016).

Equation 8: $2O^{2-} \rightarrow O_2\ (g) + 4e^-$

2.2.3 Components and Materials of R-SOCs

In order to facilitate the reactions described above in Section 2.2.1 for fuel cell operation, the relevant reactants need to be transported to the cell, requiring two separate flows, one for hydrogen and one for oxygen. It is important that these flows are balanced properly. If the flow rate for the reactants is too low, the fuel cell will not have sufficient fuel to operate at expected efficiency. If the flow rate of the reactants is too high, not all of the fuel will be utilized and again

efficiency will suffer. Therefore, the fuel cell must have some way to regulate the reactant flow rates. This usually comes in the form of flow field plates (O'Hayre et al., 2016).

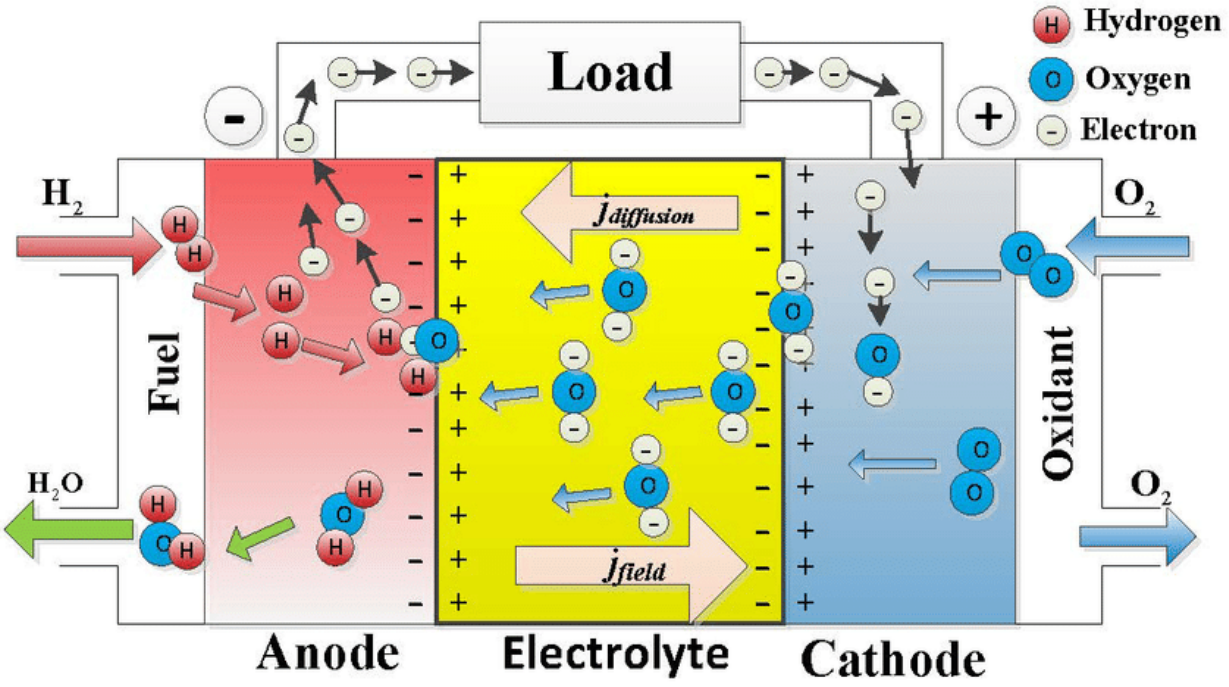

Figure 2: Typical SOFC flow diagram (Wang et al., 2019)

In fuel cell operation, once the flow of hydrogen reaches the fuel cell, it enters a porous electrode on the fuel side. The material used for this particular component is an important factor in the successful operation of the fuel cell. The electrochemical reaction occurs at what is known as the triple phase boundary (TPB), which is where the gaseous fuel, electrode, and electrolyte meet. Therefore, the fuel and air electrode materials must be permeable to allow for the flow of gas, but also electrically conductive. Additionally, due to the high operating temperatures of R-SOCs, the material must have high thermal stability.

For the fuel side of the cell, this is usually accomplished with the use of a Nickel Yttria-Stabilized Zirconia (Ni-YSZ) cermet. The YSZ in the cermet provides exceptional resistance to thermal expansion, allowing more mechanical stability when bound to a thermally

sensitive electrolyte. The nickel allows the anode to maintain high electrical conductivity, while also acting as a catalyst for the oxidation of the fuel (Maric & Mirshekari, 2020).

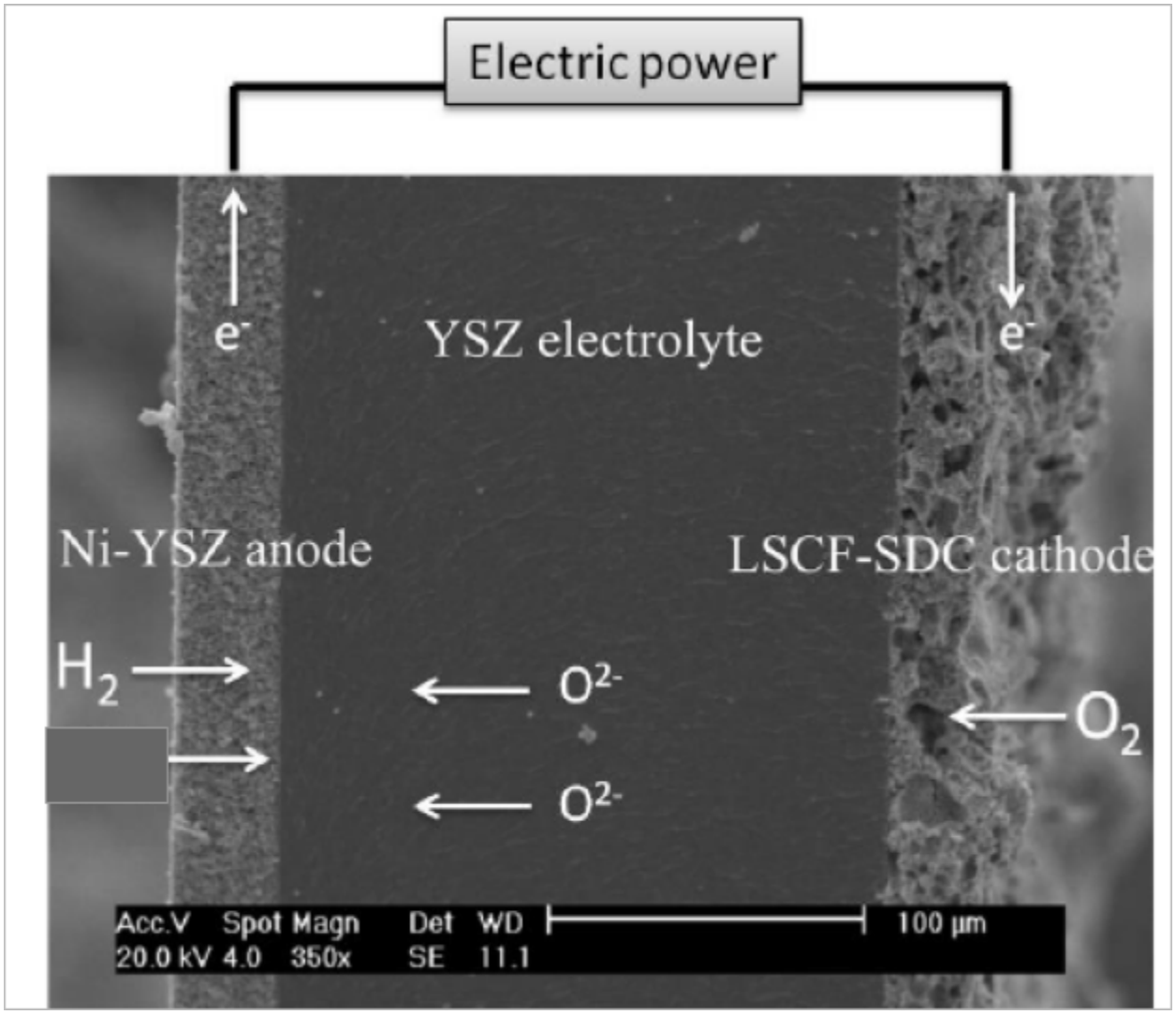

Figure 3: Microscopic view of major SOFC components (common materials) (Nascimento et al., 2012)

For the air side of the cell, the oxygen gas flow enters a porous electrode in fuel cell operation mode. The design considerations for the air electrode are similar to those of the fuel electrode; the material must have high electrical conductivity, porosity, catalytic activity, and a compatible thermal expansion coefficient. Due to the kinetics of the reduction reaction, the air

electrode must have good performance as an ionic conductor in order to extend the TPB. The materials found to fulfill these requirements are perovskites. Their formula of $ABO_{3-\delta}$, with A and B denoting cations, allows for various chemical compositions. Historically, the most common perovskite used for SOFCs has been strontium-doped lanthanum manganite, with a formula of $La_{1-x}Sr_xMnO_{3\pm\delta}$, also known as LSM (Sun et al., 2009).

These two half reactions must be separated by an electrolyte or ion conductor at the critical phase point, to allow for the flow of oxygen ions. Electrolytes are typically constructed of an oxygen ion-conductive ceramic. That ceramic must meet certain criteria: electrically insulating, to prevent the flow of electrons and force them to generate a current between the anode and the cathode, dense structure as it must be of sufficient density to prevent flow of hydrogen and oxygen gas, and only allow for the flow of oxygen ions, sufficient ionic conductivity (the electronic conductivity of the electrolyte must be sufficiently low in order to provide a high energy conversion efficiency) also the oxide ion conductivity must be high to minimize the ohmic loss, and thermal stability, since the electrolyte is exposed to its fuel at elevated temperatures (Aussielo, n.d.)

The most common material used for R-SOC electrolytes is Yttria-Stabilized Zirconia (YSZ), the same material commonly used in the cermet of the fuel side, as it is completely non-reactive with the anode and cathode at typical operating temperatures. Cells running at lower temperature ranges (less than 600C) may benefit from the use of a different material, such as Gadolinium or Samarium-doped cerium dioxide (CeO_2) as the ionic conductivity of YSZ at lower temperatures is insufficient. Other materials that could be used for the electrolyte include scandia-stabilized zirconia, lanthanum gallates, and LSMG or LSCF compounds (La, Sr)(Mg,

Ga)O_3 or (La, Sr)(Co, Fe_2O_3) some of which have improved performance at more intermediate temperatures (Aussielo, n.d) (Gómez & Hotza, 2016).

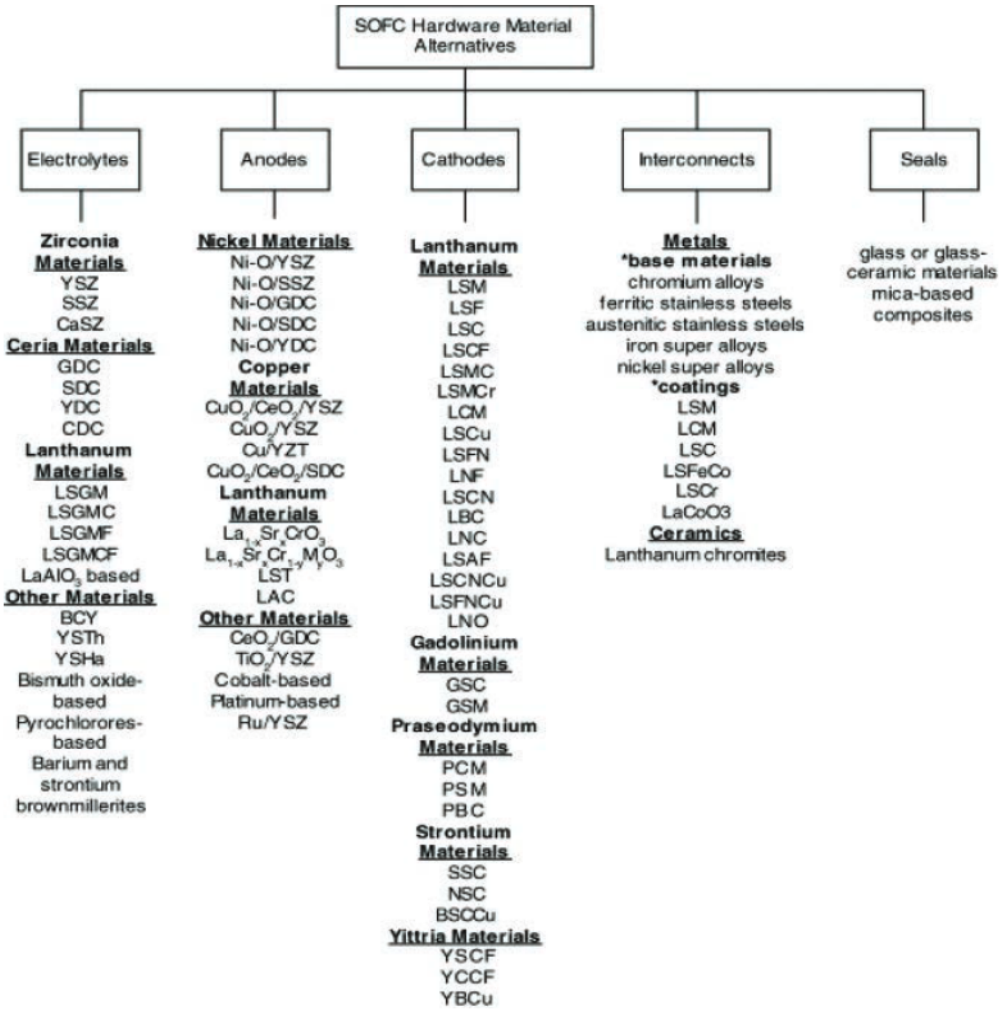

Figure 4: List of common SOFC hardware materials (Maric, 2020)

Together, with the electrolyte separating them, the half reactions occur at both the fuel and air sides. The result, as stated, is the byproducts of water and mass amounts of energy. This is due to the fact that the formation of the intermolecular hydrogen bonds and intramolecular covalent bonds are exothermic, meaning that these aforementioned chemical reactions release large amounts of energy (rather than using up energy like in an SOEC).

More goes on with these reactions than just their reactants and byproducts though, which is why thermodynamics of these cells have to be taken into account too. The two most important thermodynamic properties to understand the electrochemical reactions of these cells are: energy and voltage. The reasoning behind energy being so important is that energy is, as stated, one of the outputs of these reactions, but it is also used to calculate the total voltage of the cell too (see equation 5 in the next section for further information). The reasoning behind voltage being so important is that voltage is the electrical output that actually determines whether a fuel cell is: efficient, effective, and useful in a number of different environments or situations. Voltage is also the unit and property used to demonstrate and measure many of the important losses that need to be analyzed to determine where a fuel cell is lacking efficiency and how one may fix said lack of efficiency. One is activation losses, which are the losses caused by an overly large amount of the activation energy used in a reaction (see equation 8 in the next section for further information), and which are measured and analyzed in volts.

2.2.4 Thermodynamics of SOECs

In order to construct a thermodynamically and electrochemically accurate model of an R-SOC, we must have a thorough understanding of the governing equations for the cell operating in both SOFC and SOEC directions. This section will cover the thermodynamic principles related to the SOEC mode of the R-SOC, as incorporating the SOEC module into the R-SOC model is the main focus of this work.

Before examining the governing equations of SOECs, it is important to understand the concept of Gibbs free energy. As discussed in section 2.1.1, energy can be defined as the ability to do work. Gibbs free energy, often denoted by G, is used to describe the theoretical maximum

work that can be extracted from a thermodynamically isolated process at a constant pressure and temperature. The change in Gibbs free energy ΔG, is given by the equation below, where ΔH is enthalpy change, T is temperature in Kelvin, and ΔS is entropy change (Flowers et al., 2019):

Equation 9: $\Delta G = \Delta H - T\Delta S$

The reversible voltage of the cell can be determined thermodynamically, and is dictated by the Gibbs free energy available in the reaction. The equation below is used to calculate the reversible voltage of the cell E_r, where ΔG is the Gibbs free energy change, n is the number of moles of electrons, and F is Faraday's constant (AlZahrani & Dincer, 2017):

Equation 10: $E_r = \frac{\Delta G}{nF}$

The equation above cannot be used to determine the real voltage of the cell, as it does not take any variables into consideration other than the thermodynamically ideal Gibbs free energy change. Therefore, we must rely on the Nernst equation to get us closer to an accurate voltage approximation. The Nernst voltage E_n is given below, where R is the universal gas constant, p_{H_2}, p_{O_2}, and p_{H_2O} are the partial pressures of hydrogen, oxygen, and water vapor respectively, and T is the temperature of the reaction (Wang et al., 2020):

Equation 11: $E_n = \frac{\Delta G}{nF} + \frac{RT}{nF} ln\left(\frac{p_{H_2}\sqrt{p_{O_2}}}{p_{H_2O}}\right)$

The Nernst voltage is a closer approximation of the actual performance of an SOEC, but there are additional losses that occur during operation. For this study, the equation used to determine all polarization curves will be some variation of the equation below, where E_{cell} is the real voltage of the cell, E_n is the Nernst voltage, ΔE_{act} is the activation polarization, ΔE_{ohm} is the ohmic polarization, and ΔE_{conc} is the concentration polarization (O'Hayre et al., 2016):

Equation 12: $E_{cell} = E_n + \Delta E_{act} + \Delta E_{ohm} + \Delta E_{conc}$

It is important to note that the above equation is the same format when the R-SOC is being analyzed in SOFC mode; the polarization losses are instead subtracted from the Nernst voltage as the cell is producing electricity. As discussed above, this equation is extremely important as it dictates the structure of SOFC and SOEC polarization curves.

Polarization curves are the most widely used metric for R-SOC performance, and they are also commonly used to analyze other types of electrochemical fuel cells. A polarization curve, also known as a *j-V* curve, is a depiction of the relationship between the current and the voltage of the cell. The current is often expressed in terms of current density (A/cm^2) in order to accurately compare cells with different areas. Polarization curves can be seen as a type of efficiency curve for fuel cells, as the amount of fuel consumed directly relates to the current of the cell, and a drop in cell potential brings a corresponding drop in power per unit of fuel (O'Hayre et al., 2016).

There are three main regions of a polarization curve based on the equation above. These zones are labeled in Fig. 2, and correspond to the polarizations in the above equation. At low current densities, activation loss is the most significant. For intermediate current density values, ohmic losses generally dominate, resulting in a linear segment of the *j-V* curve. Finally, at higher current densities, concentration losses result in a sharp increase in cell voltage.

Activation losses in electrochemical cells are caused by reaction kinetics. What this means is that the activation losses of a cell are based on the rate at which a reaction occurs. If a cell's temperature were to increase, this would generally speed up the chemical reactions as the reactants require less energy to undergo the reaction, therefore the activation losses of the cell

would be lowered. This is because the cell now requires less energy (in the form of voltage) to start and finish its electrochemical reactions (Laidler, 2008).

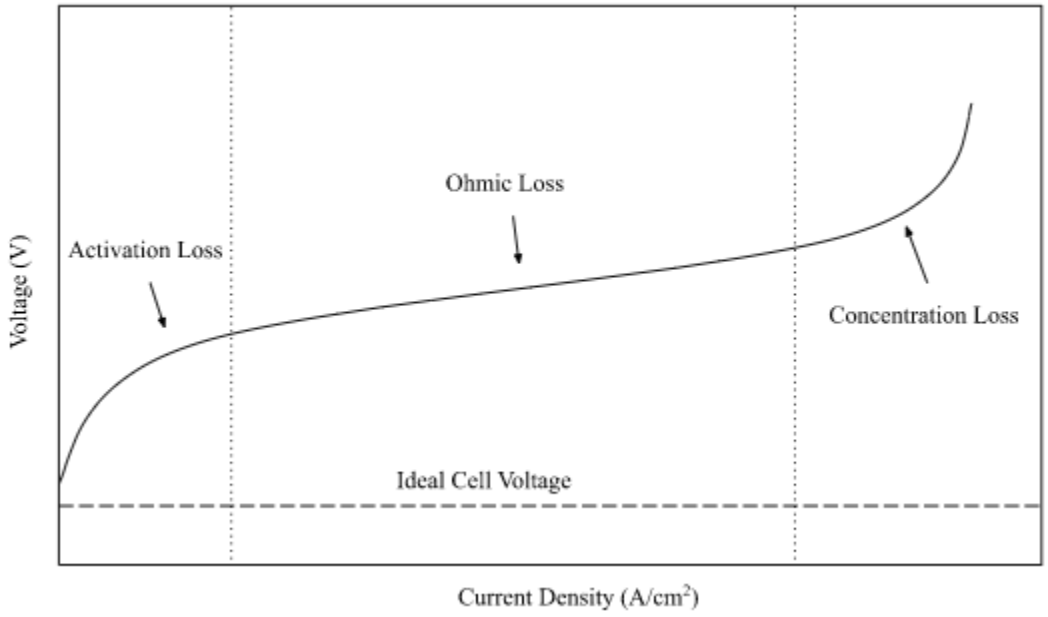

Figure 5: Example polarization curve of an electrolysis cell

To determine the total activation loss, we sum the activation losses of the anode and cathode separately. Terms with a subscript *a* denote anodic values, and terms with a subscript *c* denote cathodic values. These letters are also commonly replaced by *i* to denote that there are two corresponding forms for an equation. The equation below characterizes total activation loss, where n_i is the number of transferred electrons, j is the current density, $j_{0,i}$ is the exchange current density, and α is the transfer coefficient (Wang et al., 2020):

Equation 13: $$\Delta E_{act} = \frac{RT}{Fn_a\alpha} sinh^{-1}\left(\frac{j}{2j_{0,a}}\right) + \frac{RT}{Fn_c\alpha} sinh^{-1}\left(\frac{j}{2j_{0,c}}\right)$$

To find the exchange current density, the equation below is used where $E_{act,i}$ is the activation energy, not to be confused with the activation polarization ΔE_{act}, and γ_i is the pre-exponential factor (Wang et al., 2020):

Equation 14: $j_{0,i} = \gamma_i exp\left(\frac{-E_{act,i}}{RT}\right)$

Ohmic losses in electrochemical cells are caused by the ionic and electrolytic resistance. The resistance to the flow of ions through the electrolyte is generally the largest contributor to ohmic loss (Maric & Mirshekari, 2020). For the same reason that current density is used when considering current, a concept known as Area Specific Resistance (ASR) is used when calculating ohmic losses. ASR takes into consideration the area of the cell to account for the scaling of resistance with area. To find the ASR, the equation below is used:

Equation 15: $R_{ASR} = p_{ionic}d_{ionic} + p_e d_e = p_a d_a + p_e d_e + p_c d_c$

The a, e, c, p, and d in this equation stand for anode, electrolyte, cathode, resistivity, and thickness, respectively. The ionic resistance is $p_a d_a + p_c d_c$ because the anode and cathode are where ions are flowing in the cell (anode having positively flowing ions, and the cathode having negatively flowing ions). The electrolytic resistance is $p_e d_e$ because the electrolyte doesn't have multiple parts in order to find its resistance. The sum of these two resistance is the total ASR for the ohmic losses. Additionally, this has to be multiplied by the current density (represented by J) to get the voltage yielded from the ohmic losses, as seen in the equation below:

Equation 16: $\Delta E_{ohm} = R_{ASR}J$

Concentration losses in electrochemical cells are caused by any sort of "buildup" in concentration within the cell. This means that when a cell's current density is too high, or when a cell is experiencing a backup of reactants or products (meaning that the reactions aren't happening fast enough, or the products aren't evacuating themselves from the cell quick enough), the cell loses efficiency, and therefore experiences concentration losses. These losses can be calculated using the equation:

Equation 17: $\Delta E_{\text{conc}} = \frac{RT}{zF} \ln\left(1 - \frac{j}{j_L}\right)$

The R in this case no longer stands for resistance, but stands for the universal gas constant. The z and F being other constants: the constant number of moles of electrons that are transferred in our redox reaction, and the Faraday constant. And, finally, the j being the current density, and the j_L being the limiting current density (Maric, et al, 2020) .

In addition to calculating the losses involved in the simulation of an SOEC module, it is also important to know the equations used to calculate efficiency. Efficiency is a good metric to use to determine effective performance in a range of operating conditions. While it can be useful to see voltage as calculated above, efficiency gives us insight into the ratio between the predicted voltage given by the Gibbs free energy and the actual voltage calculated by adding the ohmic, activation, and concentration losses. In a conventional thermodynamic heat engine process, efficiency is usually given by dividing the work gained, W_{out} by the heat put in, Q_{in} as shown by Equation 18. In the case of the SOEC, the voltage efficiency η_{vol} is given by Equation 19, where E_n is the Nernst voltage and E_{cell} is the actual voltage of the cell (Menon et al., 2013).

Equation 18: $\eta_{th} = \frac{|W_{out}|}{Q_{in}}$

Equation 19: $\eta_{vol} = \frac{E_n}{E_{cell}}$

2.2.5 Relationships Between Reactions, Components, and Thermodynamics

The relationship between a cell's reactions, its components, and its thermodynamics are what ties everything together and allows the cell to work properly and efficiently. In our case, the components are the materials that build the cell. This includes, but is not limited to the anode, cathode, electrolyte, interconnects, seals, etc. The reactions are what take place within those

components. This includes, but is not limited to the half reactions that take place in both the anode and the cathode. And, lastly, all these components, materials, and reactions are only able to take place with the proper thermodynamics laws, conditions, constants, and properties taking place in harmony with each other.

2.3 Software Modeling of R-SOCs

As previously mentioned, R-SOCs utilize both an SOFC and an SOEC operational mode, acting as electrical power and fuel generation respectively. R-SOCs and their modes have previously been modeled by other research groups for the purpose of thermodynamic analysis, typically digitally using chemical simulation software. This study will use mathematical models combined with software to model R-SOCs. The software that our group will be using to replicate and build on the previous iteration of this project will be IDAES and Aspen Plus. Before going into the methodology for our software simulations, the following subsections will detail basic overviews and findings from several previous studies done using both software programs as examples of their framework and capabilities. It is important to note that both programs are relatively new, with IDAES being released just six years ago in 2016, and Aspen Plus being released in 1982, and therefore examples of past R-SOC research utilizing IDAES is comparatively scarce.

2.3.1 Software Modeling in Aspen Plus

Since Aspen Plus is a chemical process simulation software, many studies that utilize the program to analyze R-SOCs are doing so to determine the functionality of R-SOCs within larger systems. For example, a study done in 2013 by Redissi and Bouallou (2013) focused on the

co-electrolysis of CO_2 with H_2O using an SOEC module in order to reduce CO_2 emissions and produce syngas. They constructed an Aspen Plus model to simulate the steps required to conduct the co-electrolysis, with the SOEC module being one small part of their larger flowsheet. Their study simulated the electrolysis process first using two REquil reactor components in Aspen Plus to account for the reverse water gas shift reaction. Next in their flowsheet was an RStoic reactor component to simulate the electrolysis step in the SOEC, configured with a CO_2 conversion rate of 0.05 and an H_2O conversion rate of 0.98. Ultimately, their study focused on the economic viability of co-electrolysis of CO_2 and H_2O and found that it is not yet competitive with other technologies, but with further development of SOECs it could prove to be an efficient way to produce syngas and valorize CO_2.

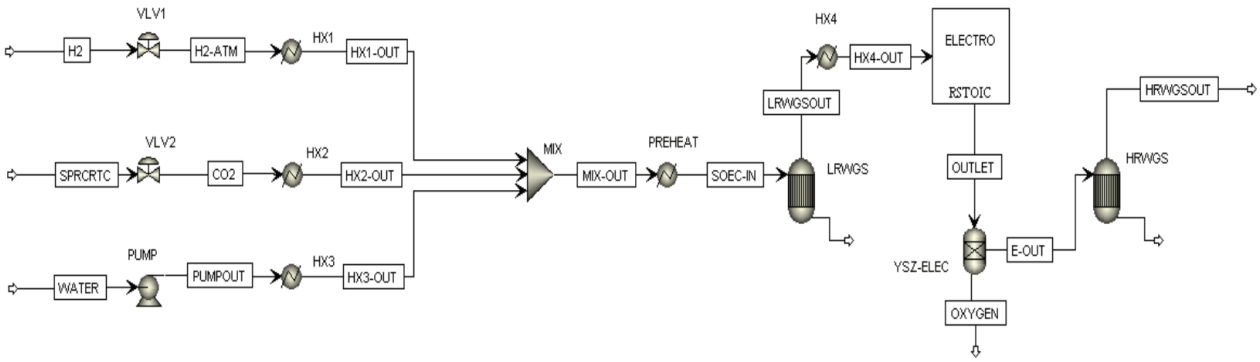

Figure 6: Syngas production flowsheet from Redissi and Bouallou (2013)

Another study conducted by Hauck, Herrmann, and Spliethoff in 2017 examined closely the behavior of a modeled R-SOC is Aspen Plus. The model presented in this study consisted of an R-SOC which contained two separate modules to represent the SOFC and SOEC modes. The work of Hauck et al. (2017) proves to be the most relevant to this work, as the SOEC flowsheet is presented and examined in detail. It is important to note that similar to Redissi and Bouallou's work in 2013, Hauck et al. (2017) focus on an SOEC running with CO_2 and H_2O, therefore it requires additional steps and reactors. As shown in Figure 7 below, the SOEC block contains a

RGibbs reactor, Mixer, RStoic, Separator, a second RGibbs reactor, a second Separator, and a recycle stream for unreacted H_2O. The study found that the performance of the R-SOC is extremely dependent on the materials used and parameters like activation energy and conductivity. From the experiments run, CO_2 was determined to have a positive effect on performance of the electrolysis step of operation. It was determined that using air instead of oxygen decreases operational voltage, yielding better performance in SOEC mode, but worse performance in SOFC mode. A higher concentration of H_2 was found to positively affect performance. Additionally, it was found that increasing temperature yields increased voltage in SOFC mode and decreased voltage in SOEC mode, leading to an overall improvement in performance (Hauck et al., 2017).

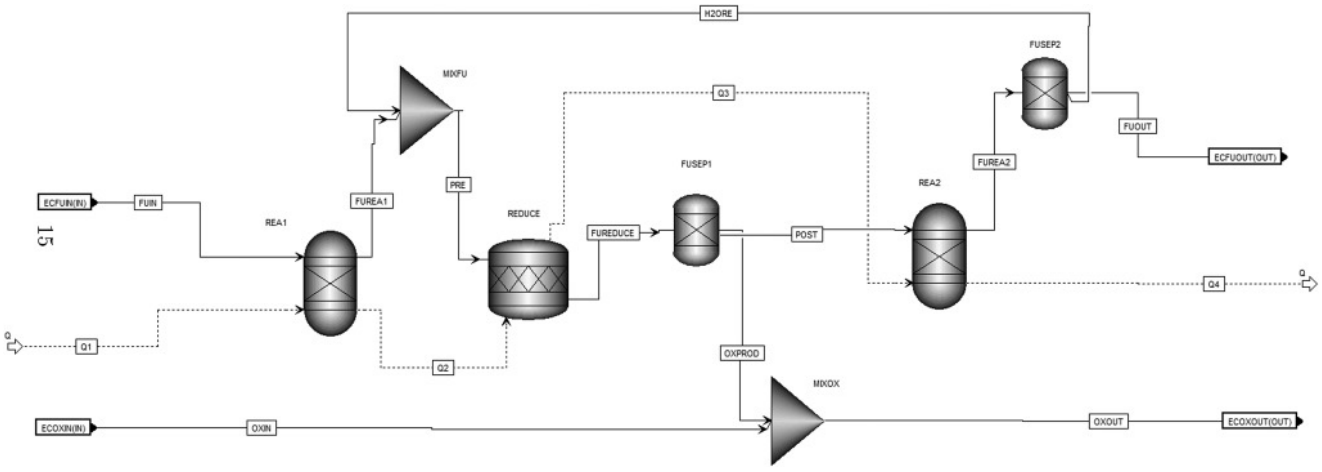

Figure 7: SOEC Block from Hauck et al. (2017)

Perhaps the most extensive study conducted to analyze R-SOC systems was conducted by Mottaghizadeh et al. in 2017. The research group constructed a complete, independent R-SOC system in Aspen Plus by thermally optimizing the plant and its components. Featured in this model are many components for heat recovery and latent heat utilization such as heat storage tanks. Similar to the studies reviewed previously, Mottaghizadeh et al. focused on both SOFC

and SOEC operation with CO_2 in the fuel stream. As shown in Figure 8 below, the flowsheet for the SOEC block in this study consists of a preliminary RGibbs reactor to simulate the RWGS of the stream containing water and carbon dioxide. Next, the equalized stream enters an RStoic reactor block where it is reacted according to stoichiometric settings, then separated by a Separator block into oxygen and fuel streams. The fuel stream is reacted in another RGibbs block before mixing with the oxygen stream and exiting the SOEC system. Ultimately, this study found that increasing operating pressure improves the efficiency of the reactor, but decreases the efficiency of the entire system.

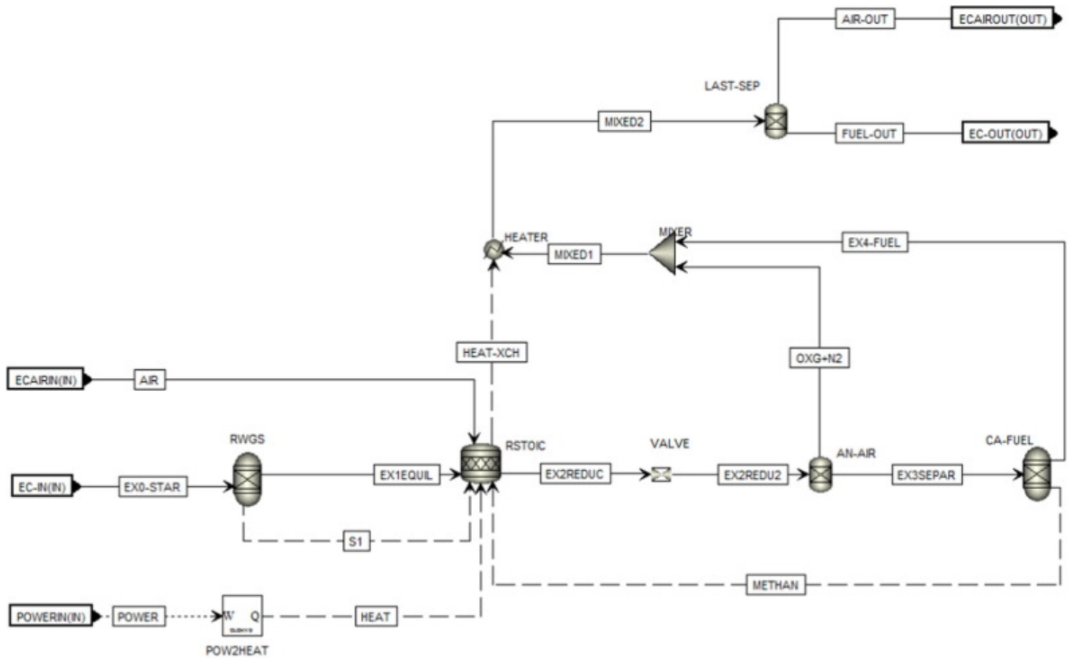

Figure 8: SOEC Block from Mottaghizadeh et al.

The studies examined above give us an idea of how to construct an SOEC block in Aspen Plus given our operating parameters. It must feature an RStoic reactor which is properly configured such that the reaction occurs according to the stoichiometry of water electrolysis. Additionally, we learn that we will need components to achieve the proper temperature and

pressure for the reaction such as Heater blocks. Additionally, we must consider incorporating a recycled stream of non-reacted water to simulate the continuous nature of the electrochemical reactions in an SOEC.

2.3.2 Software Modeling in IDAES

IDAES is primarily used to simulate transient thermal flow as well as chemical processes. A recent study done by Gentile, Vesely, Ghouse, Goyal, and Kapat in 2022 focused on modeling an air cooler to be used to cool supercritical CO_2 gas used as a working fluid in heat engines utilizing the Brayton cycle. Our solid oxide simulation isn't too different from this, as we are also using a gas (vapor form) of H_2O, which is another supercritical fluid that is similar to CO_2.

In our case, however, we'll be using IDAES to model our "Polarization Curves" for our R-SOCs. IDAES is a great program for this, as it simply utilizes Python to allow the user to code a number of parameters that need to be set for said curves. Once this is completed, the curves can then be plotted through Juniper (the Python software platform that is most notably used for IDAES), and then after that, the user can just complete this cycle until a proper number of samples are collected.

3.0 Methodology

The following chapter that will cover the main procedural methods used for the modeling of the aforementioned thermodynamic processes. Utilizing two chemical process simulation softwares IDAES (Institute of Design of Advanced Energy Systems) and Aspen Plus (of AspenTech software), relevant process parameters were both calculated and visualized. After successfully following up on and replicating the previous group's research and simulation processes, our group built on those results to test new process parameters and develop new models for comparison and to provide recommendations to SOFC researchers and future project groups on the benefits and disadvantages of each modeling package.

3.1 Software: Aspen Plus

AspenTech provides one of the leading process simulation software packages in the chemical and energy industries, and is similar in form and function to IDAES. Its primary strength lies in its ability to simulate sophisticated, rigorous chemical processes and how reactions, compounds, systems, and even electrolyte solutions react within a modeled system via complex mathematical calculations. Aspen Plus is a software within the larger AspenTech software catalog, and specializes in steady state chemical process simulation. In this type of software, the user constructs a model of the chemical process of interest, and the software determines the behavior of the various components and flows using complex mathematical models (AspenTech, n.d.).

3.1.1 Aspen Plus Advantages

Aspen Plus excels in providing the user with a straightforward interface through which they can construct chemical models containing many components and materials. Additionally, Aspen Plus provides users with powerful methods to analyze chemical processes through sensitivity and convergence analysis. The data can then be processed through Fortran code or Excel spreadsheets to create curves that determine the effects of the analyzed parameters (Ortega, n.d.). Each step in creating a chemical process model in Aspen Plus is clearly presented to users by the use of a "next" button, which sequences to the next required input for the simulation to run. Once all parameters are input by the user, the "next" button will run the simulation. However, this functionality depends on the user's expertise in constructing accurate and detailed flowsheets, a task which can be difficult for users new to Aspen Plus.

3.1.2 Aspen Plus Limitations

Aspen Plus is a steady state chemical process simulator, meaning it is incapable of modeling dynamic chemical processes without significant user input and control. Since Aspen Plus is designed for large scale chemical processes, it is limited to simulating chemical reactions through single blocks, meaning it struggles to simulate detailed steps in chemical reactions, such as the individual electron movements in the R-SOC reactions. Aspen Plus also lacks the ability to analyze the fluid dynamics or the electrical behavior of systems without the use of user defined calculator blocks.

3.2 Software: IDAES

IDAES is an up-and-coming multi-scale modeling and optimization framework currently for all development stages of advanced energy systems from materials to process, to system to market. Utilizing Python as its base language, it is capable of creating and simulating dynamic models and processing data of varying types through use of algebraic algorithms. It is also capable of automated modeling and optimizing thermodynamic, physical property and kinetic models from experimental data, which allows for the design and modeling of conceptual systems, power plants, dynamic process operations, chemical reactions, and more. IDAES can also provide reliable simulation data based on existing models from similar software for individual components as well as larger scale operations involving stacks/circuits and even entire electrical grids.

3.2.1 IDAES Advantages

As IDAES is an open-source software, it can be changed by any user according to their needs/desired application of the software. It is capable of running both steady-state and transient simulations, with similar functionality to Aspen. Preset models all consist of unit models for each individual component in the modeling system, and each unit model can be written/changed in any level of code.

3.2.2 IDAES Limitations

A disadvantage of IDAES lies in its inconvenient software installation - outdated instructions and specific installation methods meant that typical installation methods would

fulfill certain installation requirements, but not be able to initialize the simulation program. As the software is new, it does not yet have a convenient dedicated installer for multiple OS options. While it possesses some similarities to Aspen, it does not yet possess a similar graphical user interface that would aid in the visualization and optimization of simulated flows and models.

3.3 Selecting a Mathematical R-SOC Model

A number of different components and parts may be used to power an SOFC, however, many of these only help to improve the thermodynamic efficiency of the SOFC. In regards to this project, only three vital parts of the stack are required to ensure proper operation of the SOFC. This includes the electrolyte, electrodes, and any of the interconnects between the components. This is considered to be the most simple model of a Solid Oxide Fuel cell. The air flow input is led through the cathode to pass over oxygen ions to the opposite side. On the opposite side, the fuel flow input leads through the anode and retrieves the oxygen ions being transported through the movement of electrons in the electrolyte and the electric current.

3.3.1 Fuel Cell Mathematical Model

Certain assumptions about the thermodynamic models and processes involved in the simulations were necessary, so that the results were appropriate. Additionally, various operating parameters were selected from previous studies of SOFC systems. Assumptions and parameters are covered below:

- Components are perfectly thermally insulated. Material insulation properties don't allow for the heat transfer between the system and its surroundings; waste heat would lead to a less thermally efficient process, and therefore less efficient cell operation and output.

- All gasses supplied to the SOFC system are ideal gasses. In addition, partial pressures of ideal fuel gas mixtures will be considered, but not the specific individual partial pressures of other non-fuel ideal gasses present in those mixtures.
- The output of the fuel cell is pure water. All full is utilized, reacted, and forms water without excess hydrogen or oxygen remaining.
- Operating temperature is maintained throughout the thermal process.
- System is steady-state and in thermal equilibrium. State variables such as internal energy, gibbs free energy, exergy, etc. do not change over time, and there is no imbalance in thermal energy within the system.
- Current density is uniform throughout the cell. Non-uniform current density would lead to less predictable energy losses.
- The resistance of the cell stays constant, defined by the thickness and ionic conductivity of the electrolyte, and the ohmic loss term, $r_{ohmic,const}$.

Table 1: Constants for SOFC Electrochemical Model

Constant Description	Symbol	Value	Units
Universal gas constant	R	8.314	J/K mol
Faraday's constant	F	96485	C/mol
Reference pressure	P_ref	1	atm
Reference temperature	T_0	298.15	K
Moles of charge electrons transferred in reaction	n_e	2	mol
Entropy change of reaction at STP	d_s	-0.04434	kJ/K

Table 2: Parameters for SOFC Electrochemical Model

Parameters	Symbol	Value	Units	Reference
Input anolyte pressure	H2_p	0.5	atm	Chehadeh et al., 2022
Output anolyte pressure	H2O_p	0.5	atm	Chehadeh et al., 2022
Catholyte pressure	O2_p	0.21	atm	Chehadeh et al., 2022
Transfer coefficient	a	0.5	-	O'Hayre et al., 2016
SOFC Resistance	R_ohm	0.057	ohm*cm^2	Hauck et al., 2017
Limiting current density	i_L	0.65	A/cm^2	Chehadeh et al., 2022
Electrolyte thickness	thick_e	0.00125	cm	Hauck et al., 2017
Electrolyte ionic conductivity	ion_e	333.3	1/(ohm*cm)	Hauck et al., 2017
Pre-exponential factor: fuel side	gam_f	205100	A/cm^2	Ni et al., 2007
Pre-exponential factor: oxygen side	gam_o	1344000	A/cm^2	Ni et al., 2007
Activation energy: fuel side	e_f	120000	J/mol	Ni et al., 2007
Activation energy: oxygen side	e_o	100000	J/mol	Ni et al., 2007
Fuel utilization factor	fuel_u	1	-	Chehadeh et al., 2022

To create an SOFC model with these parameters, we must first calculate the Gibbs free energy change of the reaction. This is done by referencing the chemical data of the reaction, finding the change in enthalpy and the change in entropy. Putting these values into the equation below yields the Gibbs free energy change:

Equation 20: $\Delta G = -241.82 + T * 0.044423$

Next, the equation below can be used to predict the voltage thermodynamically, accounting for changes in entropy, concentration, and temperature:

Equation 21: $E_n = \frac{-\Delta G}{nF} + \frac{\Delta S}{nF}(T - T_0) - \frac{RT}{nF} ln\left(\frac{p_{H_2}\sqrt{p_{O_2}}}{p_{H_2O}}\right)$

We also must account for the various losses which occur within the cell. In this study, ohmic loss, activation loss, and concentration loss are considered. For ohmic loss, the equation below is used to approximate ΔE_{ohm}, where j is current density, δ_{el} is the thickness of the

electrolyte, σ_{el} is the ionic conductivity of the electrolyte, and $r_{ohmic,const}$ is the SOFC resistance obtained from previous studies.

Equation 22: $\Delta E_{ohm} = j * \left(\frac{\delta_{el}}{\sigma_{el}} + r_{ohmic,const}\right)$

In order to calculate the concentration losses, the constant *c* must be calculated, where α is the transfer coefficient:

Equation 23: $c = \left(\frac{RT}{nF}\right)\left(1 + \frac{1}{\alpha}\right)$

Next, the concentration losses can be calculated using the equation below where j_L is limiting current density (O'Hayre et al., 2016):

Equation 24: $\Delta E_{conc} = c * ln\left(\frac{j_L}{j_L - j}\right)$

The activation loss is found by using Equation 13 and Equation 14 from Section 2.2.4. Finally, all of the losses, ΔE_{ohm}, ΔE_{act}, and ΔE_{conc} can be subtracted from the thermodynamically predicted voltage in order to complete the SOFC model. This equation can be used to analyze the system in various states with different temperatures, pressure, fuel concentrations, and current densities:

Equation 25: $E_{cell} = E_n - \Delta E_{act} - \Delta E_{ohm} - \Delta E_{conc}$

To calculate the voltage efficiency of the fuel cell, the cell voltage is divided by the Nernst voltage. This can be multiplied by one hundred to obtain a percent value. Efficiency can also be measured in terms of hydrogen production efficiency, but voltage efficiency was favored for this study as heat generation and consumption was not thoroughly considered for our model (Menon et al., 2013):

Equation 26: $\eta_{vol} = \frac{E_{cell}}{E_n}$

3.3.2 Electrolyzer Cell Mathematical Model

As covered in the section above, a mathematical model was constructed based on existing literature to simulate the electrochemical behavior of an SOFC in various operating conditions. By using similar parameters to the SOFC model, and combining modeling equations from various sources, we were able to construct a corresponding SOEC electrochemical model. The constants used for this model are shown in Table 1, and the parameters are shown in Table 2. The assumptions for this model are as follows:

- System is isothermal, and all components are thermally insulated
- The fuel supplied to the SOEC system is an ideal gas after heating
- All the gasses supplied to the SOEC system are pure. An oxygen partial pressure of 0.21 is utilized to simulate oxygen within air, but no other gasses from air are considered.
- The steam utilization factor is 0.6
- Cell structure is planar
- Current density is uniform throughout the cell
- Operating temperature is constant through each individual simulation
- System is steady-state and in thermal equilibrium
- The resistance of the cell stays constant, defined by the thickness and ionic conductivity of the electrolyte, and the ohmic loss term, $r_{ohmic,const}$.

Table 3: Constants for SOEC Electrochemical Model

Constant Description	Symbol	Value	Units
Universal gas constant	R	8.314	J/K mol
Faraday's constant	F	96485	C/mol
Reference pressure	P_ref	1	atm
Reference temperature	T_0	298.15	K
Moles of charge electrons	n_e	2	mol

transferred in reaction			
Entropy change of reaction at STP	d_s	0.04434	kJ/K

Table 4: Parameters for SOEC Electrochemical Model

Parameters	**Symbol**	**Value**	**Units**	**Reference**
Input anolyte pressure	H2_p	0.5	atm	Chehadeh et al., 2022
Output anolyte pressure	H2O_p	0.5	atm	Chehadeh et al., 2022
Catholyte pressure	O2_p	0.21	atm	Chehadeh et al., 2022
Transfer coefficient	a	0.5	-	O'Hayre et al., 2016
SOEC Resistance	R_ohm	0.057	ohm*cm^2	Hauck et al., 2017
Limiting current density	i_L	0.65	A/cm^2	Chehadeh et al., 2022
Electrolyte thickness	thick_e	0.00125	cm	Hauck et al., 2017
Electrolyte ionic conductivity	ion_e	333.3	1/(ohm*cm)	Hauck et al., 2017
Pre-exponential factor: fuel side	gam_f	205100	A/cm^2	Ni et al., 2007
Pre-exponential factor: oxygen side	gam_o	1344000	A/cm^2	Ni et al., 2007
Activation energy: fuel side	e_f	120000	J/mol	Ni et al., 2007
Activation energy: oxygen side	e_o	100000	J/mol	Ni et al., 2007
Steam utilization factor	steam_u	0.6	-	AlZahrani & Dincer, 2017

The SOEC model was constructed by utilizing the same general set of equations as the SOFC model with some adjustments. The most notable difference is that voltage losses are added to the thermodynamically predicted voltage, as shown in Equation 7**.** In order to properly calculate the Gibbs free energy change for various temperatures, according to Equation 4, we need the temperature and the entropy and enthalpy changes of the reaction. These are obtained from chemical reference literature, and the equation below is constructed to find Gibbs free energy change (Atkins et al., 2018):

Equation 28: $\Delta G = 241.82 - T * 0.044423$

Using the Gibbs free energy change, we can calculate a voltage at various temperatures. However, temperature also affects entropy. Additionally, pressure and concentration affect the

operating voltage. Equation 13 yields energy in kJ, so a unit conversion to J is needed in Equation 14, but it is left out for clarity. Therefore, the equation below is used to calculate the thermodynamically predicted voltage (O'Hayre et al., 2016):

Equation 29: $$E_n = \frac{\Delta G}{nF} - \frac{\Delta S}{nF}(T - T_0) - \frac{RT}{nF} ln\left(\frac{p_{H_2}\sqrt{p_{O_2}}}{p_{H_2O}}\right)$$

Next, the model calculates the various losses associated with SOEC operation. First, the activation losses were calculated using models found in existing literature on SOEC models. There are multiple ways to approximate activation loss, but the equations used in this study are used as they allow for a more accurate comparison to other studies. These activation loss models are used in R-SOC and SOEC studies by Alzahrani & Dincer (2017), Hauck et al. (2017), and Wang et al. (2019) among others. The model uses Equation 13 and Equation 14 which can be found in Section 2.2.4. Concentration loss is calculated in the same manner as the SOFC model, using Equation 23 and Equation 24 above.

The ohmic losses were modeled using the same equation as the SOFC ohmic losses; we maintain the same assumptions as well for consistency between models (Hauck et al., 2017):

Equation 30: $$\Delta E_{ohm} = j * \left(\frac{\delta_{el}}{\sigma_{el}} + r_{ohmic,const}\right)$$

The losses covered above were added to the Nernst voltage calculated in Equation 14, as this is an SOEC model and losses correspond to an increase in operating voltage. Finally, the voltage was calculated in this way for various current densities up to the limiting current density of 0.65 A/cm^2. Using this mathematical model for the electrochemical behavior of the SOEC, we are able to produce polarization curves for the cell under operating conditions defined by the parameters in Tables 3 and 4. These mathematical models give us a good approximation of the behavior of an SOEC. The SOFC and SOEC models can be combined to construct a polarization

curve for the R-SOC system on a single cell level. We can also calculate the cell voltage efficiency by using Equation 19. Additionally, they can be used as a framework to process the data output from the Aspen Plus simulations. Values like Gibbs free energy change can be determined by the software models at various temperatures, and input into the mathematical models to form simulation specific polarization curves.

3.4 Aspen Plus Simulation Setup

This section covers the setup steps for the Aspen Plus fuel cell model and the electrolysis cell model. For groups looking to replicate the work of this study, the information below should contain the necessary steps and parameters.

3.4.1 Aspen Plus Fuel Cell Model

The Aspen Plus SOFC model was recreated using information from the previous iteration of this project. To begin constructing the model in Aspen Plus, the simulation settings were configured in the Specifications tab under the Setup menu when in Simulation mode. The simulation settings selected for the fuel cell model are shown in Figure 27 (See Appendix A).

Next, components were added. For this model there are only three components: diatomic hydrogen, diatomic oxygen, and water. This was done under the Specifications tab in the Components menu seen in Figure 28 (See Appendix A).

Once the components were added, the main flowsheet was constructed by adding the necessary material flows and blocks. HEATER1, HEATER2, HX-CAT-1, and HX-CAT-2 are all heater blocks. SOFC-AN is an RGibbs reactor, and SOFC-CAT is a Separator. These blocks are connected by material streams as shown below:

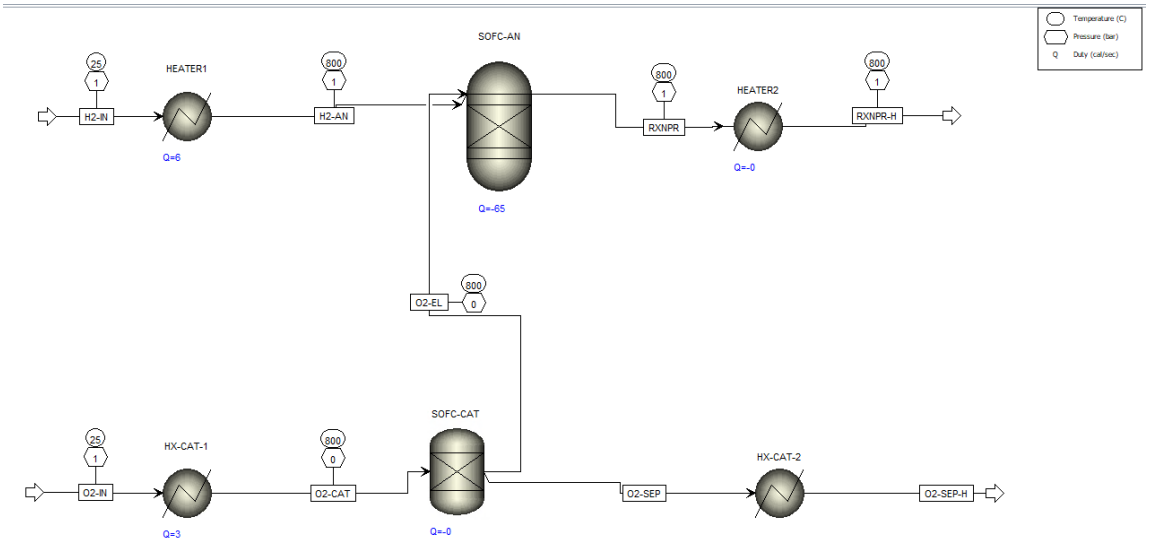

Figure 9: Components in SOFC model

In order for the simulation to run properly, operating conditions must be specified for the input streams. For the streams H2-IN and O2-IN, a mole flow of 0.03275 mol/min and 0.016375 mol/min were chosen respectively and a temperature of 298.15 K was chosen to reflect standard conditions. For H2-IN, a pressure of 1 atm was selected, and for O2-IN, a pressure of 0.21 atm was chosen to reflect the partial pressure of O_2 within air.

Next, the settings for each block must be specified. First, the heaters are used to bring the gas from ambient temperature to the selected operating temperature and pressure of the cell. In the flowsheet above, HEATER1 is set to bring the H2-IN stream to 1073 K and 0.5 atm. Similarly, HX-CAT-1 is configured to bring the O2-IN stream to 1073 K and 0.21 atm. A separator, SOFC-CAT is included for simulating fuels that must be purified such as air or methane. In this simulation, pure oxygen is used so no separation occurs. The output of the separator is configured to allow pure O_2 to flow to the Gibbs reactor, SOFC-AN. The settings for the Gibbs reactor are shown in Figure 30, and under the Products tab it is set to consider all components as products.

The output pressure and temperature for water is specified in HEATER2 at 1073 K and 1 atm. The simulation can now be run in order to obtain chemical results for the reaction that takes place in an SOFC by advancing with the Next button. The results can be seen in the Results tab.

3.4.2 Aspen Plus Electrolyzer Cell Model

The Aspen Plus electrolyzer cell model was adapted from a previous study done in 2017 by Hauck, Hermann, and Spliethoff. In this study, researchers developed a comprehensive R-SOC model in Aspen Plus with modes of operation corresponding to SOFC and SOEC modes. Their SOEC module included components not needed for this study, as their work focused on running the SOEC with CO_2 to the water feed flow in electrolysis mode.

The SOEC model in Aspen Plus was constructed using the same workflow as the SOFC model. First, the simulation settings were selected to initialize the flowsheet and simulation. Next, all of the necessary components were added: water, diatomic hydrogen, and diatomic oxygen. The steps remain the same as with the fuel cell model.

After the necessary components were added, the flowsheet was constructed. As shown in the figure below, the flowsheet consists of a mixer, heater, RStoic reactor, two separators, and a condenser (a HEATER block).

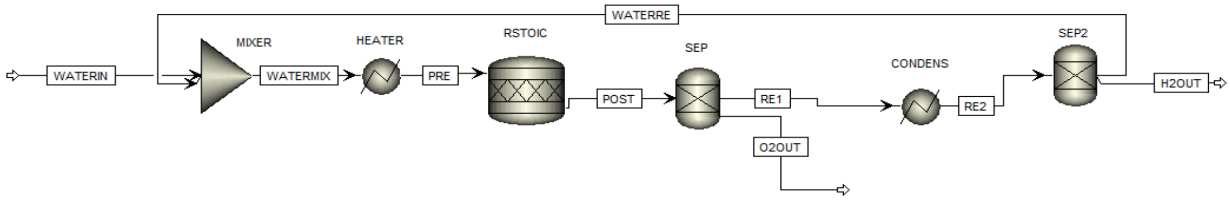

Figure 10: SOEC Flowsheet

As with the SOFC model, operating conditions must be given to the necessary number of material flows in order for the simulation to run. In this case, the only material flow which

requires input is WATERIN, which is set to 298.15 K, 1 atm, and a flow of 0.03275 mol/min. After specifying the operating conditions for the materials, the behavior of each block in the flowsheet must be defined. For the RSTOIC reactor, the temperature and pressure was set to 1073 K and 1 atm and the reaction shown below was added to the Reactions tab; a screenshot, Figure 32, can be found in Appendix A.

The HEATER in the flowsheet was set to a temperature of 1073 K and 1 atm. The first separator, SEP, is set to separate all of the oxygen gas from the POST stream. RE1 continues to the condenser CONDENS where a temperature of 298.15 K and pressure of 1 atm was selected. After the RE1 stream, containing hydrogen and water, is condensed, SEP2 is able to separate the remaining unreacted water and recycle it in stream WATERRE back to the mixer. After this setup process, the simulation can be run at various operating temperatures and pressures.

3.5 IDAES Simulation Setup

IDAES installation involves the use of a user's command console on their personal computer, Anaconda installer (compatible with Python) as well as Github to download the most up-to-date version of IDAES. As stated in the "advanced user installation instructions" on the IDAES official website, before beginning installation, users will have to create a Github account and Git application for desktop must be installed, with which an additional repository must be forked via Github so that the platform is properly installed. Installation of Miniconda3 (part of Anaconda) is necessary to install all of the relevant Python packages and to initiate the program. After Miniconda3 is installed, the IDAES package needs to be installed via the Miniconda3 terminal prompt. In the Miniconda3 terminal, the fork needs to be cloned using a set of commands, and an upstream remote must be added. After the fork is cloned, the Python

environment for IDAES must be created in the terminal prompt, and the IDAES requirements and extensions can be installed. Once IDAES has been properly installed and the IDAES Python environment has been created, programs and models can be first test-run for errors in the conda prompt. Finally, following official IDAES "getting started" instructions (on Github, not the IDAES website), the software can be initiated via Jupyter, where tutorials and example simulations can be run before creating custom projects (Note: It is crucial that the Conda prompt remain open during any Jupyter operations, as it is used to initialize and monitor IDAES behavior. If the prompt is closed before Jupyter, the notebook will lose connection to any python operations it is using from your computer and cease to function).

As IDAES does not possess an integrated graphical interface like Aspen, there is no visual fuel cell model or existing individual component framework to visualize the SOEC process, so all results were generated from mathematical models only. All constants and input parameters were defined first (Universal Gas Constant (R), Faraday Constant (F), Reference Pressure (P_ref), Limiting Current Density + Correction Factor (i_L and a), Transfer Coefficient (B), pre-exponential factors and activation energies for the Anode and Cathode (gam_a, gam_c, e_a, e_c), cell operating temperature (1073 K, variable), fuel utilization fraction (assumed to be 100%, so 1), input and output anolyte pressure (H2_p and H2O_p, assumed to be 0.5 for pure anolyte, and 0.5 again as it is assumed that all anolyte it utilized to form H2O) catholyte pressure (O2_p, assumed to be 0.21 as air is approximately 21% oxygen), and cell surface area resistance (R_ohm, assumed to be 0.5 ohm cm^2) and categorized in a table. The Nernst Term (cell potential) was calculated first, followed by Gibbs Energy Change, and then Open Circuit Voltage, Actual Current Density, all three loss calculations (Activation, Concentration, Ohmic), Cathode Exchange current density, actual voltage, rate of current and total power produced. To

generate the polarization curves, the current density and actual voltage produced are needed. The current density in code is constructed simply of a numeral array from zero (or some value close to zero, depending on the range you want to view) to the calculated maximum current density, split into intervals of the user's choice (ex. i_act = np.arange(0.0, 0.65, 0.01) is a code formula for current density, constructing an array using the numpy module that contains values from 0 to 0.65 in intervals of 0.01). The actual voltage produced is a multi-variable formula, that includes the open circuit voltage and all the relevant loss values, all of which must be calculated beforehand prior to be called upon in the actual voltage formula. All formulas for those variables are formatted in code as they were provided in our reference. The formula for open circuit voltage is E_rev = ((Gibb/(2*F)) + nernst term)*-1, and the formulas for all process losses are as follows:

Activation loss:

```
i_0a = gam_a + ((H2_p/P_ref)*(H2O_p/P_ref)*np.exp(e_a/(R*T)))
```

Ohmic Loss:

```
E_ohm = i_act*R_ohm
```

Concentration Loss (Note: Limiting current density is calculated first):

```
i_Ladj = i_L*((H2_p/P_ref)**a)
E_conc = ((R*T)/(2*F))*np.log(1-(i_act/i_Ladj))
```

Once all of those variables are calculated, the final formula for actual voltage produced ($E_{act} = E_{rev} - E_{ohm} + E_{conc} + E_{activ}$) can be run. Note, for SOEC mode, the addition and subtraction of values in the actual voltage formula are switched.

4.0 Results

There are three primary sets of results, each using a different methodology. First, there are results from the mathematical models as covered in Section 4.1 for the fuel cell and electrolysis cell, with no input from software. Next, there are thermodynamic results taken from the Aspen Plus simulations and input into the mathematical models, the results of which are covered in Section 4.2. Finally, IDAES is used to run a Python script which generates polarization curves for each mode of the R-SOC based on another set of mathematical models. The IDAES results are presented in Section 4.3. The differences in results between each methodology are covered in the Discussion Section 5.4.

4.1 Mathematical Models

The multiple forms of electrochemical loss were isolated and analyzed to assess the effectiveness of our loss models. The electrochemical losses were calculated using the same methods for both the SOFC and SOEC. These losses can be isolated graphically at a set temperature (in this case 1273 K) to depict the different behavior of each modeling equation with a variation in current density. The equations used in the order of the graphs shown below were Equation 22, Equation 24, and Equation 13. The results show that ohmic and activation losses are both linearly approximated within this range, and both increase with current density. Activation loss is displayed on a log scale for current density. For ohmic losses given by Equation 22, this linear relationship is defined by the current density multiplied by a constant resistance term, often called Area Specific Resistance (ASR). For our model, we assume that the ASR is constant, thus the linear relationship will not change with temperature. For the activation loss, calculated by Equation 22, the graph below is the region of an inverse hyperbolic sine

approximation of activation loss. The concentration losses calculated by Equation 13 behave differently, and increase at an increasing rate as the current density approaches the limiting current density, a result of the logarithmic term within the equation. This can be seen in the polarization curves in Figure 12 as either a sharp drop off in voltage for the SOFC mode, or a sharp increase for the SOEC mode.

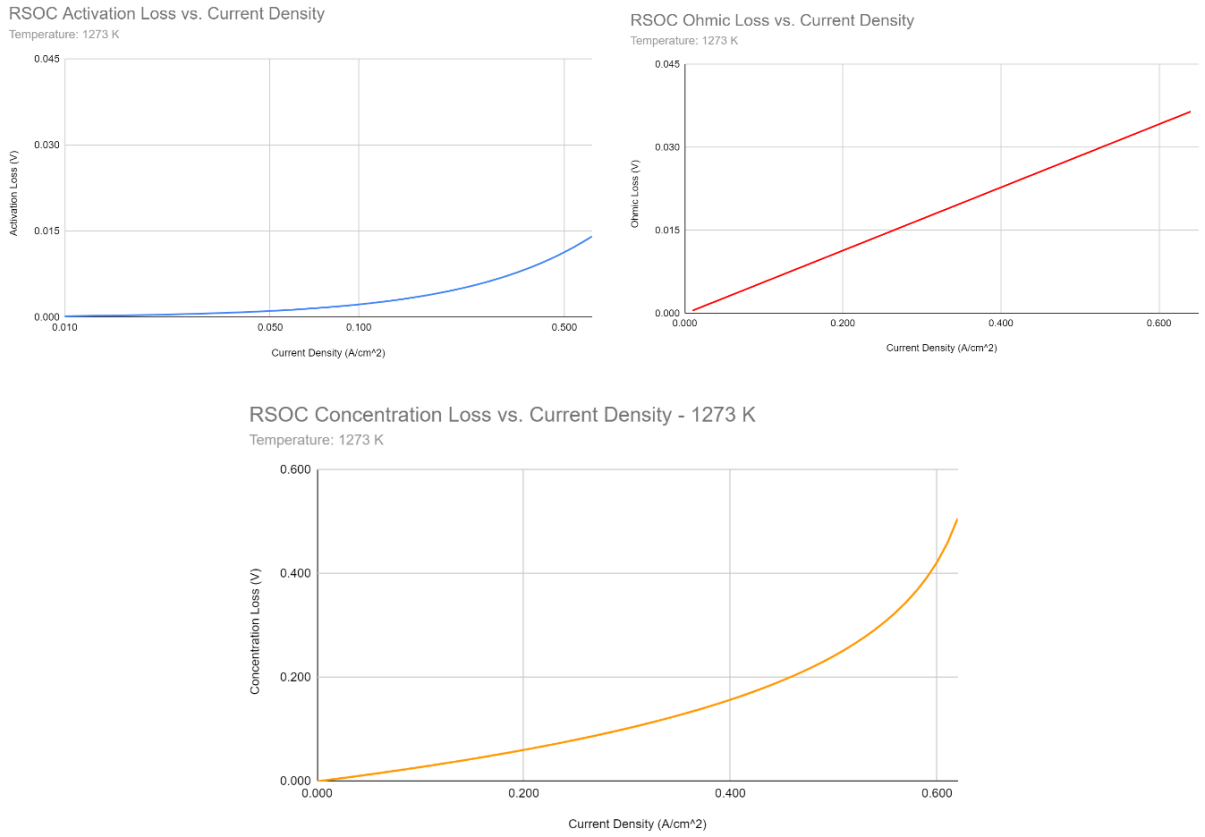

Figure 11: Activation Loss, Ohmic Loss, and Concentration Loss Respectively vs. Current Density at 1273 K

The mathematical models were used to manually generate a set of polarization curves for three different temperatures, 1073 K, 1173 K, and 1273 K. These results rely strictly on the equations covered in Section 3.3, and prove to be a simple, software-free way to simulate the SOFC and SOEC. Because the equations used to calculate ΔG in the mathematical model is the

same for both the SOFC and SOEC mode, the graphs can be combined to form an R-SOC polarization curve which is continuous between modes, as shown in Figure 12. In this graph, positive current density values represent SOFC mode, and negative current densities represent SOEC mode.

In addition to the polarization curves in Figure 12, voltage efficiency curves were generated for each operating condition that was examined using the mathematical model and Equations 26 and 19 for the SOFC and SOEC respectively. The efficiency results show a similar relationship to current density that the voltage results showed. The operating voltage of the cell decreases with increasing current density, as does efficiency as shown in Figure 13. The effect of temperature on the efficiency of the cell is small based on the modeling equations we used. Each temperature at which the fuel cell model was run exhibits a different relationship with current density. At 1073 K the efficiency remains mostly linear through the mid-range current density values, while being slightly less efficient than higher temperatures. At very high current densities however, running the cell at 1073 K can be more efficient than at 1173 K according to our results. Running the simulation at 1273 K yields slightly better efficiencies than 1073 K at mid-range current densities, and a temperature of 1173 K seems to be most efficient at all current densities.

The SOEC voltage efficiency graph generated as shown in Figure 14 suggests that with our model there is not a strong relationship with voltage efficiency and operating temperature. As with the SOFC model, the efficiency results suggest that operating the cell at 1173 K yields the highest voltage efficiency. Current density however, seems to affect the voltage efficiency much less with the SOEC than with the SOFC. At lower current densities, the operating voltage of the cell is much closer to the thermodynamically predicted voltage. As the cell approaches the

limiting current density, the voltage efficiency decreases, but not nearly as much as the voltage efficiency of the SOFC does.

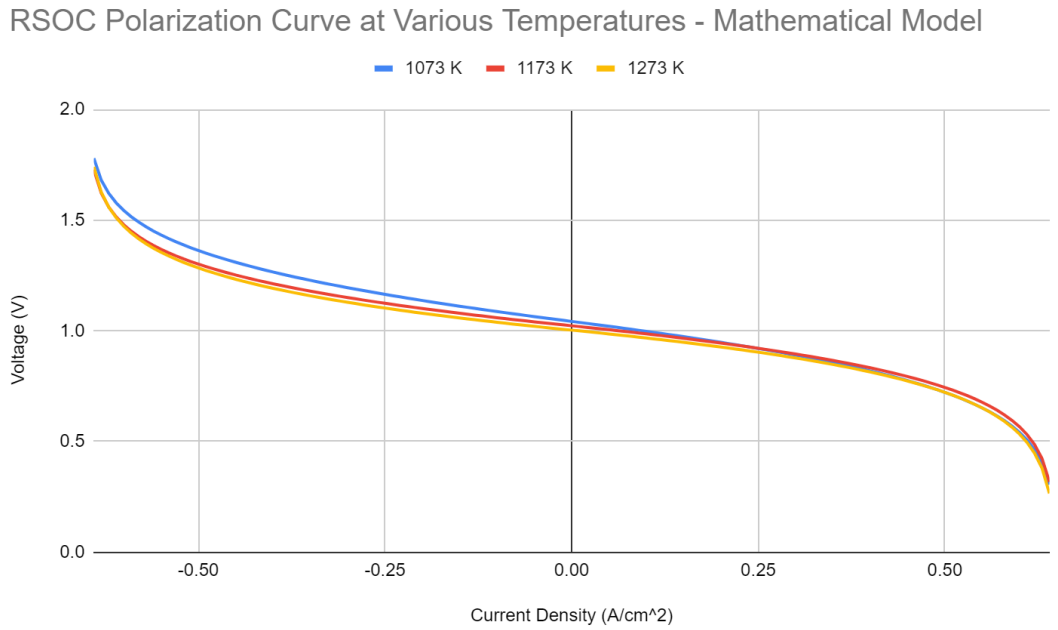

Figure 12: R-SOC Polarization Curve at Various Temperatures - Mathematical Model

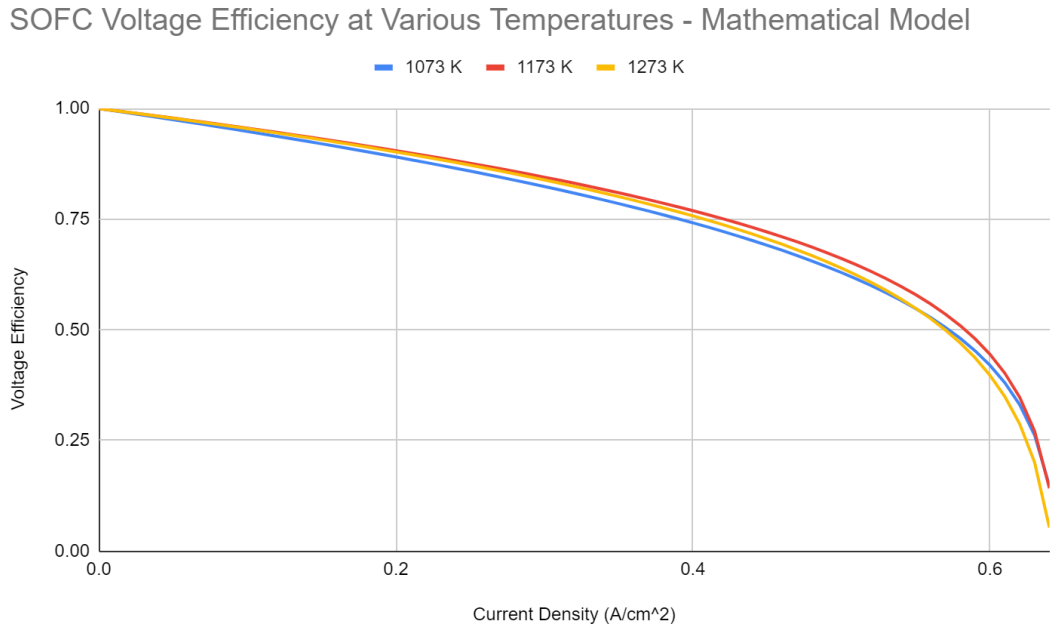

Figure 13: SOFC Voltage Efficiency - Mathematical Model

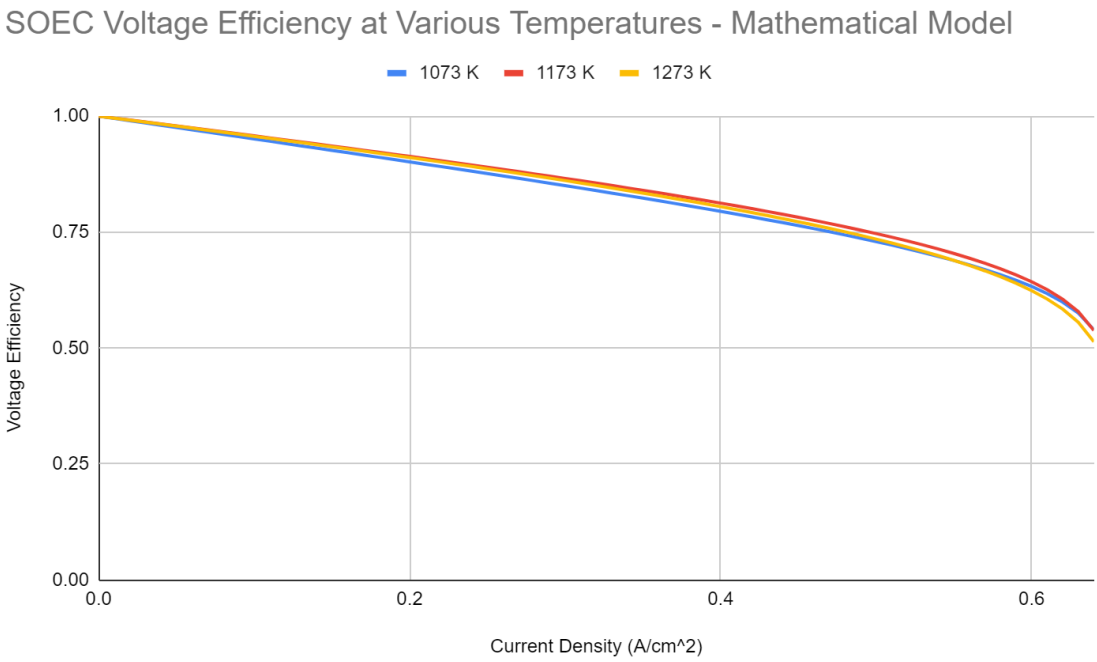

Figure 14: SOEC Voltage Efficiency - Mathematical Model

The results from the mathematical model polarization curves also suggest that changing partial pressures can have a significant effect on performance. The polarization curves shown below were generated at a constant temperature to analyze the effects of partial gas pressures. As shown in Figure 15, in SOFC mode voltage increases when H_2O partial pressure is increased relative to H_2 partial pressure. Similarly, we can see by looking at Equation 21 that higher voltage is also achieved if O_2 partial pressure is decreased. For SOEC mode, a lower voltage is achieved with an increase in H_2 partial pressure relative to H_2O partial pressure. Equation 29 also shows that voltage will decrease with an increase in O_2 partial pressure.

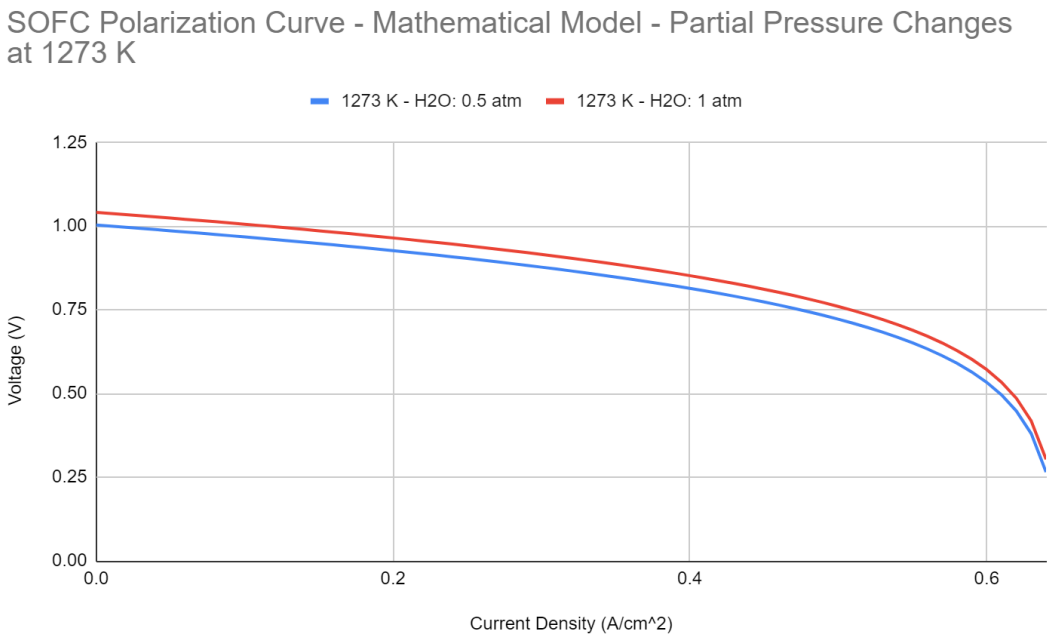

Figure 15: SOFC Polarization Curve - Mathematical Model - Partial Pressure Changes at 1273K

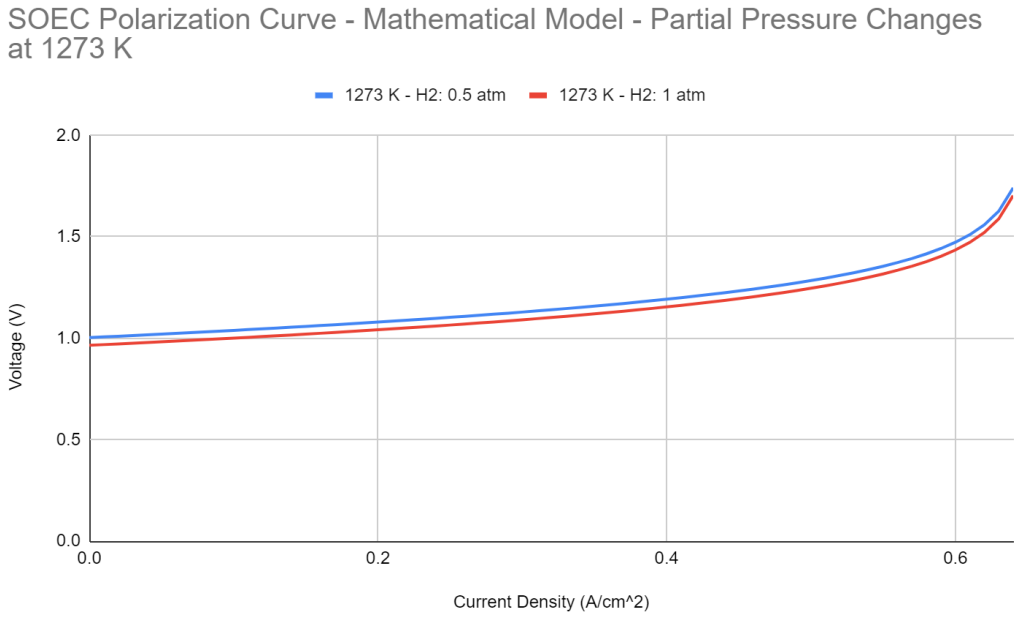

Figure 16: SOEC Polarization Curve - Mathematical Model - Partial Pressure Changes at 1273K

4.2 Results of the Aspen Simulations

4.2.1 Fuel Cell Simulation Results - Aspen Plus

The fuel cell simulation was run successfully in Aspen Plus, yielding the results tables seen in Appendix B. Each table shown corresponds to different temperatures at which the simulation was run. In these tables, the columns denote specific material flows within the model and the rows contain thermodynamic and chemical information. Notably, in the RXNPR column, we see that the mole fraction of the material flow is a majority H_2O, meaning fuel utilization in this simulation is high. If one were to adjust the ratio of mole flow of hydrogen to mole flow of oxygen, the mole fraction of H_2O in the RXNPR column would change accordingly. This simulation was run to mimic stoichiometric operation of an SOFC, in which the fuel and air flow rates are balanced to match the stoichiometry of the chemical reaction which takes place in the fuel cell.

The Gibbs energy is the most notable result from these simulations, specifically the change in Gibbs energy. The material flow before the reaction step in the simulation is O2-EL, meaning the Gibbs energy for this flow is before chemical reaction. Similarly, the RXNPR material flow is after the fuel cell reaction. Therefore, the change in Gibbs energy can be calculated. At 1073 K, 1173 K, and 1273 K, the change in Gibbs energy from the simulation was calculated to be -165.3 kJ/mol, -156.3 kJ/mol and -147.1 kJ/mol respectively. These values were input into the mathematical models covered in Section 3.3.1, using the parameters given in Table 2 to generate simulation specific polarization curves, such as the curve below. It is important to note that the mathematical models for the electrochemical losses are not changed by inputting Gibbs free energy change from Aspen Plus. The parameter that is adjusted by inputting Aspen

Plus data is the thermodynamically predicted voltage found with Equations 21 and 29 for the SOFC and SOEC respectively.

Our polarization curve in Figure 12 from Aspen Plus results show that higher temperature yields a higher voltage, with the exception of very high current densities in which a temperature of 1173K may yield higher voltage than 1273K. The voltage values from the Aspen Plus polarization curve are significantly lower than expected. Generally, at close to zero current density, the voltage should remain quite high at around 1.0 V. In the Aspen Plus SOFC curve however, the voltage at low current densities is closer to 0.80 V. The behavior of the curve in terms of the loss equations is correct, but we expected the voltage to be higher.

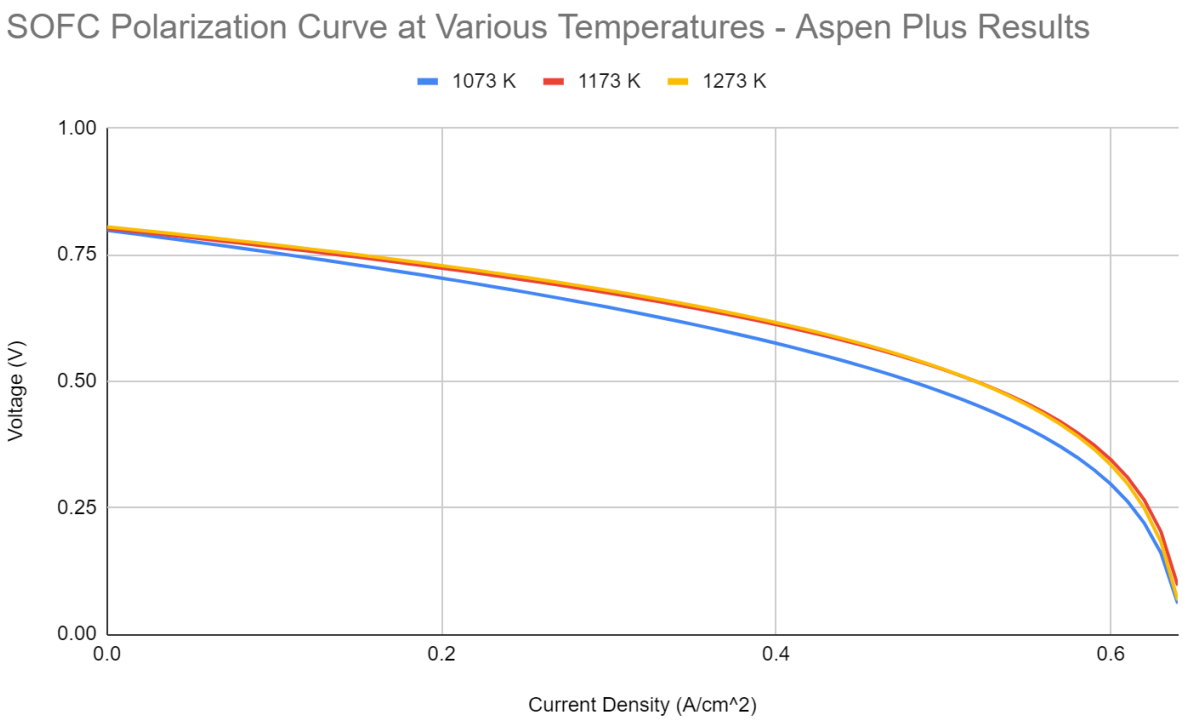

Figure 17: Fuel Cell Polarization Curve Generated from Aspen Plus Results - Varying Temperatures

4.2.2 Electrolysis Cell Simulation Results - Aspen Plus

The electrolysis cell in Aspen Plus, set up using the parameters and settings described in Section 3.4.2, was run to obtain the results table cataloged in Appendix C. The results table showed that the POST material stream exiting the RStoic reactor had mole fractions for H_2O, H_2 and O_2 of 0.31, 0.46, and 0.23 respectively. Therefore, after the RStoic reactor, only a molar fraction of about 0.69 of H_2O underwent the electrolysis reaction. Additionally, the recycled water stream worked as expected. The mixture of water and hydrogen was successfully condensed and separated in order to simulate the continuous nature of the reactions.

From the results tables at each operating condition, the Gibbs free energy was obtained for the material flows before and after the reaction. The change in Gibbs free energy could then be calculated. Next, the Gibbs free energy change could be input into the mathematical models covered in Section 3.3.2 and used to generate the polarization curves shown in Figure 14.

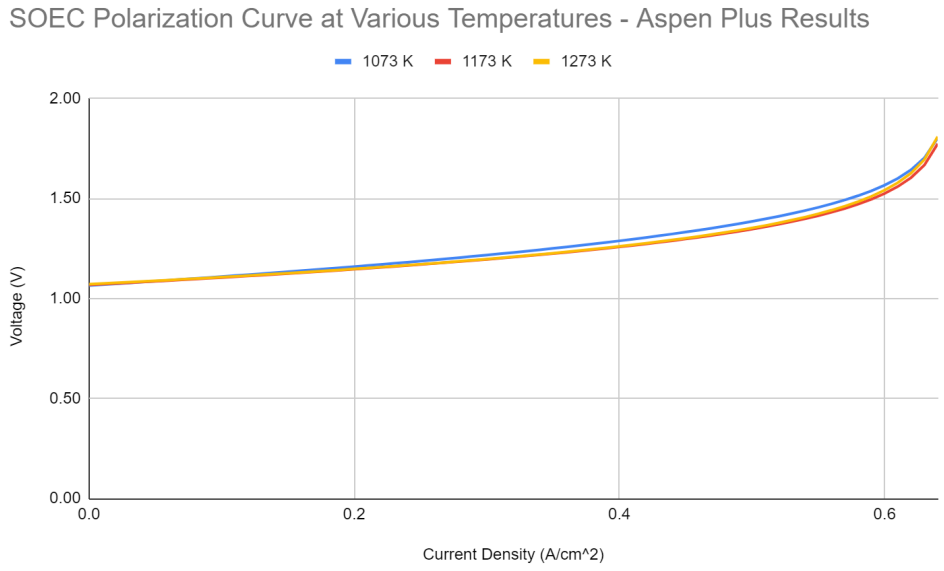

Figure 18: Electrolysis Cell Polarization Curve Generated from Aspen Plus Results - Varying Temperatures

The polarization curves in Figure 18 show that as temperature increases, the operating voltage of the SOEC generally decreases. These changes in voltage are not as large as the Aspen Plus SOFC or the SOEC mathematical model. Additionally, a relationship with current density shows that approaching the limiting current density of the cell significantly increases the operating voltage. The graph appears to have two clear zones, a linear zone from low current densities to around 0.5 A/cm^2 and a curved profile at higher current densities. The linear zone represents ohmic and activation losses, and the steeper region of the graph is due to the concentration losses. The voltages for the Aspen Plus SOEC are closer to the expected value of 1.0 V as shown by the mathematical models.

4.3 Results of the IDAES Simulations

4.3.1 Fuel Cell Results - IDAES

The IDAES full simulations were also used to produced polarization curves in both SOEC and SOFC mode at the same temperature thresholds (1073K, 1173K, and 1273K) as the Aspen simulations, and to determine how varying temperatures affected the overall efficiency of the cell (see Section 5 Discussion for more information). These trends were calculated along with invidivial energy loss values, theoretical, reduced, and actual voltages, and rate of current and power produced, all in separate lists (see Appendix 10.4 and 10.5 for SOFC and SOEC simulation results, respectively).

As shown in figure below, results for the SOFC polarization curves varied only somewhat significantly with temperature change, with the trends being: the higher the temperature, the lower the initial voltage and final voltage output of the cell & the higher the temperature, the higher the overall efficiency of the cell. However, although these results agree with our Aspen

simulation results, they were converse from the previous year's results (see our discussion chapter for a further analysis of this).

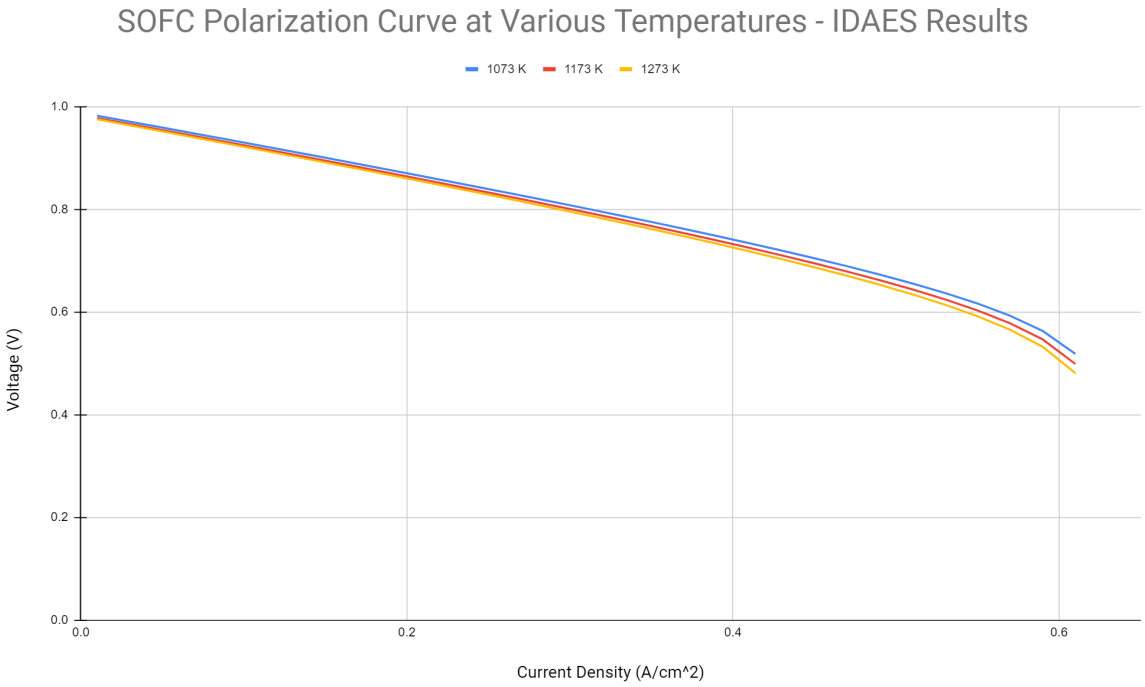

Figure 19: Combined Fuel Cell Polarization Curves

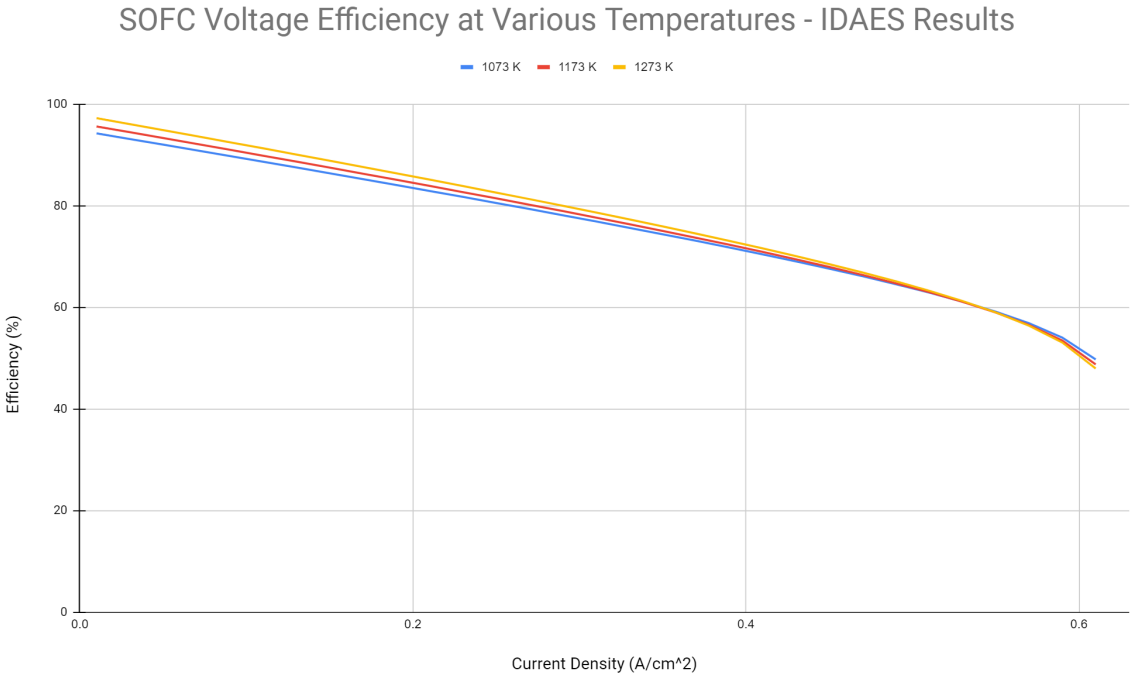

Figure 20: Combined Fuel Cell Voltage Efficiencies

An important aspect that does match up with both our Aspen Plus simulations, our IDAES simulations, and the previous year's simulations is that all sections of loss are agreeable in the way that they are orientated. Like with our Aspen simulations, the activation and ohmic losses appear to trend linearly and negatively. However, once concentration losses go beyond current densities of around 0.5 A/cm^2, the results of the simulation begin to differ.

As stated in a couple of paragraphs prior, and as seen by the figure above, the efficiency of the cell directly correlates with its temperature, as when the operating temperature of the cell rises, the efficiency of the cell rises as well. Another important thing of note though is that once current density becomes to increase, not only does efficiency begin to drop, but once current density becomes high enough, the relation between efficiency and temperature becomes inverted. Therefore, when current density is approximately higher than .5, cell efficiency at higher temperatures begin to intersect and decrease beyond the cell efficiencies at lower temperatures.

4.3.2 Electrolysis Cell Results - IDAES

Unlike the Aspen SOEC simulations, change in Gibbs free energy for each run was changed by modifying operating temperature, not obtained from preoperative and postoperative material flows. The polarization curves in Figure 21 show again that as operating temperature increases, the overall trend in operating voltage decreases, and that as current density approaches its limit the operating voltage increases sharply. The behavior remains mostly linear until voltage spikes (curving upwards) as limiting current density is achieved.

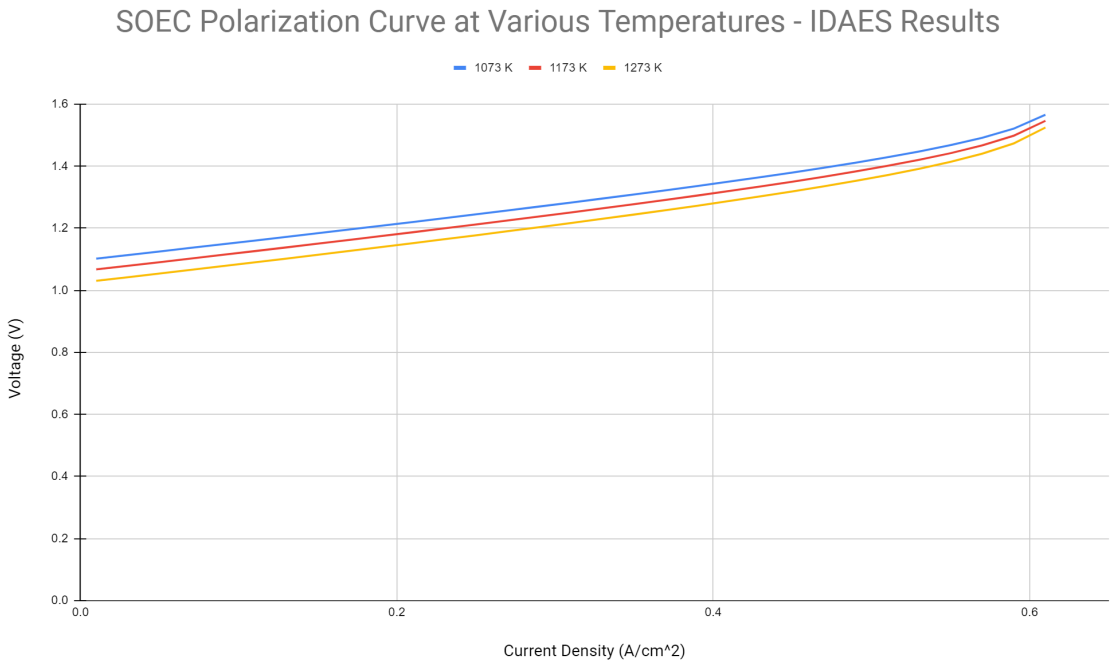

Figure 21: Combined Electrolyzer Cell Polarization Curves

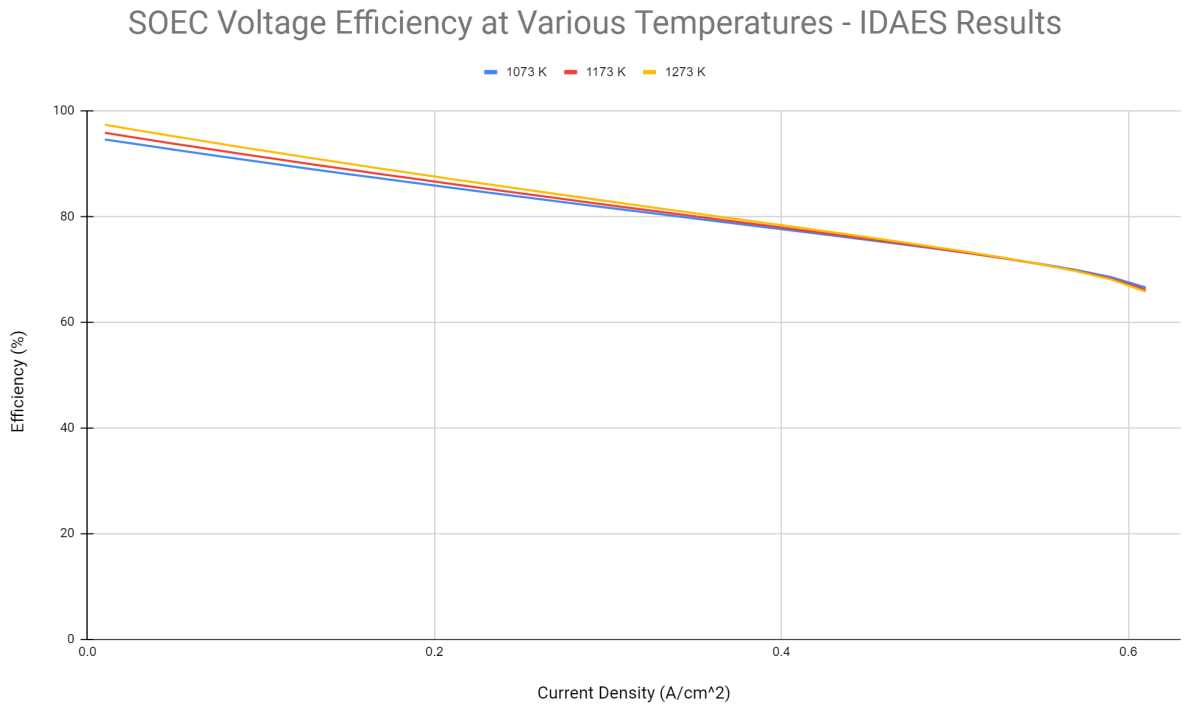

Figure 22: Combined Electrolyzer Cell Voltage Efficiencies

As with the Aspen simulations, the SOEC voltage efficiency graph in Figure 22 suggests that voltage efficiency is only moderately influenced by cell operating temperature. Just like the SOFC model, the efficiency results suggest that operating the cell at 1173 K yields the highest voltage efficiency. Current density however, seems to significantly affect the voltage efficiency. At lower current densities, the operating voltage of the cell is much closer to the thermodynamically predicted voltage. As the cell approaches the limiting current density, the efficiency decreases significantly.

5.0 Discussion

5.1 Analysis of Mathematical Model

The mathematical models used for this research were adapted from O'Hayre et al. (2016), Hauck et al. (2017), Menon et al. (2013), and Jørgensen & Fath (2008). The different methods from each of these sources were utilized to collectively build simple yet comprehensive SOFC and SOEC models. Based on these models we have found that they may overestimate electrochemical losses in SOFC mode, leading to a relationship with temperature that is more limited than expected. There is little change in voltage within the temperature range of 1073K to 1273K. Additionally, though activation losses are present, they were not as significant as we had expected. We have determined through isolating the various forms of loss that activation loss and ohmic loss exhibit a nearly linear relationship between current density and voltage. Concentration loss, however, significantly increases as the current density approaches the limiting current density. Our mathematical models have also helped us in analyzing the effects of partial pressure changes on the SOFC and SOEC systems. A significant advantage to using a mathematical model for the SOFC and SOEC systems is that it allows us to quickly change parameters and observe the effects. This allowed us to determine that partial pressure significantly affects operating voltage.

In summary, we believe that mathematical models are a crucial part of an R-SOC model. We recommend that for improved SOEC operation, temperature is increased. We cannot make a similar recommendation for SOFC mode as our results are not supported by other literature. Activation loss in our model may be underestimated, and we recommend future groups pay close attention to the activation loss model they select to ensure it functions properly. Future groups should carefully consider the use of the entropy change term, and more thoroughly research

when it should and should not be utilized. For an SOFC, we would recommend maximizing the H_2O partial pressure relative to the H_2 partial pressure, and decreasing the O_2 partial pressure. For SOEC mode, to decrease voltage we recommend maximizing H_2 partial pressure relative to H_2O partial pressure, while increasing the O_2 partial pressure.

5.2 Analysis of Aspen Plus Simulations

The SOFC Aspen Plus model was adapted from the previous iteration of this project. The flowsheet was adapted slightly to carry the O_2 material stream out of the SOFC-CAT into the SOFC-AN shown in Figure 11. The previous iteration of the flowsheet separated this one stream into two. This change seemed to work properly, and more intuitively structured the flowsheet. Another consideration with the SOFC flowsheet in Aspen Plus has to do with the extra components, notably the SOFC-CAT separator and the heaters HEATER2 and HX-CAT-2. These components are not needed if pure oxygen is fed into the fuel cell, and Aspen Plus throws a warning as certain material streams and components are not used. This flowsheet setup would be useful for running air through the SOFC, but in this case the functionality was not utilized.

The SOFC polarization curves generated in our study show an expected relationship between operating voltage and temperature for the fuel cell. At higher temperatures, a higher operating voltage was obtained. This result is backed up by other studies; in fact, most other fuel cell simulations have found this relationship. That is, in most cases it has been found that operating voltage increases with temperature for an R-SOC operating in fuel cell mode. O'Hayre et al. (2016), Chehadeh et al. (2022), Wang et al. (2020), and Hauck et al. (2017) determined that Nernst voltage decreases with increasing temperature, but due to the kinetics at high temperature overall voltage of the fuel cell increases. As temperature increases, according to Hauck et al.

(2017), the kinetics of the reaction improve. Kinetics are modeled by the equation for activation loss, meaning our model for activation loss is accurate. Another important consideration from our Aspen Plus SOFC results is that the simulation predicted much lower voltage than expected. In order to obtain a predicted voltage for the Aspen Plus results, the Gibbs free energy change is used. Therefore, the reaction step in the SOFC flowsheet in Aspen Plus is likely inaccurately modeled. Before combining the SOFC and the SOEC flowsheets to construct an R-SOC in Aspen Plus, it is very important that the SOFC flowsheet is modeled properly and the predicted voltage is verified with other work. This will allow future groups to combine these flowsheets into cell modules, and eventually into a stack module or a complete system model.

The SOEC mode in Aspen Plus appears to have the expected relationship with temperature, therefore to improve the mathematical model further consideration must be given to the changes in loss calculation when operating in SOFC mode. Our results from the Aspen Plus SOEC simulation suggest that it is better to run an SOEC at high temperatures as it reduces the voltage required. The same result has been found by Hauck et al. (2017), AlZharani & Dincer (2017), and Wang et al. (2020). Based on our results, to obtain the highest voltage efficiency at all current density values, an operating temperature of 1273 K is suggested. Our SOEC results suggest that it is most efficient to run a cell at low current densities when possible when considering the voltage efficiency only. Work that has used an alternative efficiency metric such as hydrogen production efficiency also suggests that lower current densities and higher temperatures are more efficient (Menon et al., 2013).

Another difference between our results and the work of other groups is the range of current densities. This is a selected parameter, defined mostly by the limiting current density which we chose to be 0.65 A/cm^2 to make our results more comparable to the previous iteration

of the project. Other work, such as the work done at Saint-Gobain, shows simulations run at current densities ranging from -2.0 to 2.0 A/cm^2. Consideration must be given in future work to what the current density range and limiting current density will be to allow for comparison with other studies that are most relevant.

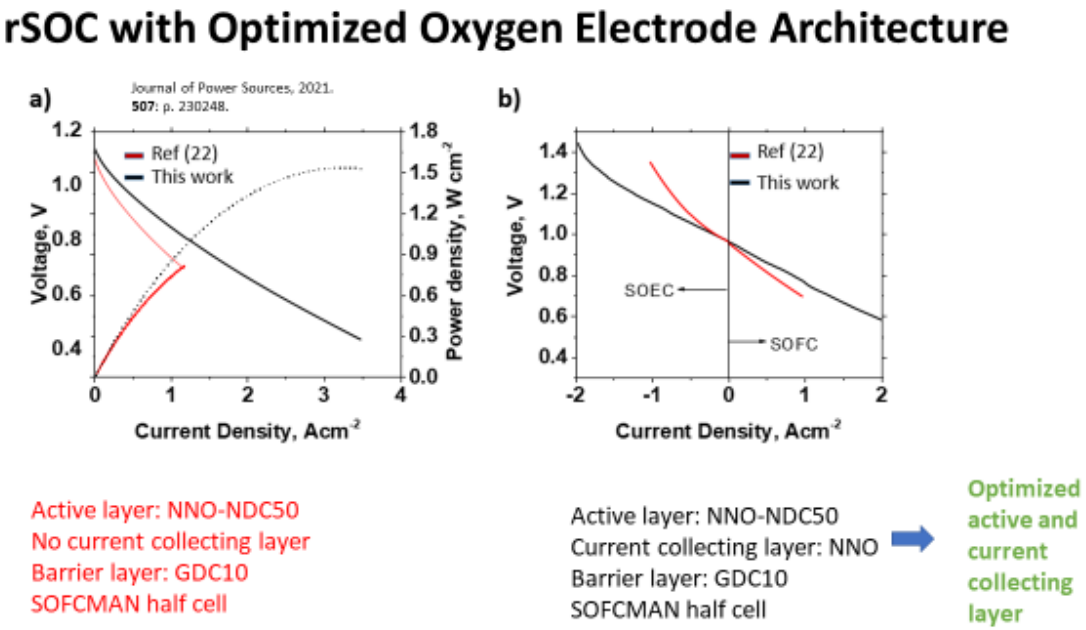

Figure 23: Experimental R-SOC Model at Saint Gobain

5.3 Analysis of IDAES Simulations

The IDAES simulations were also adapted from the previous iteration of this project, with the majority of the code being reused for SOFC simulations in particular. The polarization curves for those simulations again displayed an inversely proportional relationship between operating voltage and temperature, which contrasts to other fuel cell simulations run by other research groups. The cause(s) again could be linked to inaccurate loss approximations during operation, and overestimating thermodynamically predicted voltage for SOFC mode. Results from SOEC mode also again display the expected relationship with temperature. Much of the

conclusions drawn from Aspen Plus results hold true for the IDAES runs as well, although similar studies, especially ones with similar parameters used during experimentation, as well as determining the importance of including or not including the entropy change term were unable to be located.

The lack of these studies (and therefore this slight lack of analyses when compared to our Aspen Plus analyzes) using IDAES was most likely due to the fact that IDAES is not nearly as widely used as ASPEN is. This is simply because IDAES is a much newer program than Aspen, and so it has had less industry use as of currently. However, this may be subject to change in the future with outside companies (such as Mapex for example) actively trying to update IDAES' framework abilities day by day. For more information on this topic, as well as other potential supplemental material (or replacement softwares) to IDAES, you may view our recommendations chapter (specifically section 6.1 down below).

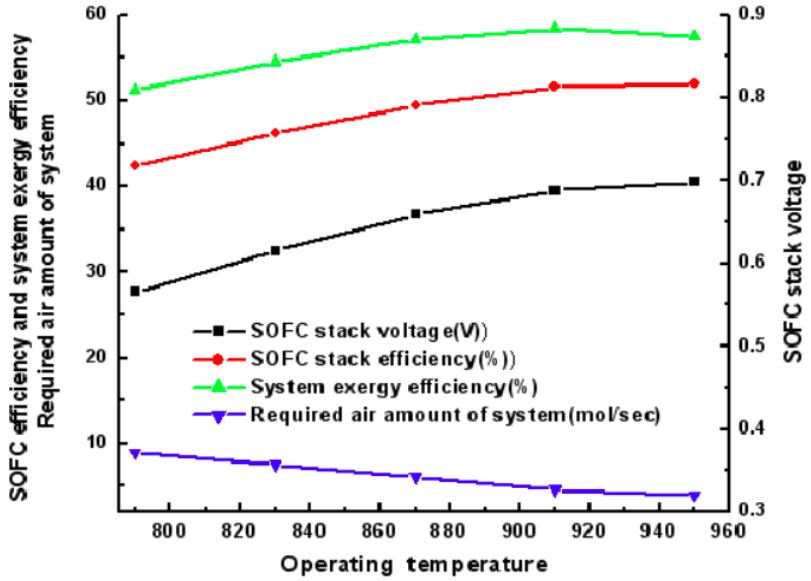

Figure 24: SOFC stack outputs (voltage, efficiency, etc.) (Duan et al., 2022)

However, one last thing to discuss in this IDAES analyzes section that wasn't fully covered in our ASPEN analyses section is further delving into the topic of voltage efficiency

versus temperature of the cell. As seen in the figure above, normally, as the operating temperature of a fuel cell increases, the voltage efficiency of that fuel cell increases as well. This is most due to a couple factors. The first factor would be that it is generally easier for the cell to do greater amounts of work at higher operating temperatures thereby increasing the cell's overall efficiency. In addition to this, the other factor would be that at higher operating temperatures the reaction rate of these cells' half reactions would be higher thereby causing the amount of activation losses of the cells to be lower thereby also increasing the cell's efficiency.

One thing that is important to note though that is as seen in the previous result's chapter is that once current density passes a certain point (of around .5), then the relationship between the cell's efficiency and the operating temperature generally becomes inverted. Again, what this means is that eventually (with high enough current density at, or past .5), the efficiencies of the higher temperatures and lower temperatures will intersect and then the higher temperatures will become less efficient, and the lower temperature will become more efficient. There are a couple of likely reasons for why this may occur. The first reason is that as current density becomes concentration losses begin to increase (curve down) thereby causing a more drastic decrease in efficiency. The other reason is that being at a high temperature specifically is more likely to increase the concentration of gas in a fuel cell thereby causing an even more drastic decrease in efficiency thereby causing the higher temperatures to now have lower efficiencies and the lower temperatures to now have higher efficiencies.

5.4 Comparison of Results

To effectively evaluate the differences between our methods, the methods of the previous iteration of this project, and the methods of other studies, it is useful to select one operating

condition and combine polarization curves onto one graph. The polarization curves below depict the SOFC and SOEC models at 1273 K using the mathematical models, the Aspen Plus results, results from the previous iteration of the project (Chehadeh et al., 2022), and the IDAES results.

During SOFC operation, all models presented in this study with the exception of the IDAES models exhibited an extremely similar loss modeling relationship. This is due to the fact that the same equations were used for loss modeling, and the changes made between these different methods focused mostly on the predicted voltage calculated by Equation 21.

Another important takeaway from these results is the difference in modeling the concentration losses between the graphs generated with use of the mathematical models (mathematical models and Aspen results), our IDAES work, and the work done by Chehadeh et al. Overall, the most conservative estimate for concentration loss is found in the results by the previous iteration of the project, Chehadeh et al., and the most aggressive estimate is given by the mathematical models. Additionally, there are slight differences in activation loss approximations as well. The work with Aspen and the mathematical models estimate a more significant activation loss at low current densities, as seen by the slight difference in slope between the Mathematical Model and Chehadeh et al. in Figure. All of this suggests that the mathematical models contain more aggressive estimates for voltages, decreasing the predicted performance of the cell especially with the consideration of the Entropy Change Term in Equation 21.

Figure also shows the difference in predicted voltage between each modeling method. The previous iteration of this project predicts the highest operating voltage for the SOFC, and the Aspen Plus SOFC model from this work predicts the lowest voltage. The difference between these extremes is about 0.25 V. The IDAES simulation from this group predicts a slightly lower

voltage than both the Mathematical Model and Chehadeh et al., suggesting that either the ohmic loss model is more aggressive, or the predicted voltage is lower. The mathematical model provides a good intermediate prediction between these two, while also predicting a much higher concentration loss.

For the SOEC results comparison, shown in Figure, we have determined that the methods used in this study are all acceptable models of an SOEC. The Aspen Plus SOEC model predicts higher activation and concentration loss than the IDAES model, therefore the voltage from the IDAES results is slightly higher at the intermediate current densities. The small difference in voltage between the mathematical model and the Aspen Plus SOEC suggest that the Aspen flowsheet accurately models an SOEC. Therefore, little changes need to be made to the Aspen Plus SOEC before implementing it into a complete R-SOC model.

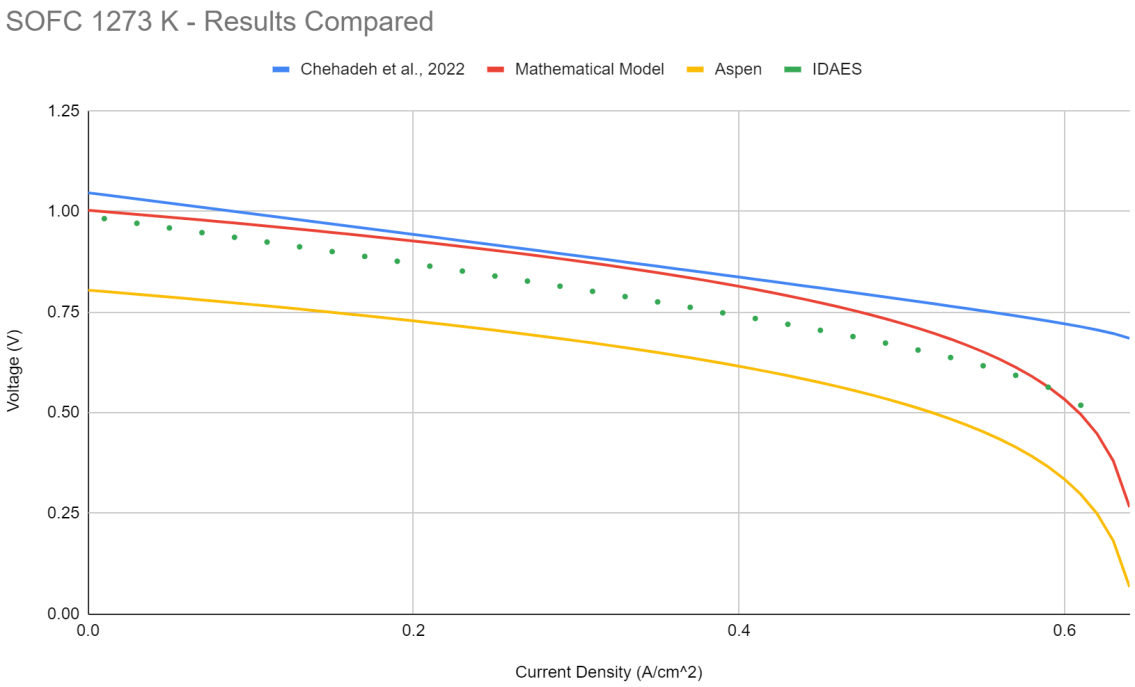

Figure 25: SOFC Output Voltage Comparison (1273 K)

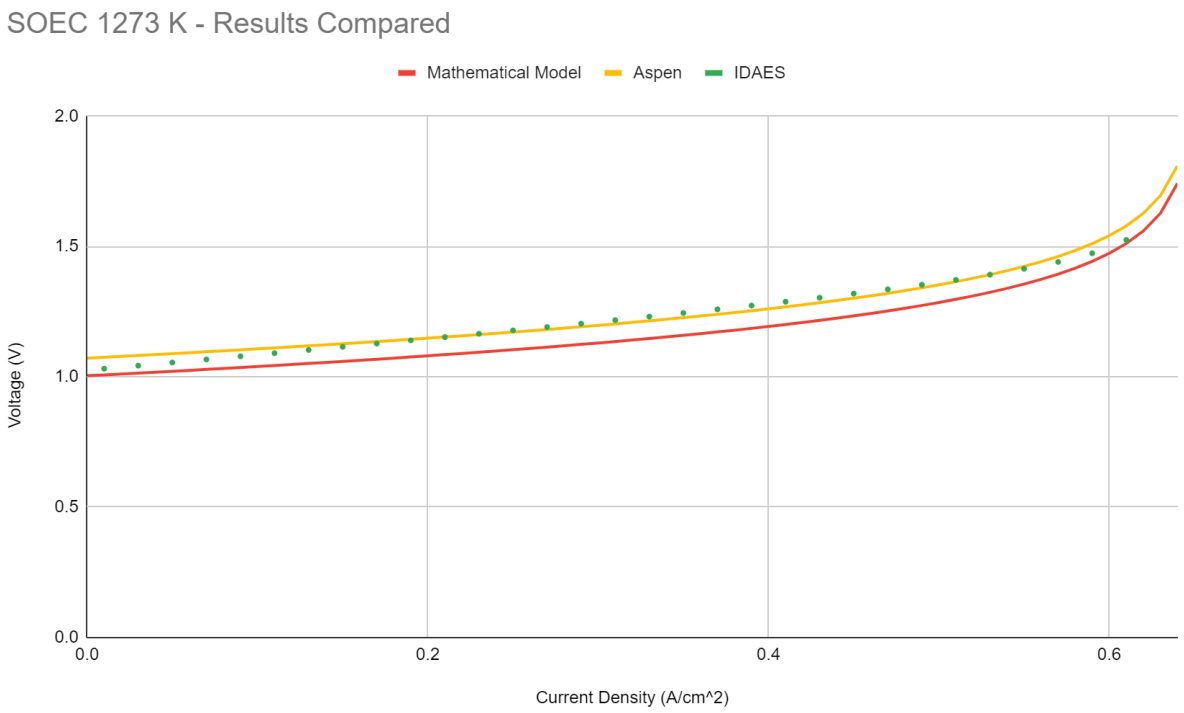

Figure 26: SOEC Output Voltage Comparison (1273 K)

6.0 Recommendations

There are many ways in which our study could be improved upon by future work. R-SOC technology has the potential to aid the world in the transition to sustainable energy production, but the technology continually needs more research and understanding. This section will cover improvements that could be made to this study, and how future research groups might improve and build upon our results. This section is broken into two parts: General recommendations (software setup tips, communication, etc.) and specific recommendations (modeling strategies and softwares, sources, etc.).

6.1 Specific Recommendations

6.1.1 Modeling Softwares - IDAES

IDAES proved to be a difficult software to use. It is described as a complex modeling framework software, but it functions more as a base software platform that would require other add-ons to create anything of relevant use. For example, the company, MapEx, is currently developing a beta that would give IDAES an extensive graphical interface. However, as the program stands currently, that interface is not yet integrated.

A lot of this is most likely due to the fact that IDAES is not just a software company. IDAES, which stands for the Institute for the Design of Advanced Energy Systems, is a whole organization started by the Department of Energy, and the National Energy Research Laboratory. They specialize in doing research on emerging and advancing energy systems both in the United States and abroad. In addition to this, they also created an IDAES software in 2019 (three years after the Institute's founding in 2016). Because this software is so new and because the Institute

itself has so much other research and projects going on, it is understandable to say the software is "underdeveloped" to say the least.

However, as previously stated, companies like Mapex are trying to incorporate add-on features into IDAES, and considering the program's code and information went fully open-source a couple of years ago, we are sure that more improvements will be coming to the software soon. Because of this, our recommendations would be this: Before your attempts to use IDAES begin, try contacting and looking into other companies like Mapex that do in fact add on additional features directly in conjunction with IDAES' interface. Or, another (potentially even better option) would be to just explore other softwares that could replace IDAES all together. This may include softwares like: EES, gPROMs, etc.

6.1.2 Modeling Softwares - Aspen Plus

Unlike IDAES, Aspen Plus is a much older software that was established back in the 1980s. Because of this, it already has an extensive framework and graphical user interface allowing users to create chemical process flowsheets. It works particularly well for diagrams, chemical, or mathematical modeling. Aspen Plus is an incredibly powerful software, and our group recommends its use for future work in simulating R-SOCs.

Due to the workflow of this study, and the attempt to recreate results from the previous iteration of the project, we have created the SOFC and SOEC models separately. Therefore, combining the results to form a polarization curve for an R-SOC is impractical. Additionally, this work cannot give input into efficiency relationships for an R-SOC as the cells were modeled separately without all of the components to allow for reversible use. We recommend future research groups improve the Aspen Plus SOFC mode, and attempt to combine the SOFC and

SOEC modules to form an Aspen Plus R-SOC model. Designing the cell such that it can be run in both SOFC and SOEC directions depending on user input will allow future groups to make suggestions on R-SOC operation and design. Creating an R-SOC model in Aspen Plus at the single cell scale is a necessary step in creating a comprehensive R-SOC stack model. These individual models could then be combined to model a complete R-SOC system and analyze the application of electrical loads at a system level. This would require more careful consideration to the components and blocks used, and a future group would need to verify that blocks are accurate representations of real R-SOC components through experimental testing. A crucial step in creating a comprehensive Aspen Plus R-SOC model will be successfully implementing the modeling equations with calculator blocks into the flowsheet to control parameters, define operational behavior, and extract results without an external mathematical model.

6.1.3 Modeling Parameters & Assumptions

Simulations that take place early on in a project's lifespan (meaning with the first, or second group) normally do not have the luxury of simulating anything other than ideal conditions. This stems from the fact that it is already difficult to get initial simulations running, and so incorporating non-ideal parameters from the start would be unnecessarily difficult. Because of this, our simulations are run on mostly ideal standards:

- Fuel utilization is at 1 (or 100%), meaning it is assumed there's no fuel left over at the end of use.
- All fuel intake is pure in the case of the SOFC, meaning it's assumed that all sources of hydrogen, and oxygen are 100% hydrogen, and oxygen.

- Temperatures are all above 1000K and below 1500K, which is an ideal condition for a cell to run at (Duan et al., 2022).
- Materials within the cell don't degrade, or lose efficiency over time.

Additional groups may want to improve on this by removing some of these assumptions, or making modifications to them. Some ideas for non-ideal standards may be the following:

- Set fuel utilization for different trials, one might want to use different values within a range between .75 - .85 (75% to 85%), as this is the current standard efficiency of solid oxide cells (Bari & Sistani, 2019).
- Assume that all fuel intake is NOT pure, and discuss what may or may not happen if contaminants were to potentially interact with the cell. The DOE (Department of Energy), and NERL (National Energy Research Laboratory) have some research on this that you might want to further investigate (Energy Education, 2018).
- Try simulating 1-2 trials of non-ideal operating temperatures (along with your other simulations). For example, a low non-ideal temp could be 700K, and at a high non-ideal temp could be 1550K. These temperatures are considered "non-ideal", as this is where the standard laws of efficiency for a solid oxide cell break down and become reversed (Duan et al., 2022).
- Materials do naturally degrade over time, and will eventually contaminate the fuel cell process, consequently causing a decrease in efficiency. A potential method to account for this would be to add in a "time factor" into your simulation rather than just standard temperature parameters. Additionally, if ambition and time is on your side, it might be a good idea to look into "alternative" materials (insert PEM material types) that increase

efficiency, lower contamination, and are biodegradable . This is where we just began to look into as our project was ending, and with climate change on the rise, it might be necessary for a group to continue on (Stambouli & Traversa, 2002).

Other assumptions may be necessary to simulate the fuel cell processes as realistically as possible - use Saint-Gobain as an additional resource to confirm current assumptions and inquire about new ones that may or may not be missing.

6.2 General Recommendations

6.2.1 Installation Help - IDAES

For this project IDAES had to be installed individually on our personal computers after complying with installation instructions from the official website and Github, the latter of which one will need an account to use. The software is open source and free to use, so it can be downloaded by anyone at no cost and tailored to their specific needs. Installation and initialization instructions will be linked below:

Official website: Advanced User Installation — IDAES v1.13.0 (idaes-pse.readthedocs.io)

Github: GitHub - IDAES/idaes-pse: The IDAES Process Systems Engineering Framework

A cursory knowledge of Python and the necessary modules used for the simulations (numpy for mathematical operations, matplotlib for graphing, etc.) will help in understanding existing and creating new code for the project. Also, it is important to note (and it is stated in the instructions) that there are two popular methods of installing the necessary modules for the

simulations to use - pip install or miniconda. It is vital that only one of these is used for all program/module installation, not both.

6.2.2 Installation Help - Aspen Plus

For this research, Aspen Plus v11 was run on a remote desktop server maintained by the Academic Resource Center (ARC) at Worcester Polytechnic Institute (WPI). Obtaining the software itself for personal use is very expensive, therefore it is necessary for student groups conducting work using Aspen Plus to do so through an existing institution.

To connect to the WPI remote desktop on which Aspen Plus is installed, one must first connect either to a WPI specific network or to the GlobalProtect VPN. Next, open the Windows Start menu and search for Remote Desktop Connection. Enter the proper address for the remote server, in this case *arc-aspen.wpi.edu*. Enter your username and password to connect.

For operating the software and creating complex flowsheets, there are a number of informative tutorials that can be found online. These tutorials cover most functionalities of Aspen Plus, and could be very useful in any attempt to create an R-SOC model. There are also numerous tutorials which cover analytical methods in Aspen Plus such as sensitivity studies and generating graphs within the software.

6.2.3 Contacting Authors

Some of this section may seem self explanatory, but we thought it was important to provide some details about how future groups might want to go about contacting others for help on their project. The WPI emails of the authors of this report can be found in the table below, along with Gmail addresses and phone numbers. Do not hesitate to contact us with any questions

about the work completed in this paper, we would be happy to answer any and all questions to the best of our ability.

Name	**WPI Email**	**Gmail**	**Phone Number**
Stephen Davis	srdavis@wpi.edu	stephendavis1313@gmail.com	516-666-0820
Alexander Kochling	ajkochling@wpi.edu	kochlingalexander@gmail.com	617-893-0468
Sam Krimmel	sjkrimmel@wpi.edu	samkrimmel37@gmail.com	802-291-3712
Group Alias	gr-fuelcellmqp@wpi.edu	N/A	N/A

For example, the things that this might be applicable for would be: coding in Python / Jupyter / IDAES, coding and graphing in ASPEN, installation guides to the programs, assumptions that were made and what might be able to be gotten rid of for the next research group, etc. We hope this section proves to be one of the most helpful sections in the paper for whoever is reading this.

7.0 Conclusion

Throughout this project, an understanding of R-SOCs, the materials that they require, and the thermodynamics behind their operation was developed. In addition to this, models of both SOFC mode and SOEC mode were created to determine the difference in voltages and efficiencies of these cells at varying temperatures. To ensure positive variability in potential results, two softwares were used to create these models: Aspen Plus and IDAES.

Before running simulations in these softwares though, multiple sources were examined to determine the correct mathematical equations for each type of model. After assessing a variety of sources, a mathematical model was selected which requires little adjustment between SOFC and SOEC modes, making it easier to later combine the two to form an R-SOC model. A software model was created in Aspen Plus using a combination of methods from the work of other research groups. The Aspen Plus simulations were run to obtain chemical quantities which were input into the mathematical model and polarization curves. An IDAES model was coded to calculate said chemical quantities, which were then scatter plotted to create our polarization curves. Those curves (for both Aspen Plus and IDAES) were then overlaid on each other with the help of Google Sheets.

The Aspen Plus simulations and the coding run on IDAES were largely similar when it comes to the results. For the SOFC model, it was found in both cases that actual voltage increases with increasing temperature; a result which is supported by other SOFC studies. For the SOEC model, it was found that voltage decreased with increasing temperature; also a result supported by other work. Therefore, for efficient operation of the R-SOC, we suggest that the cell is run at high temperature in general; 1173 K is ideal. Additionally, based on our results we have found it is best to run the cell at low current densities to maximize efficiency.

The first trial simulations for the SOEC models were developed through this project with the same software used for the first SOFC trial simulations done in the previous year. Notably, combining the SOFC and SOEC models proposed in this research could provide an accurate model of an R-SOC. While our results represent definite progress, there is still much more research to be done. It is recommended that future research is also carried out in Aspen Plus and that the model is constructed at the system level, utilizing individual cell models to create stacks. Holding discussions with organizations running experiments on R-SOCs, especially Saint Gobain, should be considered to ensure that components used in the simulation are set up and behave realistically, and supported by experimental data. The R-SOC model should also be examined under a wider range of operating parameters, with changes in gas compositions, fuel utilizations, cell dimensions, or different materials. Hopefully, with developments from future research, newer results will be able to accurately model a reversible solid oxide cell system with maximized efficiency and lower cost.

8.0 References

Abbaker, O., Wang, H., & Tian, Y. (2019). Voltage control of solid oxide fuel cell power plant based on intelligent proportional integral-adaptive sliding mode control with anti-windup compensator. *Transactions of the Institute of Measurement and Control. 42*(9). https://doi.org/10.1177/0142331219867779

AlZahrani, A. A., & Dincer, I. (2017). Thermodynamic and electrochemical analyses of a solid oxide electrolyzer for hydrogen production. *International Journal of Hydrogen Energy. 42*(33), 21404-21413. https://doi.org/10.1016/j.ijhydene.2017.03.186

American Society of Mechanical Engineers, (2012). *Society policy.* ASME. https://www.asme.org/wwwasmeorg/media/resourcefiles/aboutasme/get%20involved/advocacy/policy-publications/p-15-7-ethics.pdf

Amiri, A., Vijay, P., Tadé, M. O., Ahmed, K., Ingram, G. D., Pareek, V., & Utikar, R. (2015). Solid oxide fuel cell reactor analysis and optimisation through a novel multi-scale modelling strategy. *Computers & Chemical Engineering*, *78*, 10–23. https://doi.org/10.1016/j.compchemeng.2015.04.006

AspenTech. (n.d.). *Aspen Plus.* https://www.aspentech.com/en/products/engineering/aspen-plus

Atkins, P., de Paula, J., & Keeler, J. (2018). *Atkins' Physical chemistry 11e: Volume 1.* Oxford University Press.

Ausiello, A. (n.d.) Development of a system for electric energy production based on fuel cells fueled by biogas produced with anaerobic digestion of biomass. https://1library.net/document/yr191roq-development-electric-energy-production-produced-anaerobic-digestion-biomass.html

Bari, E., & Sistani, A. (2019). *Biodegradable Material*. Biodegradable Material - an overview | ScienceDirect Topics. Retrieved from https://www.sciencedirect.com/topics/engineering/biodegradable-material

Chehadeh, M., Ourdyl, T., Blechinger-Slocum, D., & Tabandeh, M. (2022). *A thermodynamic analysis of solid oxide fuel cells.* Worcester Polytechnic Institute.

Denker, J. (2014). *Modern Thermodynamics.* http://www.av8n.com/physics/thermo/#contents

Doherty, W., Reynolds, A., & Kennedy, D. (2014). Process simulation of biomass gasification integrated with a solid oxide fuel cell stack. *Journal of Power Sources. 277,* 292-303. https://doi.org/10.1016/j.jpowsour.2014.11.125

Duan, L., Zhang, X., & Yang, Y. (2022). *Exergy analysis of a novel SOFC hybrid system with zero-CO_2 emission*. Find and Share Research.

Energy Education. (2018). *Thermal efficiency.* Energy Education. https://energyeducation.ca/encyclopedia/Thermal_efficiency

Flowers, P., Theopold, K., Langley, R., & Robinson, W. R. (2019). *Chemistry 2e.* https://openstax.org/details/books/chemistry-2e?Book%20details

Gentile, R., Vesely, L., Ghouse, J. H., Goyal, V., & Kapat, J. S. (2022). Transient analysis of a supercritical carbon dioxide air cooler using IDAES. *Journal of Energy Resource Technology. 145*(2). https://doi.org/10.1115/1.4054860

Gómez, S. Y., & Hotza, D. (2016). Current developments in reversible solid oxide fuel cells. *Renewable and Sustainable Energy Reviews. 61*, 155-174. https://doi.org/10.1016/j.rser.2016.03.005

Hall, N. (2021, May 13). *Entropy of a Gas*. NASA. Retrieved from https://www.grc.nasa.gov/www/k-12/airplane/entropy.html

Hauck, M., Herrmann, S., & Spliethoff, H. (2017). Simulation of a reversible SOFC with Aspen Plus. *International Journal of Hydrogen Energy. 42*(15), 10329-10340. https://doi.org/10.1016/j.ijhydene.2017.01.189

Jørgensen, S. E., & Fath, B. D. (2008). *Encyclopedia of Ecology.* Elsevier Science.

Laidler, K. J. (2008). chemical kinetics | Definition, Equations, & Facts. Encyclopedia Britannica. https://www.britannica.com/science/chemical-kinetics

Macedo, D. A., Cesario, M. R., Souza, G. L., Cela, B., Paskocimas, C. A., Martinelli, A. E., Melo, D. M. A., & do Nascimento, R. M. (2012). Infrared spectroscopy techniques in the characterization of SOFC functional ceramics. *Infrared Spectroscopy - Materials Science, Engineering and Technology.* https://doi.org/10.5772/34884

Maric, R., & Mirshekari, G. (2020). Fundamental aspects of solid oxide fuel cells. *Solid Oxide Fuel Cells*. CRC Press. https://doi-org.ezpv7-web-p-u01.wpi.edu/10.1201/9780429100000

Menon, V., Janardhanan, V. M., & Deutschmann, O. (2013). A mathematical model to analyze solid oxide electrolyzer cells (SOECs) for hydrogen production. *Chemical Engineering Science*, *110*, 83-93. https://doi.org/10.1016/j.ces.2013.10.025

Miller, D. C., Siirola, J., Burgard, A. (2010). *Applications driving IDAES process systems engineering framework capabilities.* Institute for the Design of Advanced Energy Systems.

Mottaghizadeh, P., Santhanam, S., Heddrich, M. P., Andreas Friedrich, K., & Rinaldi, F. (2017). Process modeling of a reversible solid oxide cell (r-SOC) energy storage system utilizing

commercially available SOC reactor. *Energy Conversion and Management. 142,* 477-493. https://doi.org/10.1016/j.enconman.2017.03.010

National Renewable Energy Laboratory. (n.d.) *Hydrogen & fuel cells: Contaminants.* National Renewable Energy Laboratory. https://www.nrel.gov/hydrogen/contaminants.html

Ni, M., Leung, M. K. H., & Leung, D. Y. C. (2007). Parametric study of solid oxide fuel cell performance. *Energy Conversion and Management*, *48*(5), 1525-1535. https://doi.org/10.1016/j.enconman.2006.11.016

Office of Fossil Energy and Carbon Management. (n.d.). *Why SOFC technology?*. Energy.gov. https://www.energy.gov/fecm/why-sofc-technology

O'Hayre, R., Cha, S., Colella, W. G., & Prinz, F. B. (2016). *Fuel cell fundamentals.* John Wiley & Sons.

Ortega, E. (n.d.) *What is Aspen Plus?* ChemEngGuy. https://www.chemicalengineeringguy.com/the-blog/process-simulation/what-is-aspen-plus/

Oryshchyn, D., Harun, N. F., Tucker, D., Bryden, K. M., & Shadle, L. (2018). Fuel utilization effects on system efficiency in solid oxide fuel cell gas turbine hybrid systems. *Applied Energy, 228*(C). https://doi.org/10.1016/j.apenergy.2018.07.004

Redissi, Y., & Bouallou, C. (2013). Valorization of carbon dioxide by co-electrolysis of CO_2/H_2O at high temperature for syngas production. *Energy Procedia, 37,* 6667-6678. https://doi.org/10.1016/j.egypro.2013.06.599

Service, R. F. (2020). *Next generation water splitter could help renewables power the globe.* Science.

https://www.science.org/content/article/next-generation-water-splitter-could-help-renewables-power-globe

Stambouli, A. B., & Traversa, E. (2002). Fuel cells, an alternative to standard sources of energy. *Renewable and Sustainable Energy Reviews, 6*(3), 295-304. https://doi.org/10.1016/S1364-0321(01)00015-6

Steinberger-Wilckens, R. (2016). *Advances in medium and high temperature solid oxide fuel cell technology.* CISM International Centre for Mechanical Sciences. https://doi-org.ezpv7-web-p-u01.wpi.edu/10.1007/978-3-319-46146-5_1

Sun, C., Hui, R., & Roller, J. (2010). Cathode materials for solid oxide fuel cells: a review. *Journal of Solid State Electrochemistry, 14,* 1125-1144. https://doi.org/10.1007/s10008-009-0932-0

The Hidden Costs of Fossil Fuels | Union of Concerned Scientists. (2008). Www.ucsusa.org. https://www.ucsusa.org/resources/hidden-costs-fossil-fuels#:~:text=There%20are%20two%20main%20methods

Wang, C., Chen, M., Liu, M., & Yan, J. (2020). Dynamic modeling and parameter analysis study on reversible solid oxide cells during mode switching transient processes. *Applied Energy, 263.* https://doi.org/10.1016/j.apenergy.2020.114601

Wendel, C. H., Gao, Z., Barnett, S. A., & Braun, R. J. (2015). Modeling and experimental performance of an intermediate temperature reversible solid oxide cell for high-efficiency, distributed-scale electrical energy storage. *Journal of Power Sources, 283*(1), 329-342. https://doi.org/10.1016/j.jpowsour.2015.02.113

9.0 Appendices

9.1 Appendix A: Aspen Simulation Setup Screenshots

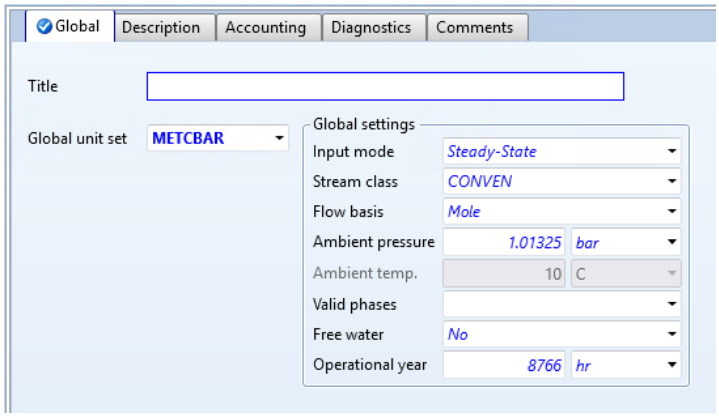

Figure 27: Simulation specifications in Aspen Plus

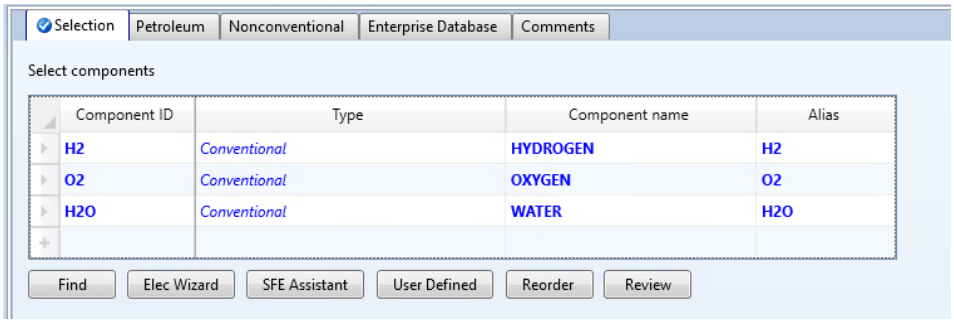

Figure 28: Components in SOFC model

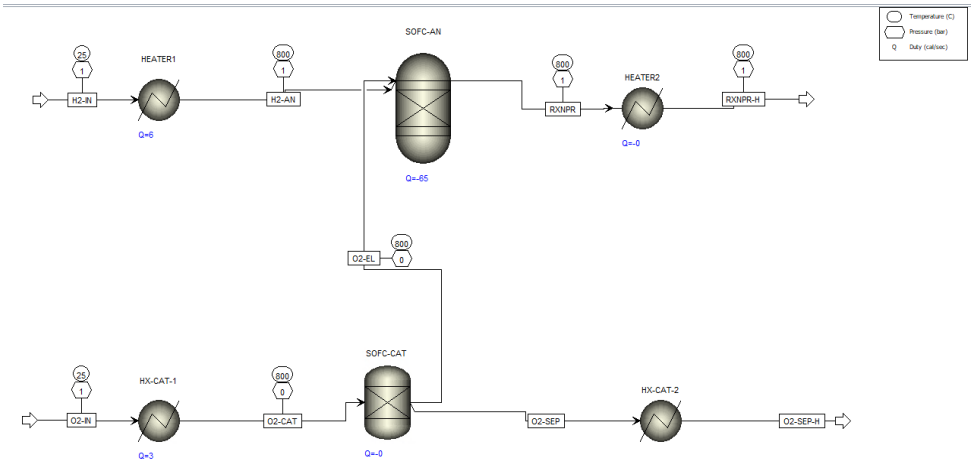

Figure 29: Components in SOFC model

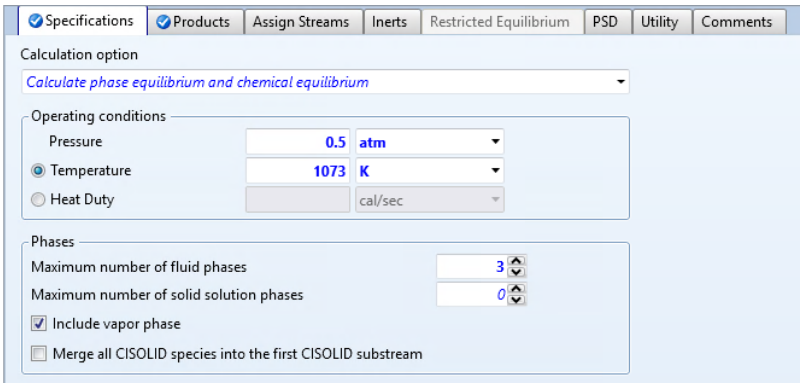

Figure 30: Settings for the RGibbs reactor in SOFC model

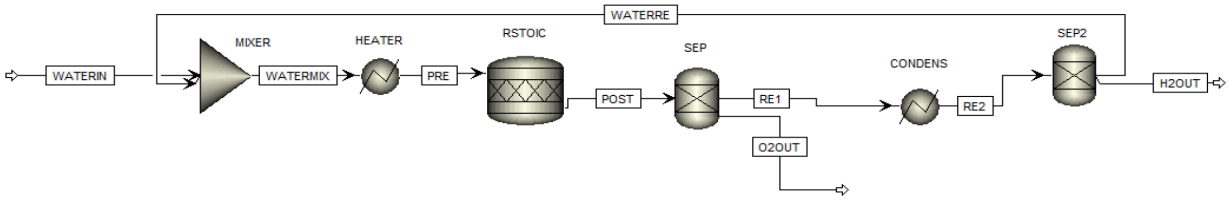

Figure 31: SOEC Flowsheet

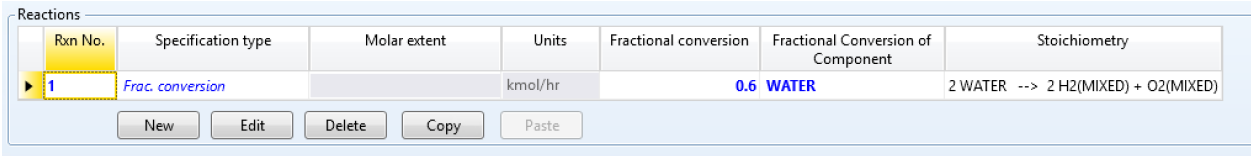

Figure 32: Settings for the RStoic reactor in SOEC model

9.2 Appendix B: Aspen Simulation Flowsheets - Fuel Cell Results

	Units	H2-AN	H2-IN	O2-CAT	O2-EL	O2-IN	O2-SEP	O2-SEP-H	RXNPR	RXNPR-H
Description										
From		HEATER1		HX-CAT-1	SOFC-CAT		SOFC-CAT	HX-CAT-2	SOFC-AN	HEATER2
To		SOFC-AN	HEATER1	SOFC-CAT	SOFC-AN	HX-CAT-1	HX-CAT-2		HEATER2	
Stream Class		CONVEN	CONVEN	CONVEN	CONVEN	CONVEN	CONVEN	CONVEN	CONVEN	CONVEN
Maximum Relative Error										
Cost Flow	$/sec									
− MIXED Substream										
Phase		Vapor Phase	Vapor Phase	Vapor Phase	Vapor Phase	Vapor Phase			Vapor Phase	Vapor Phase
Temperature	K	1073	298.15	1073	1073	298.15			1073	1073
Pressure	atm	0.5	1	0.21	0.21	1			0.5	1
Molar Vapor Fraction		1	1	1	1	1			1	1
Molar Liquid Fraction		0	0	0	0	0			0	0
Molar Solid Fraction		0	0	0	0	0			0	0
Mass Vapor Fraction		1	1	1	1	1			1	1
Mass Liquid Fraction		0	0	0	0	0			0	0
Mass Solid Fraction		0	0	0	0	0			0	0
Molar Enthalpy	J/kmol	2.28867e+07	3.72529e-09	2.52537e+07	2.52537e+07	-3.72529e-09			-2.12774e+08	-2.12774e+08
Mass Enthalpy	J/kg	1.13532e+07	1.84797e-09	789207	789207	-1.1642e-10			-1.18108e+07	-1.18108e+07
Molar Entropy	J/kmol-K	43426.6	0	53859.2	53859.2	0			8174.07	2411.02
Mass Entropy	J/kg-K	21542.3	0	1683.16	1683.16	0			453.73	133.832
Molar Density	kmol/cum	0.00567884	0.0408747	0.00238511	0.00238511	0.0408747			0.00567884	0.0113577
Mass Density	kg/cum	0.0114479	0.0823985	0.0763207	0.0763207	1.30794			0.102306	0.204612
Enthalpy Flow	kJ/sec	0.0124923	2.03339e-18	0.00689215	0.00689215	-1.01669e-18			-0.116139	-0.116139
Average MW		2.01588	2.01588	31.9988	31.9988	31.9988			18.0153	18.0153
+ Mole Flows	**mol/min**	**0.03275**	**0.03275**	**0.016375**	**0.016375**	**0.016375**	**0**	**0**	**0.03275**	**0.03275**
− Mole Fractions										
H2		1	1	0	0	0			1.20791e-06	1.20791e-06
O2		0	0	1	1	1			6.04869e-07	6.04869e-07
H2O		0	0	0	0	0			0.999998	0.999998
+ Mass Flows	**kg/sec**	**1.10033e-06**	**1.10033e-06**	**8.73301e-06**	**8.73301e-06**	**8.73301e-06**			**9.83334e-06**	**9.83334e-06**
+ Mass Fractions										
Volume Flow	cum/sec	9.6117e-05	1.33538e-05	0.000114425	0.000114425	6.67691e-06			9.61171e-05	4.80586e-05
− Gibbs energy, pure component										
H2	kJ/mol	-23.71	3.72529e-15						-23.71	-17.5263
O2	kJ/mol			-32.5373	-32.5373	-3.72529e-15			-24.798	-18.6143
H2O	kJ/mol								-221.545	-215.361
Gibbs energy, mixture	kJ/mol	-23.71	3.72529e-15	-32.5373	-32.5373	-3.72529e-15			-221.545	-215.361
+ Vapor Phase										

Table 5: Results Flowsheet from Fuel Cell Model at 1073 K

	Units	H2-AN	H2-IN	O2-CAT	O2-EL	O2-IN	O2-SEP	O2-SEP-H	RXNPR	RXNPR-H
Description										
From		HEATER1		HX-CAT-1	SOFC-CAT		SOFC-CAT	HX-CAT-2	SOFC-AN	HEATER2
To		SOFC-AN	HEATER1	SOFC-CAT	SOFC-AN	HX-CAT-1	HX-CAT-2		HEATER2	
Stream Class		CONVEN	CONVEN	CONVEN	CONVEN	CONVEN	CONVEN	CONVEN	CONVEN	CONVEN
Maximum Relative Error										
Cost Flow	$/sec									
− MIXED Substream										
Phase		Vapor Phase	Vapor Phase	Vapor Phase	Vapor Phase	Vapor Phase			Vapor Phase	Vapor Phase
Temperature	K	1173	298.15	1173	1173	298.15			1173	1173
Pressure	atm	0.5	1	0.21	0.21	1			0.5	1
Molar Vapor Fraction		1	1	1	1	1			1	1
Molar Liquid Fraction		0	0	0	0	0			0	0
Molar Solid Fraction		0	0	0	0	0			0	0
Mass Vapor Fraction		1	1	1	1	1			1	1
Mass Liquid Fraction		0	0	0	0	0			0	0
Mass Solid Fraction		0	0	0	0	0			0	0
Molar Enthalpy	J/kmol	2.59577e+07	3.72529e-09	2.87924e+07	2.87924e+07	-3.72529e-09			-2.08491e+08	-2.08491e+08
Mass Enthalpy	J/kg	1.28766e+07	1.84797e-09	899798	899798	-1.1642e-10			-1.1573e+07	-1.1573e+07
Molar Entropy	J/kmol-K	46162.7	0	57012.2	57012.2	0			11989	6225.94
Mass Entropy	J/kg-K	22899.5	0	1781.7	1781.7	0			665.492	345.593
Molar Density	kmol/cum	0.00519471	0.0408747	0.00218178	0.00218178	0.0408747			0.00519471	0.0103894
Mass Density	kg/cum	0.0104719	0.0823985	0.0698143	0.0698143	1.30794			0.0935839	0.187168
Enthalpy Flow	kJ/sec	0.0141686	2.03339e-18	0.00785794	0.00785794	-1.01669e-18			-0.113802	-0.113802
Average MW		2.01588	2.01588	31.9988	31.9988	31.9988			18.0152	18.0152
✚ Mole Flows	**mol/min**	**0.03275**	**0.03275**	**0.016375**	**0.016375**	**0.016375**	**0**	**0**	**0.0327501**	**0.0327501**
− Mole Fractions										
H2		1	1	0	0	0			5.8873e-06	5.8873e-06
O2		0	0	1	1	1			2.94457e-06	2.94457e-06
H2O		0	0	0	0	0			0.999991	0.999991
✚ Mass Flows	**kg/sec**	**1.10033e-06**	**1.10033e-06**	**8.73301e-06**	**8.73301e-06**	**8.73301e-06**			**9.83334e-06**	**9.83334e-06**
✚ Mass Fractions										
Volume Flow	cum/sec	0.000105075	1.33538e-05	0.000125089	0.000125089	6.67691e-06			0.000105075	5.25376e-05
− Gibbs energy, pure component										
H2	kJ/mol	-28.1912	3.72529e-15						-28.1912	-21.4311
O2	kJ/mol			-38.0829	-38.0829	-3.72529e-15			-29.6224	-22.8623
H2O	kJ/mol								-222.555	-215.795
Gibbs energy, mixture	kJ/mol	-28.1912	3.72529e-15	-38.0829	-38.0829	-3.72529e-15			-222.554	-215.794
✚ Vapor Phase										

Table 6: Results Flowsheet from Fuel Cell Model at 1173 K

	Units	H2-AN	H2-IN	O2-CAT	O2-EL	O2-IN	O2-SEP	O2-SEP-H	RXNPR	RXNPR-H
Description										
From		HEATER1		HX-CAT-1	SOFC-CAT		SOFC-CAT	HX-CAT-2	SOFC-AN	HEATER2
To		SOFC-AN	HEATER1	SOFC-CAT	SOFC-AN	HX-CAT-1	HX-CAT-2		HEATER2	
Stream Class		CONVEN	CONVEN	CONVEN	CONVEN	CONVEN	CONVEN	CONVEN	CONVEN	CONVEN
Maximum Relative Error										
Cost Flow	$/sec									
− MIXED Substream										
Phase		Vapor Phase	Vapor Phase	Vapor Phase	Vapor Phase	Vapor Phase			Vapor Phase	Vapor Phase
Temperature	K	1273	298.15	1273	1273	298.15			1273	1273
Pressure	atm	0.5	1	0.21	0.21	1			0.5	1
Molar Vapor Fraction		1	1	1	1	1			1	1
Molar Liquid Fraction		0	0	0	0	0			0	0
Molar Solid Fraction		0	0	0	0	0			0	0
Mass Vapor Fraction		1	1	1	1	1			1	1
Mass Liquid Fraction		0	0	0	0	0			0	0
Mass Solid Fraction		0	0	0	0	0			0	0
Molar Enthalpy	J/kmol	2.90707e+07	3.72529e-09	3.23675e+07	3.23675e+07	-3.72529e-09			-2.04082e+08	-2.04082e+08
Mass Enthalpy	J/kg	1.44209e+07	1.84797e-09	1.01152e+06	1.01152e+06	-1.1642e-10			-1.13284e+07	-1.13284e+07
Molar Entropy	J/kmol-K	48709.3	0	59936.8	59936.8	0			15594.3	9831.22
Mass Entropy	J/kg-K	24162.8	0	1873.1	1873.1	0			865.623	545.722
Molar Density	kmol/cum	0.00478664	0.0408747	0.00201039	0.00201039	0.0408747			0.00478664	0.00957328
Mass Density	kg/cum	0.0096493	0.0823985	0.0643301	0.0643301	1.30794			0.0862317	0.172463
Enthalpy Flow	kJ/sec	0.0158678	2.03339e-18	0.00883362	0.00883362	-1.01669e-18			-0.111396	-0.111396
Average MW		2.01588	2.01588	31.9988	31.9988	31.9988			18.0151	18.0151
+ Mole Flows	**mol/min**	**0.03275**	**0.03275**	**0.016375**	**0.016375**	**0.016375**	**0**	**0**	**0.0327504**	**0.0327504**
− Mole Fractions										
H2		1	1	0	0	0			2.24303e-05	2.24303e-05
O2		0	0	1	1	1			1.12161e-05	1.12161e-05
H2O		0	0	0	0	0			0.999966	0.999966
+ Mass Flows	**kg/sec**	**1.10033e-06**	**1.10033e-06**	**8.73301e-06**	**8.73301e-06**	**8.73301e-06**			**9.83334e-06**	**9.83334e-06**
+ Mass Fractions										
Volume Flow	cum/sec	0.000114033	1.33538e-05	0.000135753	0.000135753	6.67691e-06			0.000114034	5.70169e-05
− Gibbs energy, pure component										
H2	kJ/mol	-32.9362	3.72529e-15						-32.9362	-25.5999
O2	kJ/mol			-43.9321	-43.9321	-3.72529e-15			-34.7503	-27.414
H2O	kJ/mol								-223.935	-216.599
Gibbs energy, mixture	kJ/mol	-32.9362	3.72529e-15	-43.9321	-43.9321	-3.72529e-15			-223.933	-216.597
+ Vapor Phase										

Table 7: Results Flowsheet from Fuel Cell Model at 1273 K

9.3 Appendix C: Aspen Simulation Flowsheets - Electrolysis Cell Results

	Units	H2OUT	O2OUT	POST	PRE	RE1	RE2	WATERIN	WATERMIX	WATERRE
Description										
From		SEP2	SEP	RSTOIC	HEATER	SEP	CONDENS		MIXER	SEP2
To				SEP	RSTOIC	CONDENS	SEP2	MIXER	HEATER	MIXER
Stream Class		CONVEN	CONVEN	CONVEN	CONVEN	CONVEN	CONVEN	CONVEN	CONVEN	CONVEN
Maximum Relative Error										
Cost Flow	$/sec									
− MIXED Substream										
Phase		Vapor Phase	Vapor Phase	Vapor Phase	Vapor Phase	Vapor Phase		Liquid Phase	Liquid Phase	Liquid Phase
Temperature	K	298.15	1073	1073	1073	1073	298.15	298.15	298.15	298.15
Pressure	atm	1	1	1	1	1	1	1	1	1
Molar Vapor Fraction		1	1	1	1	1	0.619352	0	0	0
Molar Liquid Fraction		0	0	0	0	0	0.380648	1	1	1
Molar Solid Fraction		0	0	0	0	0	0	0	0	0
Mass Vapor Fraction		1	1	1	1	1	0.185199	0	0	0
Mass Liquid Fraction		0	0	0	0	0	0.814801	1	1	1
Mass Solid Fraction		0	0	0	0	0	0	0	0	0
Molar Enthalpy	J/kmol	3.72529e-09	2.52537e+07	-4.90781e+07	-2.12774e+08	-7.13777e+07	-1.13468e+08	-2.858e+08	-2.858e+08	-2.858e+08
Mass Enthalpy	J/kg	1.84797e-09	789207	-3.54153e+06	-1.18108e+07	-8.48155e+06	-1.3483e+07	-1.58643e+07	-1.58643e+07	-1.58643e+07
Molar Entropy	J/kmol-K	0	40883.5	36355.4	2410.73	29158.1	-62238.4	-163139	-163139	-163139
Mass Entropy	J/kg-K	0	1277.66	2623.44	133.816	3464.75	-7395.56	-9055.61	-9055.61	-9055.61
Molar Density	kmol/cum	0.0408747	0.0113577	0.0113577	0.0113577	0.0113577	0.0659659	55.173	55.173	55.173
Mass Density	kg/cum	0.0823985	0.363432	0.157394	0.204612	0.0955821	0.555145	993.957	993.957	993.957
Enthalpy Flow	kJ/sec	2.03339e-18	0.00689215	-0.0580417	-0.193566	-0.0649339	-0.103224	-0.155999	-0.259999	-0.104
Average MW		2.01588	31.9988	13.8579	18.0153	8.41564	8.41564	18.0153	18.0153	18.0153
+ Mole Flows	**kmol/sec**	**5.45833e-07**	**2.72917e-07**	**1.18264e-06**	**9.09722e-07**	**9.09722e-07**	**9.09722e-07**	**5.45833e-07**	**9.09722e-07**	**3.63889e-07**
− Mole Fractions										
WATER		0	0	0.307692	1	0.4	0.4	1	1	1
H2		1	0	0.461538	0	0.6	0.6	0	0	0
O2		0	1	0.230769	0	0	0	0	0	0
+ Mass Flows	**kg/sec**	**1.10033e-06**	**8.73301e-06**	**1.63889e-05**	**1.63889e-05**	**7.65589e-06**	**7.65589e-06**	**9.83334e-06**	**1.63889e-05**	**6.55556e-06**
+ Mass Fractions										
Volume Flow	cum/sec	1.33538e-05	2.40293e-05	0.000104127	8.00975e-05	8.00975e-05	1.37908e-05	9.89312e-09	1.64885e-08	6.59542e-09
− Gibbs energy, pure component										
WATER	kJ/mol			-215.361	-215.361	-215.361	-231.841	-237.16	-237.16	-237.16
H2	kJ/mol	3.72529e-15		-17.5263		-17.5263	9.02414			
O2	kJ/mol		-18.6143	-18.6143						
Gibbs energy, mixture	kJ/mol	3.72529e-15	-18.6143	-88.0874	-215.361	-102.664	-94.9114	-237.16	-237.16	-237.16
+ Vapor Phase										

Table 8: Results Flowsheet from Electrolysis Cell Model at 1073 K

	Units	H2OUT	O2OUT	POST	PRE	RE1	RE2	WATERIN	WATERMIX	WATERRE
Description										
From		SEP2	SEP	RSTOIC	HEATER	SEP	CONDENS		MIXER	SEP2
To				SEP	RSTOIC	CONDENS	SEP2	MIXER	HEATER	MIXER
Stream Class		CONVEN	CONVEN	CONVEN	CONVEN	CONVEN	CONVEN	CONVEN	CONVEN	CONVEN
Maximum Relative Error										
Cost Flow	$/sec									
− MIXED Substream										
Phase		Vapor Phase	Vapor Phase	Vapor Phase	Vapor Phase	Vapor Phase		Liquid Phase	Liquid Phase	Liquid Phase
Temperature	K	298.15	1173	1173	1173	1173	298.15	298.15	298.15	298.15
Pressure	atm	1	1	1	1	1	1	1	1	1
Molar Vapor Fraction		1	1	1	1	1	0.619352	0	0	0
Molar Liquid Fraction		0	0	0	0	0	0.380648	1	1	1
Molar Solid Fraction		0	0	0	0	0	0	0	0	0
Mass Vapor Fraction		1	1	1	1	1	0.185199	0	0	0
Mass Liquid Fraction		0	0	0	0	0	0.814801	1	1	1
Mass Solid Fraction		0	0	0	0	0	0	0	0	0
Molar Enthalpy	J/kmol	3.72529e-09	2.87924e+07	-4.55269e+07	-2.08493e+08	-6.78227e+07	-1.13468e+08	-2.858e+08	-2.858e+08	-2.858e+08
Mass Enthalpy	J/kg	1.84797e-09	899798	-3.28526e+06	-1.15731e+07	-8.05912e+06	-1.3483e+07	-1.58643e+07	-1.58643e+07	-1.58643e+07
Molar Entropy	J/kmol-K	0	44036.5	39519.3	6224.65	32325.3	-62238.4	-163139	-163139	-163139
Mass Entropy	J/kg-K	0	1376.19	2851.75	345.521	3841.1	-7395.56	-9055.61	-9055.61	-9055.61
Molar Density	kmol/cum	0.0408747	0.0103894	0.0103894	0.0103894	0.0103894	0.0659659	55.173	55.173	55.173
Mass Density	kg/cum	0.0823985	0.332449	0.143976	0.187168	0.0874336	0.555145	993.957	993.957	993.957
Enthalpy Flow	kJ/sec	2.03339e-18	0.00785794	-0.0538419	-0.189671	-0.0616998	-0.103224	-0.155999	-0.259999	-0.104
Average MW		2.01588	31.9988	13.8579	18.0153	8.41564	8.41564	18.0153	18.0153	18.0153
+ Mole Flows	**mol/min**	**0.03275**	**0.016375**	**0.0709583**	**0.0545833**	**0.0545833**	**0.0545833**	**0.03275**	**0.0545833**	**0.0218333**
− Mole Fractions										
WATER		0	0	0.307692	1	0.4	0.4	1	1	1
H2		1	0	0.461538	0	0.6	0.6	0	0	0
O2		0	1	0.230769	0	0	0	0	0	0
+ Mass Flows	**kg/sec**	**1.10033e-06**	**8.73301e-06**	**1.63889e-05**	**1.63889e-05**	**7.65589e-06**	**7.65589e-06**	**9.83334e-06**	**1.63889e-05**	**6.55556e-06**
+ Mass Fractions										
Volume Flow	cum/sec	1.33538e-05	2.62687e-05	0.000113831	8.75624e-05	8.75624e-05	1.37908e-05	9.89312e-09	1.64885e-08	6.59542e-09
− Gibbs energy, pure component										
WATER	kJ/mol			-215.795	-215.795	-215.795	-231.841	-237.16	-237.16	-237.16
H2	kJ/mol	3.72529e-15		-21.4311		-21.4311	9.02414			
O2	kJ/mol		-22.8623	-22.8623						
Gibbs energy, mixture	kJ/mol	3.72529e-15	-22.8623	-91.883	-215.795	-105.74	-94.9114	-237.16	-237.16	-237.16
+ Vapor Phase										

Table 9: Results Flowsheet from Electrolysis Cell Model at 1173 K

	Units	H2OUT	O2OUT	POST	PRE	RE1	RE2	WATERIN	WATERMIX	WATERRE
Description										
From		SEP2	SEP	RSTOIC	HEATER	SEP	CONDENS		MIXER	SEP2
To				SEP	RSTOIC	CONDENS	SEP2	MIXER	HEATER	MIXER
Stream Class		CONVEN	CONVEN	CONVEN	CONVEN	CONVEN	CONVEN	CONVEN	CONVEN	CONVEN
Maximum Relative Error										
Cost Flow	$/sec									
− MIXED Substream										
Phase		Vapor Phase	Vapor Phase	Vapor Phase	Vapor Phase	Vapor Phase		Liquid Phase	Liquid Phase	Liquid Phase
Temperature	K	298.15	1273	1273	1273	1273	298.15	298.15	298.15	298.15
Pressure	atm	1	1	1	1	1	1	1	1	1
Molar Vapor Fraction		1	1	1	1	1	0.619352	0	0	0
Molar Liquid Fraction		0	0	0	0	0	0.380648	1	1	1
Molar Solid Fraction		0	0	0	0	0	0	0	0	0
Mass Vapor Fraction		1	1	1	1	1	0.185199	0	0	0
Mass Liquid Fraction		0	0	0	0	0	0.814801	1	1	1
Mass Solid Fraction		0	0	0	0	0	0	0	0	0
Molar Enthalpy	J/kmol	3.72529e-09	3.23675e+07	-4.19101e+07	-2.04089e+08	-6.41934e+07	-1.13468e+08	-2.858e+08	-2.858e+08	-2.858e+08
Mass Enthalpy	J/kg	1.84797e-09	1.01152e+06	-3.02427e+06	-1.13287e+07	-7.62786e+06	-1.3483e+07	-1.58643e+07	-1.58643e+07	-1.58643e+07
Molar Entropy	J/kmol-K	0	46961.1	42477.9	9826.72	35294.1	-62238.4	-163139	-163139	-163139
Mass Entropy	J/kg-K	0	1467.59	3065.25	545.466	4193.87	-7395.56	-9055.61	-9055.61	-9055.61
Molar Density	kmol/cum	0.0408747	0.00957328	0.00957328	0.00957328	0.00957328	0.0659659	55.173	55.173	55.173
Mass Density	kg/cum	0.0823985	0.306334	0.132666	0.172465	0.0805653	0.555145	993.957	993.957	993.957
Enthalpy Flow	kJ/sec	2.03339e-18	0.00883362	-0.0495645	-0.185665	-0.0583981	-0.103224	-0.155999	-0.259999	-0.104
Average MW		2.01588	31.9988	13.8579	18.0153	8.41564	8.41564	18.0153	18.0153	18.0153
+ Mole Flows	**mol/min**	**0.03275**	**0.016375**	**0.0709583**	**0.0545833**	**0.0545833**	**0.0545833**	**0.03275**	**0.0545833**	**0.0218333**
− Mole Fractions										
WATER		0	0	0.307692	1	0.4	0.4	1	1	1
H2		1	0	0.461538	0	0.6	0.6	0	0	0
O2		0	1	0.230769	0	0	0	0	0	0
+ Mass Flows	**kg/sec**	**1.10033e-06**	**8.73301e-06**	**1.63889e-05**	**1.63889e-05**	**7.65589e-06**	**7.65589e-06**	**9.83334e-06**	**1.63889e-05**	**6.55556e-06**
+ Mass Fractions										
Volume Flow	cum/sec	1.33538e-05	2.85082e-05	0.000123535	9.50272e-05	9.50272e-05	1.37908e-05	9.89312e-09	1.64885e-08	6.59542e-09
− Gibbs energy, pure component										
WATER	kJ/mol			-216.599	-216.599	-216.599	-231.841	-237.16	-237.16	-237.16
H2	kJ/mol	3.72529e-15		-25.5999		-25.5999	9.02414			
O2	kJ/mol		-27.414	-27.414						
Gibbs energy, mixture	kJ/mol	3.72529e-15	-27.414	-95.9845	-216.599	-109.123	-94.9114	-237.16	-237.16	-237.16
+ Vapor Phase										

Table 10: Results Flowsheet from Electrolysis Cell Model at 1273 K

9.4 Appendix D: IDAES Simulation Code - Fuel Cells

(Note: If reused, remember to change all necessary parameters values to suit your needs, such as T (temperature), E_act (actual voltage calculation))

```
# Constant Values
R = 8.314 # J/K mol
F = 96485 # C/mol
P_ref = 1 # atm reference is 1atm
i_L = 6500 * 0.0001 # A/cm^2 assumed/input
a = 0.05 #Correction constant assumed/input
B = 0.5 # transfer coefficient assumed/input
gam_a = 2.0*10**8 * 0.0001 # A/cm^2
gam_c = 1.5*10**8 * 0.0001 # A/cm^2
e_a = 105000 #J/mol
e_c = 110000 #J/mol

import matplotlib.pyplot as plt
import numpy as np
import pytablewriter


from pytablewriter.style import Style
table1 = pytablewriter.MarkdownTableWriter()
table1.table_name = "SOFC Constant Values and Assumptions"
table1.header_list = ["Constant", "Symbol", "Value", "Units"]
table1.value_matrix = [
["Universal Gas Constant", "R", format(R), "J/K mol"],
["Faraday Constant", "F", format(F, ".1f"), "C/mol"],
["Reference Pressure", "P_ref", format(P_ref, ".1f"), "atm"],
["Limiting Current Density", "i_L", format(i_L, ".3f"), "A/cm^2"],
["Limiting Current Density Correction Factor", "a", format(a, ".3f"), "-"],
["Transfer Coefficient", "B", format(B, ".3f"), "-"],
["Pre-exponential Factor: Anode", "gam_a", format(gam_a, ".3f"), "A/cm^2"],
["Pre-exponential Factor: Cathode", "gam_c", format(gam_c, ".3f"), "A/cm^2"],
["Activation Energy: Anode", "e_a", format(e_a, ".3f"), "J/mol"],
["Activation Energy: Cathode", "e_c", format(e_c, ".3f"), "J/mol"]
]
table1

# Input Parameters
T = 1073 # K
fuelU = 1
H2_p = 0.5 # atm assumed that anolyte is purely H2
O2_p = 0.21 # atm air is 21% O2
```

```
H2O_p = 0.5 # atm all anolyte becomes H2O
R_ohm = 0.5 # ohm*cm^2 assumed/input

inputtable = pytablewriter.MarkdownTableWriter()
inputtable.table_name = "SOFC Input Values"
inputtable.header_list = ["Input", "Symbol", "Value", "Units"]
inputtable.value_matrix = [
["SOFC Operating Temp", "T", format(T, ".1f"), "K"],
["Fuel Utilization", "fuelU", format(fuelU, ".1f"), ""],
["Input Anolyte Pressure", "H2_p", format(H2_p, ".1f"), "atm"],
["Output Anolyte Pressure", "H2O_p", format(H2O_p, ".1f"), "atm"],
["Catholyte Pressure", "O2_p", format(O2_p, ".2f"), "atm"],
["SOFC Resistance", "R_ohm", format(R_ohm, ".2f"), "ohm*cm^2"],
]
inputtable

# Nernst Term Calculation for Open Circuit Voltage
nernstterm = ((R*T)/(2*F))*np.log((((H2_p/P_ref)*(np.sqrt((O2_p/P_ref))))/(H2O_p/P_ref)))
print("Nernst Term: " + format(nernstterm, ".2f"))


# Gibbs Energy Change Calculation
Gibb = (-241.82 + (0.044423*T))*1000

# Open Circuit Voltage Calculation
E_rev = ((Gibb/(2*F)) + nernstterm )*-1
print("Open-Circuit Voltage (in Volts): " + format(E_rev, ".3f"))

# Actual Current Density
# i_act = i_op + i_l # actual current density
# i_act = 0.32 # A/cm^2
# i_act = np.array([0.1, 0.12, 0.14, 0.16, 0.18, 0.2, 0.22, 0.24, 0.26, 0.28, 0.30, 0.32, 0.34, 0.36,
0.38, 0.4, 0.42, 0.44, 0.46, 0.48, 0.50, ])
i_act = np.arange(0.01, 0.61, 0.02)
#i_act = np.array([0.0001, 0.001, 0.01, 0.1])

# Activation Loss Calculation
# Anode Exchange Current Density
i_0a = gam_a + ((H2_p/P_ref)*(H2O_p/P_ref)*np.exp(e_a/(R*T)))

# Ohmic Loss Calculation
E_ohm = i_act*R_ohm
print("Ohmic loss: ", E_ohm)
```

```
# Concentration Loss Calculation
i_Ladj = i_L*((H2_p/P_ref)**a)
E_conc = ((R*T)/(2*F))*np.log(1-(i_act/i_Ladj))
# print("Concentration loss: " + format(E_conc, ".3f"))
print("Concentration loss: " , E_conc)


E_activ_a = np.log(i_act/i_0a)*(-(1-B)/B)*((R*T)/F)
# Cathode Exchange Current Density
i_0c = gam_c + (((O2_p/P_ref)**0.25)*np.exp(e_c/(R*T)))
E_activ_c = np.log(i_act/i_0c)*(-(1-B)/B)*((R*T)/F)
E_activ = (E_activ_a - E_activ_c)/2
# print("Activation loss: " + format(E_activ, ".3f"))
print("Activation loss: " , E_activ)
all
# Actual SOFC Voltage Calculation
E_act = E_rev - E_ohm + E_conc + E_activ
# print("Actual SOFC Voltage: " + format(E_act, ".3f"))
print("Actual SOFC Voltage (in Volts): " , E_act)

x = i_act
y = E_act
plt.scatter(x, y, marker='D', s=5)
plt.xlabel('Current Density (A/cm^2)')
plt.ylabel('Voltage (V)')
plt.title('SOFC Polarization Curve')
plt.show()

n_H2react = 1
# Rate of Current Produced by SOFC stack per mole fuel
I = 2 * n_H2react * F
print("Rate of Current Produced by SOFC stack per mole fuel:", I, "Coulombs/mole")

W_netSOFC = E_act * I
print("Total Power (in Watts): " , W_netSOFC)

x = i_act
y = E_act/E_rev
plt.scatter(x, y, marker='D', s=5)
plt.xlabel('Current Density (A/cm^2)')
plt.ylabel('Voltage Efficiency')
plt.title('SOFC Efficiency Curve')
plt.show()
```

9.5 Appendix D: IDAES Simulation Code - Electrolyzer Cells

(Note: If reused, remember to change all necessary parameters values to suit your needs, such as T (temperature), E_act (actual voltage calculation))

```
# Constant Values
R = 8.314 # J/K mol
F = 96485 # C/mol
P_ref = 1 # atm reference is 1atm
i_L = 6500 * 0.0001 # A/cm^2 assumed/input
a = 0.05 #Correction constant assumed/input
B = 0.5 # transfer coefficient assumed/input
gam_a = 2.0*10**8 * 0.0001 # A/cm^2
gam_c = 1.5*10**8 * 0.0001 # A/cm^2
e_a = 105000 #J/mol
e_c = 110000 #J/mol

import matplotlib.pyplot as plt
import numpy as np
import pytablewriter


from pytablewriter.style import Style
table1 = pytablewriter.MarkdownTableWriter()
table1.table_name = "SOEC Constant Values and Assumptions"
table1.header_list = ["Constant", "Symbol", "Value", "Units"]
table1.value_matrix = [
["Universal Gas Constant", "R", format(R), "J/K mol"],
["Faraday Constant", "F", format(F, ".1f"), "C/mol"],
["Reference Pressure", "P_ref", format(P_ref, ".1f"), "atm"],
["Limiting Current Density", "i_L", format(i_L, ".3f"), "A/cm^2"],
["Limiting Current Density Correction Factor", "a", format(a, ".3f"), "-"],
["Transfer Coefficient", "B", format(B, ".3f"), "-"],
["Pre-exponential Factor: Anode", "gam_a", format(gam_a, ".3f"), "A/cm^2"],
["Pre-exponential Factor: Cathode", "gam_c", format(gam_c, ".3f"), "A/cm^2"],
["Activation Energy: Anode", "e_a", format(e_a, ".3f"), "J/mol"],
["Activation Energy: Cathode", "e_c", format(e_c, ".3f"), "J/mol"]
]
table1

# Input Parameters
T = 1073 # K
fuelU = 1
H2_p = 0.5 # atm assumed that anolyte is purely H2
O2_p = 0.21 # atm air is 21% O2
```

```
H2O_p = 0.5 # atm all anolyte becomes H2O
R_ohm = 0.5 # ohm*cm^2 assumed/input

inputtable = pytablewriter.MarkdownTableWriter()
inputtable.table_name = "SOEC Input Values"
inputtable.header_list = ["Input", "Symbol", "Value", "Units"]
inputtable.value_matrix = [
["SOEC Operating Temp", "T", format(T, ".1f"), "K"],
["Fuel Utilization", "fuelU", format(fuelU, ".1f"), ""],
["Input Anolyte Pressure", "H2_p", format(H2_p, ".1f"), "atm"],
["Output Anolyte Pressure", "H2O_p", format(H2O_p, ".1f"), "atm"],
["Catholyte Pressure", "O2_p", format(O2_p, ".2f"), "atm"],
["SOEC Resistance", "R_ohm", format(R_ohm, ".2f"), "ohm*cm^2"],
]
inputtable

# Nernst Term Calculation for Open Circuit Voltage
nernstterm = ((R*T)/(2*F))*np.log((((H2_p/P_ref)*(np.sqrt((O2_p/P_ref))))/(H2O_p/P_ref)))
print("Nernst Term: " + format(nernstterm, ".2f"))


# Gibbs Energy Change Calculation
Gibb = (-241.82 + (0.044423*T))*1000

# Open Circuit Voltage Calculation
E_rev = ((Gibb/(2*F)) + nernstterm )*-1
print("Open-Circuit Voltage (in Volts): " + format(E_rev, ".3f"))

# Actual Current Density
# i_act = i_op + i_l # actual current density
# i_act = 0.32 # A/cm^2
# i_act = np.array([0.1, 0.12, 0.14, 0.16, 0.18, 0.2, 0.22, 0.24, 0.26, 0.28, 0.30, 0.32, 0.34, 0.36,
0.38, 0.4, 0.42, 0.44, 0.46, 0.48, 0.50, ])
i_act = np.arange(0.01, 0.61, 0.02)
#i_act = np.array([0.0001, 0.001, 0.01, 0.1])

# Activation Loss Calculation
# Anode Exchange Current Density
i_0a = gam_a + ((H2_p/P_ref)*(H2O_p/P_ref)*np.exp(e_a/(R*T)))

# Ohmic Loss Calculation
E_ohm = i_act*R_ohm
print("Ohmic loss: ", E_ohm)
```

```
# Concentration Loss Calculation
i_Ladj = i_L*((H2_p/P_ref)**a)
E_conc = ((R*T)/(2*F))*np.log(1-(i_act/i_Ladj))
# print("Concentration loss: " + format(E_conc, ".3f"))
print("Concentration loss: " , E_conc)


E_activ_a = np.log(i_act/i_0a)*(-(1-B)/B)*((R*T)/F)
# Cathode Exchange Current Density
i_0c = gam_c + (((O2_p/P_ref)**0.25)*np.exp(e_c/(R*T)))
E_activ_c = np.log(i_act/i_0c)*(-(1-B)/B)*((R*T)/F)
E_activ = (E_activ_a - E_activ_c)/2
# print("Activation loss: " + format(E_activ, ".3f"))
print("Activation loss: " , E_activ)

# Actual SOEC Voltage Calculation
E_act = E_rev + E_ohm - E_conc - E_activ
# print("Actual SOEC Voltage: " + format(E_act, ".3f"))
print("Actual SOEC Voltage (in Volts): " , E_act)

x = i_act
y = E_act
plt.scatter(x, y, marker='D', s=5)
plt.xlabel('Current Density (A/cm^2)')
plt.ylabel('Voltage (V)')
plt.title('SOEC Polarization Curve')
plt.show()

n_H2react = 1
# Rate of Current Produced by SOEC stack per mole fuel
I = 2 * n_H2react * F
print("Rate of Current Produced by SOEC stack per mole fuel:", I, "Coulombs/mole")

W_netSOEC = E_act * I
print("Total Power (in Watts): " , W_netSOEC)

x = i_act
y = E_act/E_rev
plt.scatter(x, y, marker='D', s=5)
plt.xlabel('Current Density (A/cm^2)')
plt.ylabel('Voltage Efficiency')
plt.title('SOEC Efficiency Curve')
plt.show()
```

9.6 Appendix F: IDAES Simulation Results - Fuel Cells

```
Nernst Term: -0.04
Open-Circuit Voltage (in Volts): 1.042
Ohmic loss:  [0.005 0.015 0.025 0.035 0.045 0.055 0.065 0.075 0.085 0.095 0.105 0.115
 0.125 0.135 0.145 0.155 0.165 0.175 0.185 0.195 0.205 0.215 0.225 0.235
 0.245 0.255 0.265 0.275 0.285 0.295 0.305]
Concentration loss:  [-0.00074223 -0.00226343 -0.0038364  -0.00546477 -0.00715261 -0.00890441
 -0.01072521 -0.01262068 -0.0145972  -0.01666202 -0.01882338 -0.02109078
 -0.02347515 -0.02598921 -0.02864789 -0.03146886 -0.03447322 -0.03768647
 -0.04113987 -0.04487221 -0.04893256 -0.05338418 -0.05831057 -0.06382526
 -0.07008804 -0.07733419 -0.08593114 -0.09650057 -0.11022577 -0.12983376
 -0.1645694 ]
Activation loss:  [-0.05401382 -0.05401382 -0.05401382 -0.05401382 -0.05401382 -0.05401382
 -0.05401382 -0.05401382 -0.05401382 -0.05401382 -0.05401382 -0.05401382
 -0.05401382 -0.05401382 -0.05401382 -0.05401382 -0.05401382 -0.05401382
 -0.05401382 -0.05401382 -0.05401382 -0.05401382 -0.05401382 -0.05401382
 -0.05401382 -0.05401382 -0.05401382 -0.05401382 -0.05401382 -0.05401382
 -0.05401382]
Actual SOFC Voltage (in Volts):  [0.98245429 0.97093309 0.95936013 0.94773175 0.93604392 0.92429212
 0.91247131 0.90057584 0.88859932 0.87653451 0.86437314 0.85210574
 0.83972138 0.82720732 0.81454863 0.80172766 0.78872331 0.77551005
 0.76205666 0.74832431 0.73426396 0.71981235 0.70488595 0.68937126
 0.67310849 0.65586233 0.63726538 0.61669595 0.59297075 0.56336276
 0.51862712]
```

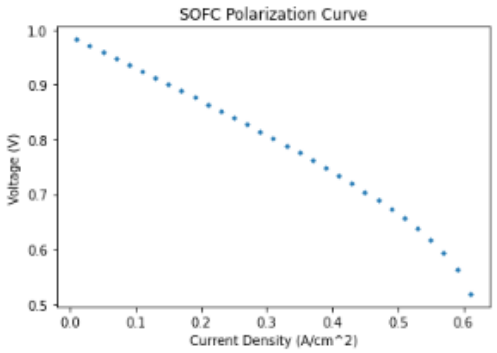


```
Rate of Current Produced by SOFC stack per mole fuel: 192970 Coulombs/mole
Total Power (in Watts):  [189584.20463412 187360.95851272 185127.72353258 182883.7958668
 180628.39457473 178360.64990841 176079.58931491 173784.12056717
 171473.01128633 169144.86388756 166798.08466438 164430.84528488
 162041.03434883 159626.19575869 157183.44934814 154709.38726207
 152199.93661661 149650.17434895 147054.07278049 144404.14224365
 141690.91636504 138902.18877806 136021.84166454 133027.97248758
 129889.74482916 126561.75360541 122973.10113253 119003.81802986
 114425.56589948 108712.11205234 100079.47593047]
```

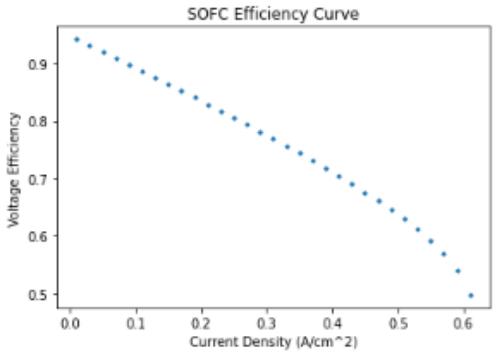

Table 11: Results from Fuel Cell Model at 1073 K

```
Nernst Term: -0.04
Open-Circuit Voltage (in Volts): 1.023
Ohmic loss:  [0.005 0.015 0.025 0.035 0.045 0.055 0.065 0.075 0.085 0.095 0.105 0.115
 0.125 0.135 0.145 0.155 0.165 0.175 0.185 0.195 0.205 0.215 0.225 0.235
 0.245 0.255 0.265 0.275 0.285 0.295 0.305]
Concentration loss:  [-0.00081141 -0.00247438 -0.00419394 -0.00597407 -0.00781921 -0.00973427
 -0.01172476 -0.01379689 -0.01595761 -0.01821486 -0.02057766 -0.02305637
 -0.02566295 -0.02841131 -0.03131778 -0.03440165 -0.037686   -0.04119873
 -0.04497397 -0.04905415 -0.05349291 -0.0583594  -0.06374492 -0.06977356
 -0.07662001 -0.08454148 -0.09393963 -0.1054941  -0.12049844 -0.14193383
 -0.17990672]
Activation loss:  [-0.03876612 -0.03876612 -0.03876612 -0.03876612 -0.03876612 -0.03876612
 -0.03876612 -0.03876612 -0.03876612 -0.03876612 -0.03876612 -0.03876612
 -0.03876612 -0.03876612 -0.03876612 -0.03876612 -0.03876612 -0.03876612
 -0.03876612 -0.03876612 -0.03876612 -0.03876612 -0.03876612 -0.03876612
 -0.03876612 -0.03876612 -0.03876612 -0.03876612 -0.03876612 -0.03876612
 -0.03876612]
Actual SOFC Voltage (in Volts):  [0.97797411 0.96631114 0.95459158 0.94281145 0.93096631 0.91905125
 0.90706076 0.89498864 0.88282791 0.87057066 0.85820786 0.84572915
 0.83312257 0.82037421 0.80746774 0.79438387 0.78109952 0.76758679
 0.75381155 0.73973137 0.72529261 0.71042612 0.6950406  0.67901196
 0.66216551 0.64424404 0.62484589 0.60329142 0.57828708 0.54685169
 0.4988788 ]
```

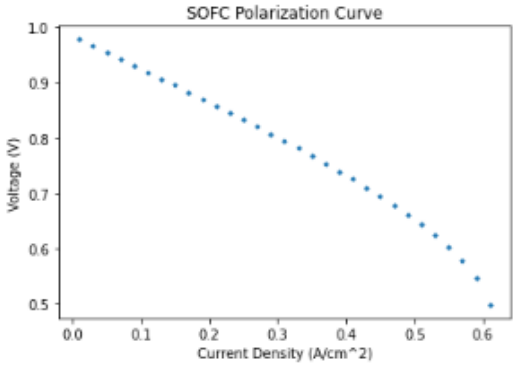


```
Rate of Current Produced by SOFC stack per mole fuel: 192970 Coulombs/mole
Total Power (in Watts):  [188719.66494266 186469.06130761 184207.5378857  181934.32525573
 179648.56969599 177349.32040094 175035.51417897 172705.95701112
 170359.30166497 167994.02030545 165608.37069801 163200.35411631
 160767.66238473 158307.61050567 155817.04989097 153292.25508486
 150728.77362435 148121.22363371 145463.0156749  142745.96206844
 139959.71420674 137090.92813076 134121.98389576 131028.93772188
 127778.0793404  124319.77206598 120576.51078854 116417.14538367
 111592.05708083 105525.97006993  96268.64279039]
```

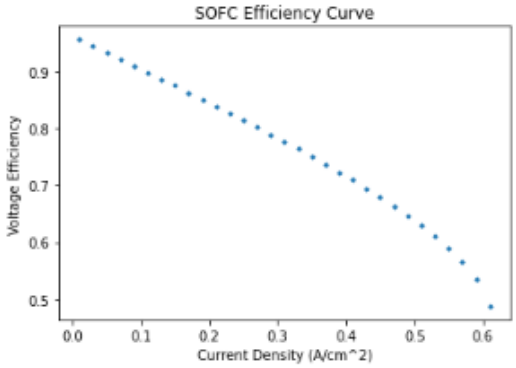

Table 12: Results from Fuel Cell Model at 1173 K

```
Nernst Term: -0.04
Open-Circuit Voltage (in Volts): 1.003
Ohmic loss:  [0.005 0.015 0.025 0.035 0.045 0.055 0.065 0.075 0.085 0.095 0.105 0.115
 0.125 0.135 0.145 0.155 0.165 0.175 0.185 0.195 0.205 0.215 0.225 0.235
 0.245 0.255 0.265 0.275 0.285 0.295 0.305]
Concentration loss:  [-0.00088058 -0.00268532 -0.00455148 -0.00648337 -0.00848581 -0.01056413
 -0.01272432 -0.01497309 -0.01731802 -0.0197677  -0.02233194 -0.02502196
 -0.02785076 -0.03083342 -0.03398767 -0.03733444 -0.04089879 -0.04471098
 -0.04880806 -0.05323609 -0.05805327 -0.06333463 -0.06917927 -0.07572186
 -0.08315198 -0.09174877 -0.10194813 -0.11448763 -0.13077112 -0.1540339
 -0.19524403]
Activation loss:  [-0.02145213 -0.02145213 -0.02145213 -0.02145213 -0.02145213 -0.02145213 -0.02145213
 -0.02145213 -0.02145213 -0.02145213 -0.02145213 -0.02145213 -0.02145213
 -0.02145213 -0.02145213 -0.02145213 -0.02145213 -0.02145213 -0.02145213
 -0.02145213 -0.02145213 -0.02145213 -0.02145213 -0.02145213 -0.02145213
 -0.02145213 -0.02145213 -0.02145213 -0.02145213 -0.02145213 -0.02145213
 -0.02145213]
Actual SOFC Voltage (in Volts):  [0.97556024 0.9637555  0.95188934 0.93995745 0.92795501 0.91587669
 0.9037165  0.89146773 0.8791228  0.86667311 0.85410888 0.84141886
 0.82859006 0.8156074  0.80245315 0.78910637 0.77554203 0.76172984
 0.74763276 0.73320473 0.71838755 0.70310619 0.68726155 0.67071896
 0.65328884 0.63469205 0.61449269 0.59195319 0.5656697  0.53240691
 0.48119679]
```

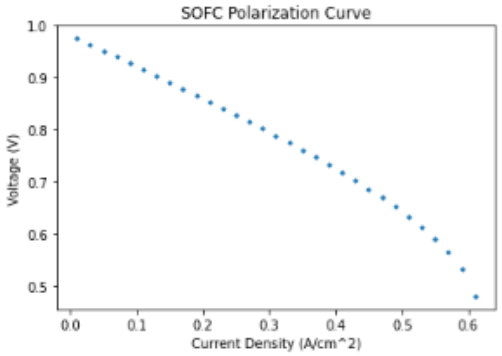


```
Rate of Current Produced by SOFC stack per mole fuel: 192970 Coulombs/mole
Total Power (in Watts):  [188253.85952044 185975.89837175 183686.08650808 181383.58891392
 179067.47908651 176736.72516273 174390.17331228 172026.52772433
 169644.32631286 167241.9109926  164817.39100089 162368.59721701
 159893.02468989 157387.75952191 154849.38470306 152273.8571769
 149656.34490134 146991.00718771 144270.69283855 141486.5161625
 138627.2463177  135678.40175272 132620.86039624 129428.63722543
 126065.14812089 122476.52479579 118578.65471381 114229.20700672
 109157.28253144 102738.56235678  92856.54391956]
```

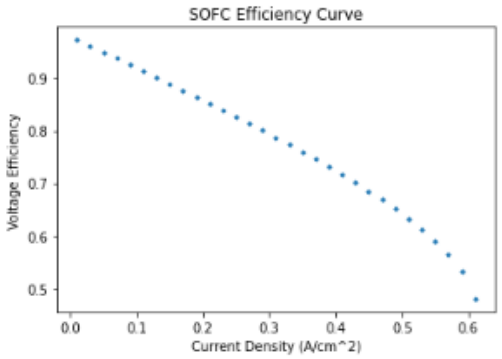

Table 13: Results from Fuel Cell Model at 1273 K

9.7 Appendix G: IDAES Simulation Results - Electrolyzer Cells

```
Nernst Term: -0.04
Open-Circuit Voltage (in Volts): 1.042
Ohmic loss:  [0.005 0.015 0.025 0.035 0.045 0.055 0.065 0.075 0.085 0.095 0.105 0.115
 0.125 0.135 0.145 0.155 0.165 0.175 0.185 0.195 0.205 0.215 0.225 0.235
 0.245 0.255 0.265 0.275 0.285 0.295 0.305]
Concentration loss:  [-0.00074223 -0.00226343 -0.0038364  -0.00546477 -0.00715261 -0.00890441
 -0.01072521 -0.01262068 -0.0145972  -0.01666202 -0.01882338 -0.02109078
 -0.02347515 -0.02598921 -0.02864789 -0.03146886 -0.03447322 -0.03768647
 -0.04113987 -0.04487221 -0.04893256 -0.05338418 -0.05831057 -0.06382526
 -0.07008804 -0.07733419 -0.08593114 -0.09650057 -0.11022577 -0.12983376
 -0.1645694 ]
Activation loss:  [-0.05401382 -0.05401382 -0.05401382 -0.05401382 -0.05401382 -0.05401382
 -0.05401382 -0.05401382 -0.05401382 -0.05401382 -0.05401382 -0.05401382
 -0.05401382 -0.05401382 -0.05401382 -0.05401382 -0.05401382 -0.05401382
 -0.05401382 -0.05401382 -0.05401382 -0.05401382 -0.05401382 -0.05401382
 -0.05401382 -0.05401382 -0.05401382 -0.05401382 -0.05401382 -0.05401382
 -0.05401382]
Actual SOEC Voltage (in Volts):  [1.10196639 1.11348759 1.12506056 1.13668893 1.14837676 1.16012856
 1.17194937 1.18384484 1.19582136 1.20788617 1.22004754 1.23231494
 1.2446993  1.25721337 1.26987205 1.28269302 1.29569737 1.30891063
 1.32236403 1.33609637 1.35015672 1.36460833 1.37953473 1.39504942
 1.41131219 1.42855835 1.4471553  1.46772473 1.49144993 1.52105792
 1.56579356]
```

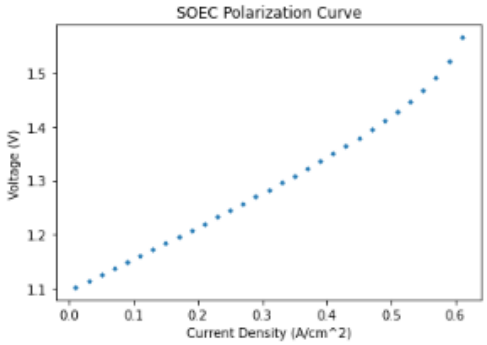


```
Rate of Current Produced by SOEC stack per mole fuel: 192970 Coulombs/mole
Total Power (in Watts):  [212646.45419762 214869.70031903 217102.93529917 219346.86296495
 221602.26425702 223870.00892333 226151.06951683 228446.53826458
 230757.64754541 233085.79494419 235432.57416736 237799.81354687
 240189.62448292 242604.46307306 245047.2094836  247521.27156967
 250030.72221514 252580.48448279 255176.58605125 257826.5165881
 260539.7424667  263328.47005368 266208.8171672  269202.68634417
 272340.91400259 275668.90522633 279257.55769921 283226.84080188
 287805.09293227 293518.54677941 302151.18290127]
```

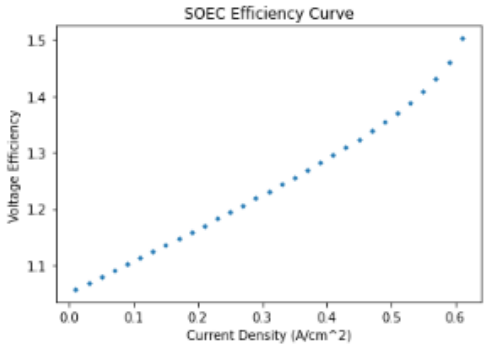

Table 14: Results from Electrolyzer Cell Model at 1073 K

```
Nernst Term: -0.04
Open-Circuit Voltage (in Volts): 1.023
Ohmic loss:  [0.005 0.015 0.025 0.035 0.045 0.055 0.065 0.075 0.085 0.095 0.105 0.115
 0.125 0.135 0.145 0.155 0.165 0.175 0.185 0.195 0.205 0.215 0.225 0.235
 0.245 0.255 0.265 0.275 0.285 0.295 0.305]
Concentration loss:  [-0.00081141 -0.00247438 -0.00419394 -0.00597407 -0.00781921 -0.00973427
 -0.01172476 -0.01379689 -0.01595761 -0.01821486 -0.02057766 -0.02305637
 -0.02566295 -0.02841131 -0.03131778 -0.03440165 -0.037686   -0.04119873
 -0.04497397 -0.04905415 -0.05349291 -0.0583594  -0.06374492 -0.06977356
 -0.07662001 -0.08454148 -0.09393963 -0.1054941  -0.12049844 -0.14193383
 -0.17990672]
Activation loss:  [-0.03876612 -0.03876612 -0.03876612 -0.03876612 -0.03876612 -0.03876612
 -0.03876612 -0.03876612 -0.03876612 -0.03876612 -0.03876612 -0.03876612
 -0.03876612 -0.03876612 -0.03876612 -0.03876612 -0.03876612 -0.03876612
 -0.03876612 -0.03876612 -0.03876612 -0.03876612 -0.03876612 -0.03876612
 -0.03876612 -0.03876612 -0.03876612 -0.03876612 -0.03876612 -0.03876612
 -0.03876612]
Actual SOEC Voltage (in Volts):  [1.06712917 1.07879214 1.0905117  1.10229184 1.11413697 1.12605203
 1.13804253 1.15011465 1.16227538 1.17453263 1.18689543 1.19937414
 1.21198072 1.22472908 1.23763555 1.25071942 1.26400377 1.27751649
 1.29129173 1.30537192 1.31981068 1.33467717 1.35006269 1.36609133
 1.38293777 1.40085925 1.4202574  1.44181187 1.46681621 1.4982516
 1.54622448]
```

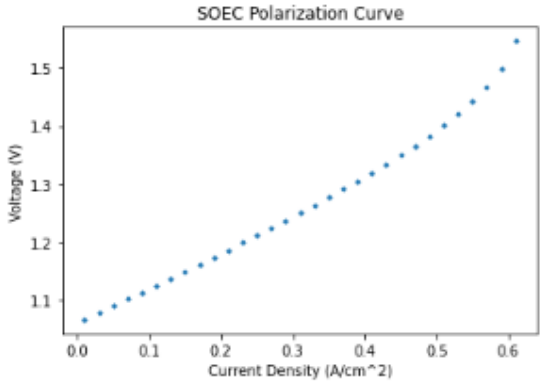


```
Rate of Current Produced by SOEC stack per mole fuel: 192970 Coulombs/mole
Total Power (in Watts):  [205923.916427   208174.52006204 210436.04348395 212709.25611392
 214995.01167366 217294.26096871 219608.06719068 221937.62435853
 224284.27970469 226649.5610642  229035.21067164 231443.22725334
 233875.91898492 236335.97086398 238826.53147868 241351.32628479
 243914.80774531 246522.35773595 249180.56569476 251897.61930121
 254683.86716291 257552.65323889 260521.59747389 263614.64364778
 266865.50202926 270323.80930368 274067.07058111 278226.43598599
 283051.52428882 289117.61129972 298374.93857926]
```

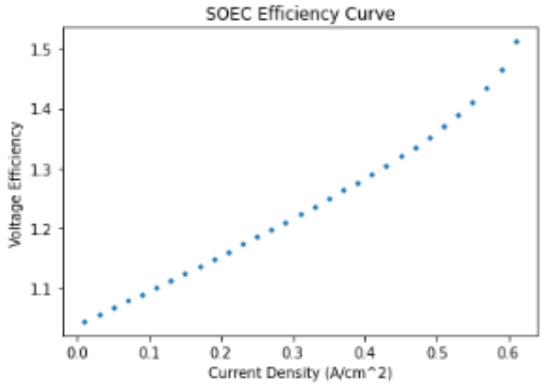

Table 15: Results from Electrolyzer Cell Model at 1173 K

```
Nernst Term: -0.04
Open-Circuit Voltage (in Volts): 1.003
Ohmic loss:  [0.005 0.015 0.025 0.035 0.045 0.055 0.065 0.075 0.085 0.095 0.105 0.115
 0.125 0.135 0.145 0.155 0.165 0.175 0.185 0.195 0.205 0.215 0.225 0.235
 0.245 0.255 0.265 0.275 0.285 0.295 0.305]
Concentration loss:  [-0.00088058 -0.00268532 -0.00455148 -0.00648337 -0.00848581 -0.01056413
 -0.01272432 -0.01497309 -0.01731802 -0.0197677  -0.02233194 -0.02502196
 -0.02785076 -0.03083342 -0.03398767 -0.03733444 -0.04089879 -0.04471098
 -0.04880806 -0.05323609 -0.05805327 -0.06333463 -0.06917927 -0.07572186
 -0.08315198 -0.09174877 -0.10194813 -0.11448763 -0.13077112 -0.1540339
 -0.19524403]
Activation loss:  [-0.02145213 -0.02145213 -0.02145213 -0.02145213 -0.02145213 -0.02145213
 -0.02145213 -0.02145213 -0.02145213 -0.02145213 -0.02145213 -0.02145213
 -0.02145213 -0.02145213 -0.02145213 -0.02145213 -0.02145213 -0.02145213
 -0.02145213 -0.02145213 -0.02145213 -0.02145213 -0.02145213 -0.02145213
 -0.02145213 -0.02145213 -0.02145213 -0.02145213 -0.02145213 -0.02145213
 -0.02145213]
Actual SOEC Voltage (in Volts):  [1.03022565 1.0420304  1.05389655 1.06582844 1.07783088 1.0899092
 1.10206939 1.11431816 1.1266631  1.13911278 1.15167701 1.16436703
 1.17719583 1.1901785  1.20333274 1.21667952 1.23024387 1.24405605
 1.25815314 1.27258117 1.28739834 1.3026797  1.31852435 1.33506694
 1.35249705 1.37109384 1.3912932  1.4138327  1.44011619 1.47337898
 1.52458911]
```

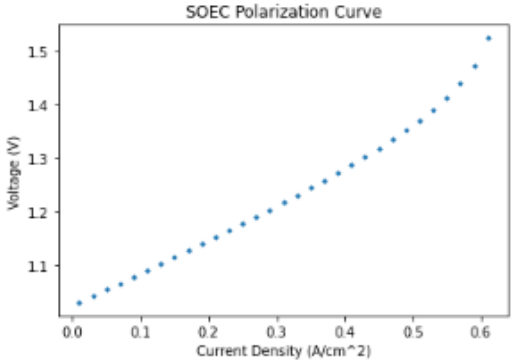


```
Rate of Current Produced by SOEC stack per mole fuel: 192970 Coulombs/mole
Total Power (in Watts):  [198802.64438712 201080.60553581 203370.41739948 205672.91499364
 207989.02482105 210319.77874483 212666.33059528 215029.97618323
 217412.1775947  219814.59291496 222239.11290667 224687.90669055
 227163.47921767 229668.74438565 232207.1192045  234782.64673066
 237400.15900622 240065.49671985 242785.81106901 245569.98774506
 248429.25758986 251378.10215484 254435.64351132 257627.86668213
 260991.35578667 264579.97911177 268477.84919375 272827.29690084
 277899.22137612 284317.94155078 294199.959988   ]
```

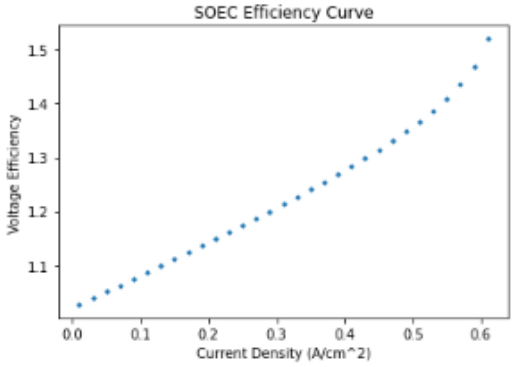

Table 16: Results from Electrolyzer Cell Model at 1273 K